19 August 2026

Divinyl-s-tetrazine as a Minimal Linchpin for Peptide Stapling, Protein Disulfide Re-bridging and Click Functionalisation

Tianyi Yang[1], Yujia Cui[2], Daria K. Wanic[1], Linwei Zeng[1], Mark R. Howarth[3,2], David R. Spring[1]

1. Yusuf Hamied Department of Chemistry, University of Cambridge

2. Department of Pharmacology, University of Cambridge

3. Engineering Biology Interdisciplinary Research Centre, University of Cambridge

Abstract

Site-selective bridging of cysteines and native disulfide bonds represents a powerful strategy for peptide and protein modification. However, most existing bis-electrophilic reagents rely on azide-alkyne cycloadditions for downstream modifications. In contrast, inverse-electron-demand Diels-Alder (IEDDA) reactions of s-tetrazines have emerged as a powerful tool in bioconjugation. Here, we report divinyl-s-tetrazine (DvTz) as a minimal linchpin in which the electron-deficient tetrazine core simultaneously activates the vinyl groups as electrophilic Michael acceptors for rapid cysteine conjugation, while also serving as a bioorthogonal handle for subsequent IEDDA ligation. DvTz enables rapid, high-yielding cysteine-selective stapling of unprotected peptides across all twenty canonical amino acids. A broad range of peptide lengths, sequence compositions and stapling distances were also demonstrated. A one-pot stapling and IEDDA sequence was also established without intermediate purification. This technology was further extended to antibody Fab fragments, achieving site-specific disulfide re-bridging and subsequent IEDDA ligation across three distinct Fab proteins, with exclusive formation of singly conjugated species and fully preserved antigen-binding activity. Collectively, this work establishes DvTz as an efficient and simple linchpin for peptide and protein modification and bioconjugation.

Divinyl-*s*-tetrazine as a Minimal Linchpin for Peptide Stapling, Protein Disulfide Re-bridging and Click Functionalisation

Tianyi Yang,[‡a] Yujia Cui,[‡b] Daria K. Wanic,[a] Linwei Zeng,[*a] Mark R. Howarth,[*bc] David R. Spring[*a]

a. Yusuf Hamied Department of Chemistry, University of Cambridge, Lensfield Road, Cambridge, United Kingdom, CB2 1EW E-mail: spring@ch.cam.ac.uk; lwzeng@zju.edu.cn

b. Department of Pharmacology, University of Cambridge, Tennis Court Road, Cambridge, United Kingdom, CB2 1PD Email: mh2186@cam.ac.uk

c. Engineering Biology Interdisciplinary Research Centre, University of Cambridge, Cambridge, United Kingdom, CB2 1GA

‡ These authors contributed equally to this work.

*Corresponding Authors

Abstract

Site-selective bridging of cysteines and native disulfide bonds represents a powerful strategy for peptide and protein modification. However, most existing bis-electrophilic reagents rely on azide-alkyne cycloadditions for downstream modifications. In contrast, inverse-electron-demand Diels-Alder (IEDDA) reactions of *s*-tetrazines have emerged as a powerful tool in bioconjugation. Here, we report divinyl-*s*-tetrazine (**DvTz**) as a minimal linchpin in which the electron-deficient tetrazine core simultaneously activates the vinyl groups as electrophilic Michael acceptors for rapid cysteine conjugation, while also serving as a bioorthogonal handle for subsequent IEDDA ligation. **DvTz** enables rapid, high-yielding cysteine-selective stapling of unprotected peptides across all twenty canonical amino acids. A broad range of peptide lengths, sequence compositions and stapling distances were also demonstrated. A one-pot stapling and IEDDA sequence was also established without intermediate purification. This technology was further extended to antibody Fab fragments, achieving site-specific disulfide re-bridging and subsequent IEDDA ligation across three distinct Fab proteins, with exclusive formation of singly conjugated species and fully preserved antigen-binding activity. Collectively, this work establishes **DvTz** as an efficient and simple linchpin for peptide and protein modification and bioconjugation.

Introduction

Site-selective chemical modification of native cysteine residues in peptides and proteins has become a cornerstone approach in bioconjugation, facilitating applications in chemical biology and novel therapeutics.[1–4] Among these approaches, a range of site-selective bis-cysteine conjugation reagents have been developed to bridge pairs of cysteines or re-bridge reduced disulfide bonds, enabling late-stage modification with diverse molecules while preserving the integrity of the

parent biomolecules. Notable examples include next-generation maleimides,[5–10] pyridazinediones,[11–14] divinylpyrimidines,[15–19] and ThioBridge™,[20–22] which have been extensively applied to peptide stapling and cyclisation,[23–27] protein modification,[28–30] and antibody-drug conjugation (Figure 1A).[31] Despite the impressive developments in this field, most existing bridging scaffolds carry an additional functional handle for downstream conjugation, often relying on established click chemistry such as copper-catalysed or strain-promoted azide-alkyne cycloaddition (CuAAC or SPAAC). In parallel, inverse-electron-demand Diels-Alder (IEDDA) reactions between 1,2,4,5-tetrazines (*s*-tetrazines) and dienophiles have emerged as a powerful biorthogonal tool with ultrafast kinetics, catalyst-free operation, compatibility with low concentrations in vivo, and utility in 'click-to-release' applications.[32] By combining cysteine labeling and IEDDA reactivity, Wu and co-workers reported a tetrazine prodrug reagent that selectively modifies cysteine on peptides, enabling subsequent bioorthogonal cleavage to release the active drug inside target cells.[33] Nevertheless, the development of bifunctional reagents based on the s-tetrazine scaffold for bis-cysteine conjugation remains limited (Figure 1B).[34–36]

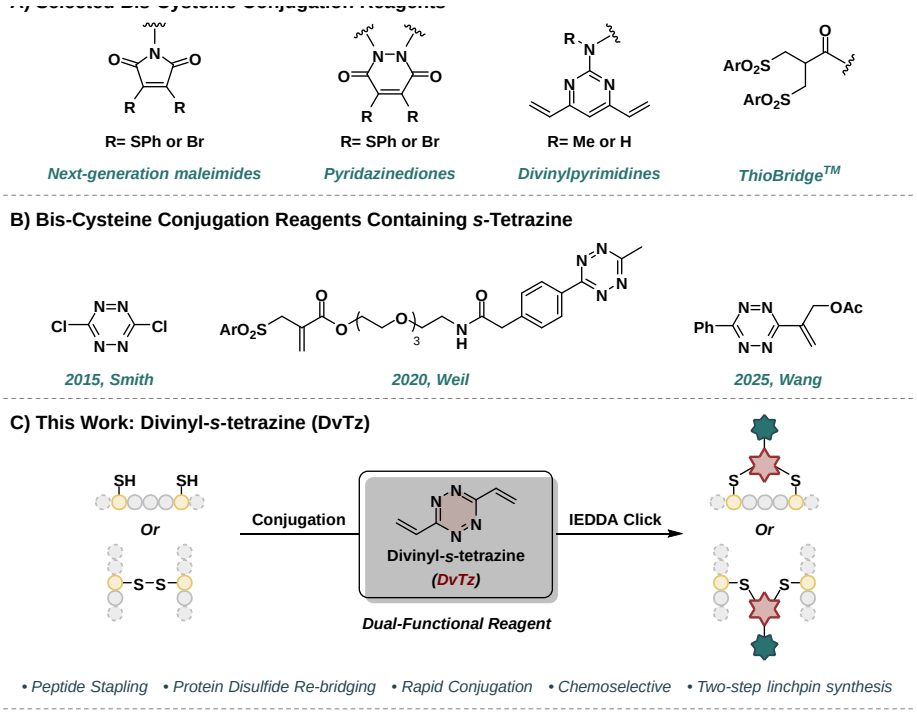

Figure 1. A) Selected examples of bis-cysteine bridging reagents; **B)** Previously reported bis-cysteine bridging reagents incorporating *s*-tetrazines; **C)** This work: divinyl-*s*-tetrazine (**DvTz**) as an effective linchpin for bis-cysteine conjugation/disulfide re-bridging and IEDDA functionalisation.

Dichloro-*s*-tetrazine was first introduced by Smith and co-workers as a photolabile trigger for peptide and protein modification,[34] with recent work reporting peptide cyclodimerisations instead of stapling with N-terminal cysteine.[37]

Separately, Weil and coworkers have developed a bis-sulfone-based tetrazine reagent.[35] Wang introduced a tetrazine allyl acetate for disulfide re-bridging and subsequent IEDDA functionalisation.[36] Inspired by this latter design, we pursued a simplified cysteine bridging agent capable of selective cysteine conjugation. Herein, we report divinyl-*s*-tetrazine (**DvTz**) as a minimal linchpin that integrates cysteine stapling and bioorthogonal IEDDA conjugation into a single scaffold. The tetrazine core simultaneously activates two vinyl warheads for rapid cysteine Michael additions and serves as a latent click handle for subsequent IEDDA ligation, obviating the need for an additional functionalisation tag. We demonstrate its application in cysteine-mediated peptide stapling and one-pot IEDDA functionalisation, extend this strategy to site-specific disulfide re-bridging of antibody Fab fragments with preserved antigen-binding activity, and evaluate its performance on an IgG1 antibody.

Result and Discussion

Peptide Stapling Optimisation

We first designed and optimised the synthesis of **DvTz** via a two-step route from commercially available starting materials (Figure S1) and evaluated its performance in peptide stapling using cysteine-containing model peptide **1** (Table 1).

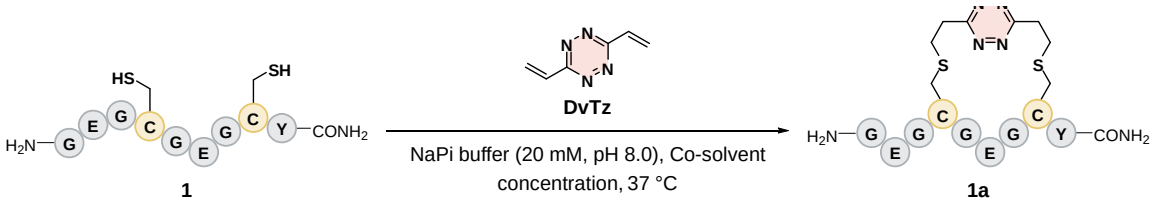

Entry	Co-solvent (v/v)	Conc. (mM)	DvTz eq.	Time (min)	Yield (%)*
1	30% MeCN	5	1.2	240	44
2	30% MeCN	2	1.2	240	52
3	30% MeCN	0.1	1.2	240	64
4	30% MeCN	0.05	1.2	240	63
5	30% MeCN	0.1	1.0	240	48
6	30% MeCN	0.1	2.0	240	91
7	70% MeCN	0.1	2.0	240	92
8	5% DMSO	0.1	2.0	240	88
9	30% EtOH	0.1	2.0	240	88
10	30% ^{i}PrOH	0.1	2.0	240	89
11	10% DMF	0.1	2.0	240	65
12	30% MeCN	0.1	2.0	15	93 (89[a], 75[b])

Table 1. Selected reaction conditions for the optimisation of peptide stapling. Peptide **1** was dissolved in NaPi buffer (20 mM, pH 8) and the corresponding co-solvent at the indicated concentration, followed by the addition of **DvTz** at the specified equivalents and incubation at 37 °C; *LC-estimated yields based on the UV absorption of peptides in HPLC-UV analysis (220 nm) of reaction mixtures; [a]Yield determined using aspirin as internal standard with calibration curve established (Figure S2); [b]Isolated yield; For full reaction condition optimisation see Table S1.

Inspired by the reported methodologies[33,38], we initiated the stapling reaction at a peptide concentration of 5 mM in a mixture of MeCN (30%) and NaPi buffer (20 mM, pH 8.0) containing 1.2 equivalents of **DvTz** (Entry 1). Under these conditions, the reaction afforded a moderate yield of 44%, accompanied by formation of side products, likely arising from undesired intermolecular reactions favoured at higher reactant concentrations. Decreasing the peptide concentration led to a concomitant increase in product yield (entries 2–4), reaching 64% at 0.1 mM, while further dilution did not provide additional improvement (Table S1). Next, we investigated the stoichiometry of **DvTz**, identifying 2.0 equivalents as optimal and affording **1a** in a 91% yield. Increasing the amount of **DvTz** beyond 2.0 equivalents did not further improve the yield, though importantly, no modification of the unprotected *N*-terminus was detected (Table S1). To ensure that our method is applicable to peptides of varying solubility and hydrophilicity, we screened a range of MeCN: buffer ratios (10–70%, entry 7 and Table S1) as well as co-solvents such as DMSO (entries 8–11) all of which led to high yields. We also assessed the effect of buffer pH over the range 6.5–8.0 and found only minor variations in yield, with high efficiency maintained throughout (Table S1). Finally, close monitoring of the reaction time course revealed that the stapling performed under the optimised conditions reached completion within 15 minutes, with a 75% isolated yield (entry 12). To validate the accuracy of our HPLC-UV based yield analysis, aspirin was used as an internal standard with isolated **1a** to construct a calibration curve (Figure S2), determining a yield of 89% under the optimal conditions (entry 12), showcasing the accuracy and viability of our analysis.

One-pot Peptide Stapling and IEDDA Functionalisation

We next turned our attention to functionalising the tetrazine linker *via* IEDDA cycloaddition. Reaction between the stapled peptide **1a** and 2.0 equivalents of bicyclo[6.1.0]nonyne (BCN) derivative **2** proceeded smoothly, reaching completion within 2 hours (Figure S3). Encouraged by this result, we explored whether the two-step sequence of peptide stapling and IEDDA could be accomplished in a single pot. To test this, **2** was directly added into the reaction mixture of peptide **1** and **DvTz** after 15 minutes, cleanly furnishing product **1b** in 74% HPLC yield and 45% isolated yield (Figure 2). This one-pot strategy therefore enables streamlined peptide stapling and subsequent bioorthogonal functionalisation in a single operation, eliminating the need for intermediate purification.

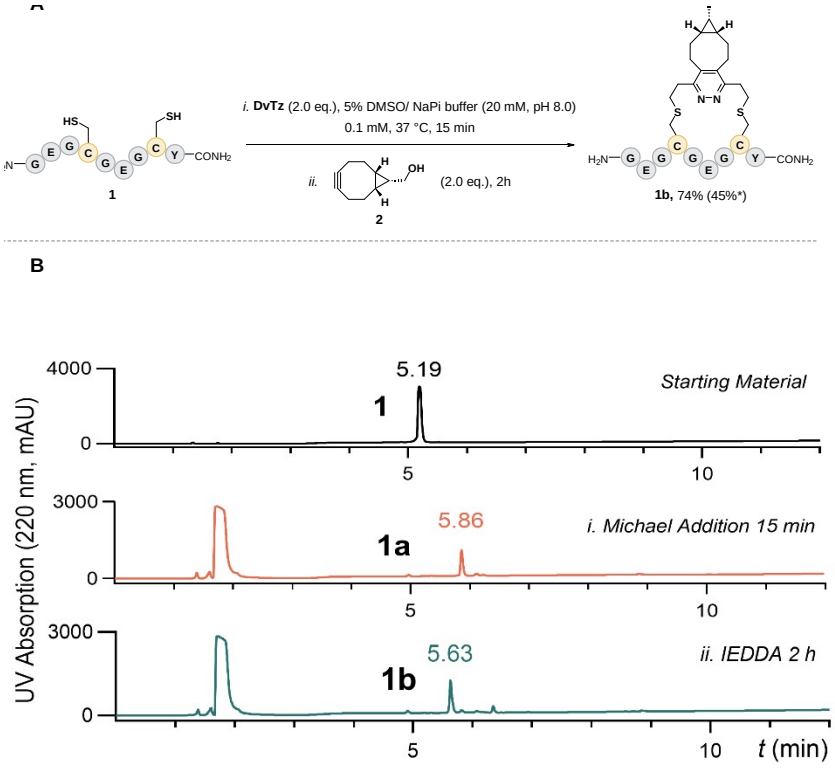

Figure 2. One-pot peptide stapling and IEDDA functionalisation. A. Reaction scheme; 2.0 equivalents of **DvTz** were added to peptide **1** dissolved in a 5% DMSO and NaPi buffer (20 mM, pH 8.0) mixture at 0.1 mM and incubated at 37 °C for 15 minutes, followed by the addition of 2.0 equivalents of **2** and incubation at 37 °C for 2 hours; LC-estimated yield based on the UV absorption of peptides in HPLC-UV analysis (220 nm) of the reaction mixture; *Isolated yield; **B.** HPLC-UV absorption traces (220 nm) of the one-pot reaction.

Peptide Stapling Scope

Having established the IEDDA reaction, we sought to explore the generality of **DvTz**-enabled peptide stapling across peptides of varying length, sequence composition, and stapling distance (Figure 3). As the stapling in model peptide **1** was applied between *i* and *i+4* residues, we first attempted to shrink the stapling distance to a single amino acid.

Tetrapeptide **3** underwent cyclisation under the optimised conditions to afford **3a** in a 73% yield. Replacing the central alanine with the bulkier valine and extending the peptide length led to peptide **4**, which gave **4a** in 81% yield. We then repositioned one cysteine to the *N*-terminus of a pentapeptide, increasing the distance to two residues, which delivered the desired stapled peptide **5a** in 67% yield. Together with the result for **3a**, these demonstrate that the method tolerates cysteine positioning at either terminus and within the peptide sequence. To challenge the capacity of the reaction to tolerate competing nucleophilic and sterically hindered side chains, peptide **6** was designed with a cysteine flanked by an unprotected *N*-terminal lysine and a bulky isoleucine. Gratifyingly, the desired product **6a** was successfully obtained in 71% yield.

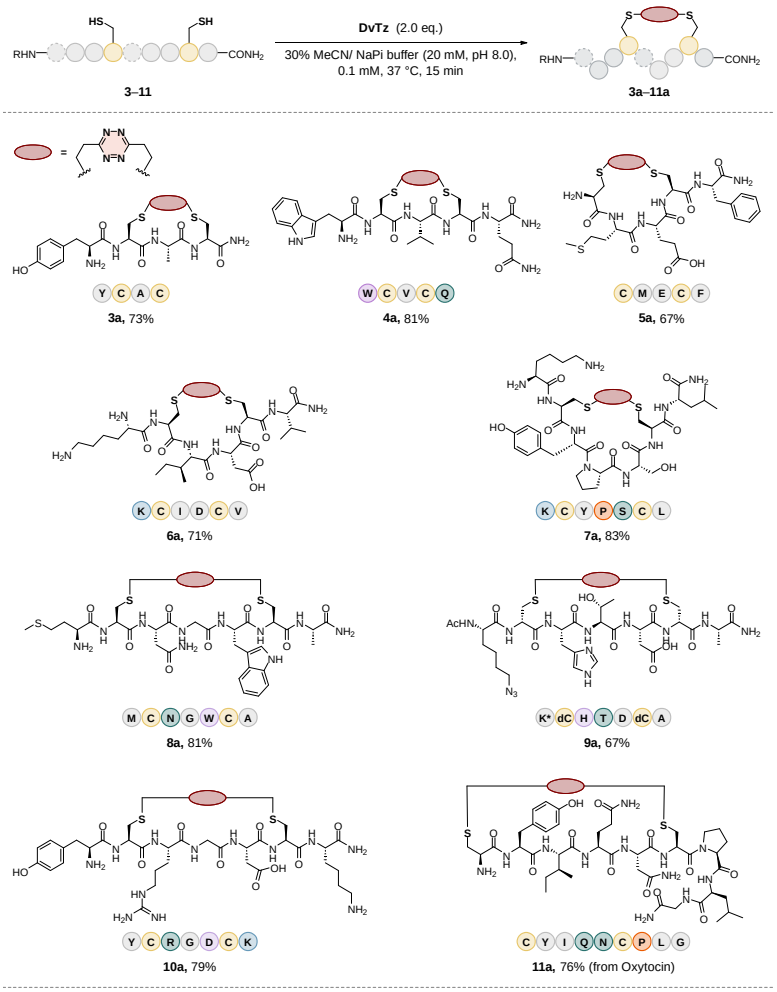

Figure 3. Peptide stapling scope with DvTz. 2.0 equivalents of **DvTz** were added to peptide dissolved in 30% MeCN and NaPi buffer (20 mM, pH 8.0) mixture at 0.1 mM and incubated at 37 °C for 15 minutes; LC-estimated yields based on the UV absorption of peptides in HPLC-UV analysis (220 nm) of reaction mixtures; dC= *D*-cysteine; K*= azidolysine

Further extension of the peptide length led to heptapeptides **7**–**10**, each incorporating a distinct set of three amino acids within the stapling region. Conformationally constrained and turn-inducing proline was introduced in peptide **7** adjacent to a nucleophilic serine residue; this is well tolerated and **7a** was produced in an excellent 83% yield. A comparable yield was found for **8a** (81%). In the case of **9a**, *D*-cysteines (dC) were employed together with the nucleophilic residues, histidine and threonine, delivering the stapled product in a 67% yield. Further to this, the side chain of the lysine in the sequence was modified to an azide (K*), showcasing the installation of two orthogonal 'click' handles for further elaboration through both IEDDAs and azide-alkyne cycloaddition. The arginine–glycine–aspartic acid (RGD) peptide sequence is widely exploited in targeted cancer therapy through its interaction with integrin receptors. Linear peptides containing this sequence are commonly modified to enhance the stability and enable payload attachment.[39–41] For this

reason, we applied **DvTz** to peptide **10**, which incorporates the RGD sequence, obtaining product **10a** in 79% yield. Lastly, applying the optimised conditions to oxytocin, a nine-amino-acid natural hormone involved in several physiological functions,[42] afforded **11a** in 76% yield. Overall, these results demonstrated that **DvTz** can serve as a rapid and highly specific bis-cysteine stapling reagent for unprotected peptides. All twenty natural amino acids, as well as D-cysteine, are compatible across a range of peptide lengths (4–9 residues), sequence compositions, and stapling distances, with products being formed in good to excellent yields.

Disulfide Re-bridging and IEDDA Functionalisation of Proteins

In recent years, small antibody fragments have attracted increasing attention mainly for drug conjugate development, offering the potential to overcome tissue penetration or retention issues suffered by antibody-drug conjugates.[43–45] The Fab fragments comprise the constant and variable domains of immunoglobulin.[46] Fab fragments have a single solvent-accessible interchain disulfide bond, rendering them well-suited for disulfide re-bridging-based strategies for payload conjugation.[47,48] Notably, a trastuzumab-derived Fab conjugate has demonstrated good stability and potent tumour growth inhibition in a mouse breast cancer model,[22] with several other approaches to Fab conjugation having since been reported.[12,30,49–51] Motivated by the excellent performance of **DvTz** on peptides, we envisaged that this reagent could be extended to interchain disulfide bond re-bridging and functionalisation of Fabs (Figure 4).

To this end, we prepared αHER2 Fab **12** from trastuzumab *via* sequential digestion by pepsin and papain. The Fab fragment was then first reduced using 10 equivalents of TCEP in TBS buffer (pH 8.0) at 37 °C for 1 h, followed by the addition of different stoichiometries of **DvTz** (15, 20 and 50 eq.) and incubation at 37 °C overnight (Figure S4). We found that 20 equivalents of **DvTz** were sufficient to fully re-bridge the interchain disulfide bond and the reaction reached completion within 1 hour to afford **12a** (Figure S4). Subsequent IEDDA with 20 equivalents of **2** furnished αHER2 Fab-DvTz-BCN **12b** in 2 hours. Both **12a** and **12b** were analysed by SDS-PAGE with reducing loading dye, where the native interchain disulfide bond in αHER2 Fab was cleaved into heavy and light chains, while both **12a** and **12b** remained intact, confirming successful disulfide re-bridging (Figure S4). Notably, a previous study of vinyltetrazines by Wang and coworkers, reported substantial over-reaction upon conjugation with a protein bearing one free cysteine, forming at least four conjugates.[38] By contrast, MS analysis of **12a** confirmed clean, single addition of **DvTz**, with no other conjugated species detected (Figure 4B and S5). The expected mass shift for the IEDDA product **12b** was likewise confirmed by MS (Figure 4B and S5).

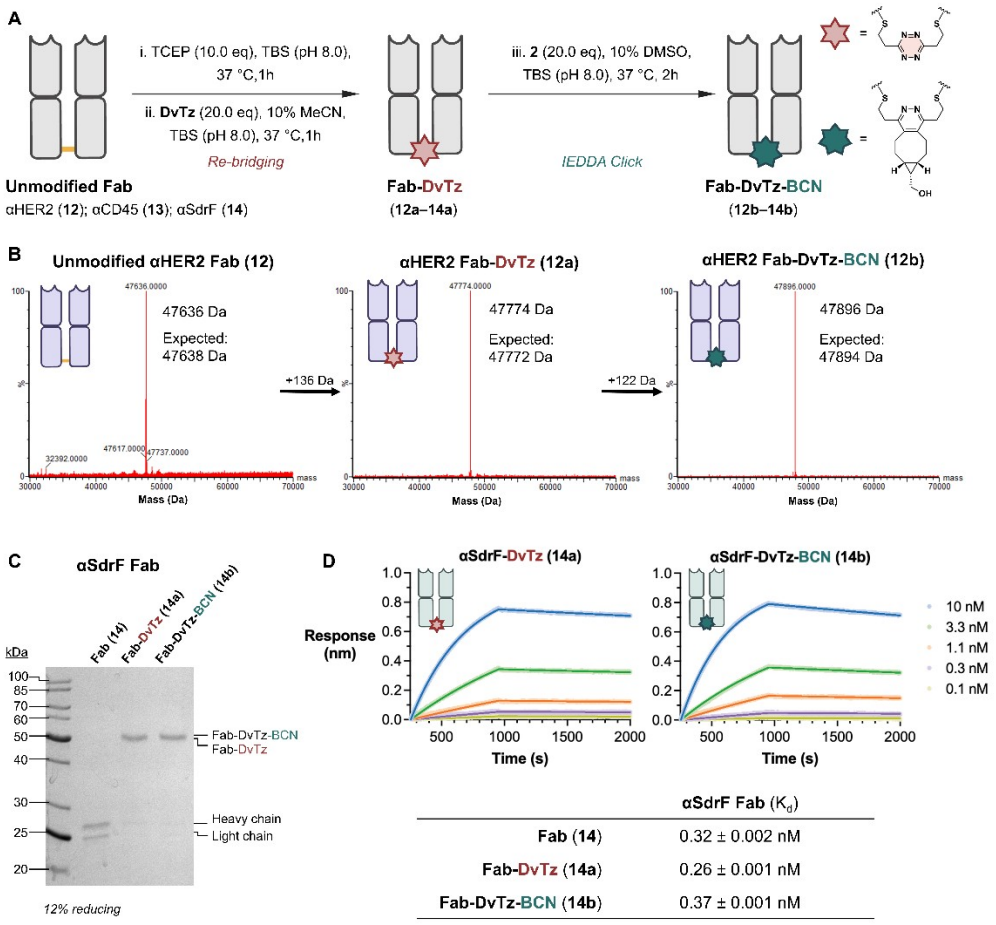

Figure 4. Disulfide re-bridging and IEDDA functionalisation of antibody antigen-binding fragments (Fabs) using DvTz. A) Schematic representation of disulfide re-bridging and IEDDA functionalisation of Fabs (disulfide bonds were coloured in yellow); the Fab was first treated with 10.0 eq. TCEP at 37 °C for 1h in TBS (1x, pH 8.0, 10 µM Fab). 20.0 eq. **DvTz** was subsequently added in MeCN (10% of the total reaction volume), and the solution was incubated at 37 °C for a further 1h. The reaction was then filtered, buffer exchanged to PBS (1x, pH 7.4) and concentrated to 10 µM Fab. Following this, 20.0 eq. **2** was added in DMSO (10% of the reaction volume), and the reaction was incubated at 37 °C for 2h prior to filtration and buffer exchange; **B)** Deconvoluted MS data of αHER2 Fab, αHER2 Fab-DvTz and αHER2 Fab-DvTz-BCN; intensity *vs.* deconvoluted mass; **C)** SDS-PAGE analysis of αSdrF Fab, αSdrF Fab-DvTz and αSdrF Fab-DvTz-BCN on 12% acrylamide gel with samples prepared using a loading dye containing 2-mercaptoethanol, followed by Coomassie Blue staining prior to visualisation; **D)** Bio-layer interferometry (BLI) characterisation of binding affinity of αSdrF Fab-DvTz and αSdrF Fab-DvTz-BCN to SdrF N2N3 domain. Biotinylated SdrF N2N3 domain was loaded onto streptavidin sensors until binding was 0.6-0.7 nm; αSdrF Fab-DvTz or αSdrF Fab-DvTz-BCN were used as analytes in PBS-T (pH 7.4, 0.05% Tween 20), with concentration ranging from 10 nM to 0.1 nM. The darker lines correspond to a fit with a 1:1 standard binding model. Table summarises dissociation constants (K_d) ± fitting error.

Beyond the αHER2 Fab generated by proteolytic digestion, we next extended the strategy to two Fabs expressed recombinantly in mammalian cells, αCD45 (**13**) and αSdrF (**14**), each bearing an engineered C-terminal polyhistidine tag for affinity purification and a SpyTag003 for modular assembly with SpyCatcher003-bearing constructs through spontaneous isopeptide bond formation.[52] CD45 is expressed at high antigen density on nucleated haematopoietic cells but is absent from non-haematopoietic tissues,[53] and radiolabelled anti-CD45 antibodies are established clinically and preclinically as

targeted conditioning and anti-leukaemic agents.[54,55] Applying the established protocol to αCD45 Fab, we observed the analogous interchain disulfide re-bridging *via* **DvTz** and IEDDA functionalization, confirmed through SDS-PAGE and MS analysis (Figure S6).

SdrF is a cell-wall-anchored adhesin from *Staphylococcus epidermidis*, a skin commensal and a major cause of prosthetic device infection.[56] SdrF mediates adherence to host collagen deposited on implanted materials, and anti-SdrF antibodies reduce colonisation of implanted devices. An αSdrF binder is therefore an attractive vehicle for small molecule payload delivery in two distinct settings. Conjugating an antibiotic through **DvTz** offers a route to localised antibacterial activity at the device surface. Alternatively, *S. epidermidis* has recently been engineered as a topical vaccine platform, displaying antigens anchored to its cell-surface proteins to redirect B cell responses;[57] here, conjugation of a small-molecule innate immune stimulator could position an adjuvant directly on the bacterial surface. Applying the re-bridging and IEDDA methods to αSdrF Fab **14** led to the formation of αSdrF Fab-DvTz **14a** and αSdrF Fab-DvTz-BCN **14b**, with SDS-PAGE and MS analysis validating the successful modification at the interchain disulfide (Figure 4C and S7). We next assessed the binding kinetic activity of these modified Fabs (**14a** and **14b**) through bio-layer interferometry (BLI), evaluating their binding affinity towards the SdrF N2N3 domain antigen (Figure 4D and S8). **14a** was found to have a dissociation constant (K_d) of 0.26 nM, while **14b** had a value of 0.37 nM, approximately the same K_d as native αSdrF Fab (0.32 nM). Collectively, these results highlight that our linchpin at the interchain disulfide has minimal impact on Fab antigen recognition, with binding activity preserved throughout re-bridging and subsequent IEDDA functionalisation. Together, these findings establish **DvTz** as an effective disulfide re-bridging reagent for small antibody fragments, enabling site-specific re-bridging and IEDDA-based functionalisation of three Fabs against structurally and functionally distinct targets. This establishes a platform for future therapeutic applications spanning oncology, immunology, and antimicrobial therapy.

Compared to a single interchain disulfide bond in Fab, human IgG1 antibodies possess four interchain disulfide bonds connecting two identical heavy chains and two identical light chains,[58] posing challenges for site-specific chemical modification.

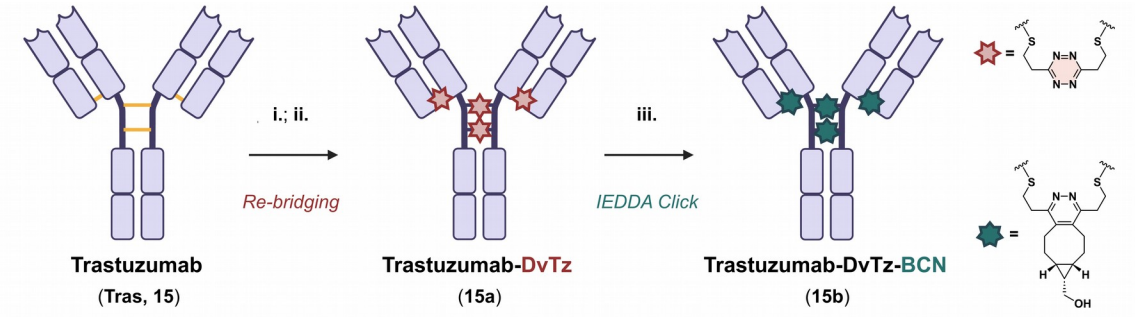

Figure 5. Disulfide re-bridging and IEDDA functionalisation of trastuzumab using DvTz. i. 10.0 eq. TCEP in TBS (1x, pH 8.0, 10 μM Tras) at 37 °C for 1h; ii. 60.0 eq. **DvTz** in 10% MeCN, TBS (1x, pH 8.0) at 37 °C for 2h; iii. 100.0 eq. **2** in 10% DMSO, PBS (1x, pH 7.4) at 37 °C overnight. Disulfide bonds were coloured in yellow.

Amongst the numerous antibodies, trastuzumab is a well-understood HER2-targeting antibody which features in several FDA-approved ADCs, as well as many more candidates currently in clinical trials and preclinical evaluation.[59,60] We therefore evaluated the performance of **DvTz** for trastuzumab re-bridging, screening a range of **DvTz** equivalents (40–80 eq.) and reaction times following TCEP reduction of the native disulfides (Figure S9). Optimal conversion was achieved with 60.0 equivalents of **DvTz** over 2 hours at 37 °C, affording predominantly the fully re-bridged antibody, with a mass increase consistent with the addition of four **DvTz** units (Figure S10). SDS-PAGE analysis of trastuzumab-DvTz (**15a**) also revealed the formation of 'half antibodies', arising from re-bridging of intrachain cysteines, a common phenomenon observed with many other reagents.[9,15,61] However, subsequent IEDDA reaction of **15a** with **2** did not proceed to full conversion, despite extensive optimisation attempts by increasing the equivalents of **2** (up to 100 eq.) and prolonging reaction time (up to overnight). MS analysis of the resulting product **15b** revealed a mixture of species, with the fully 'clicked' tetra-functionalised antibody (bearing four BCN groups) as the major product, alongside partially converted double-'clicked' species (Figure S10). We attribute this incomplete reaction to the reduced accessibility in the full IgG scaffold. Nevertheless, our BLI analysis showed preserved binding for both **15a** and **15b** compared to native trastuzumab (Figure S11).

Conclusions

In conclusion, we have developed divinyl-*s*-tetrazine (**DvTz**) as an effective dual-functional linchpin that integrates selective bis-cysteine bridging and bioorthogonal IEDDA functionalisation within a single, easily accessible reagent. The electron-withdrawing tetrazine core enhances the electrophilicity of the vinyl groups, accelerating their Michael addition with cysteine thiols. We have demonstrated that **DvTz** enables rapid (15 min), high-yielding stapling of unprotected peptides spanning all twenty proteinogenic amino acids, across a broad range of peptide lengths, sequence compositions,

and stapling distances. No side-reactions were observed with other nucleophilic residues, such as lysine and histidine, nor with the peptide N-terminus. We have also established a one-pot peptide stapling and IEDDA sequence that proceeds without intermediate purification. This chemistry was successfully extended to antibody Fab fragments, achieving site-specific, chemo-selective disulfide re-bridging and subsequent click functionalisation, further underscoring the mildness and biocompatibility of the reagent. Across all three structurally and functionally distinct Fab proteins, **DvTz** re-bridging afforded exclusively single conjugated species, in contrast to the multiple conjugated mixtures previously reported for vinyltetrazines.[38] The linchpin also gave minimal disruption to antigen recognition following modification, as evidenced by the comparable dissociation constants measured for αSdrF Fabs (**14**, **14a**–**b**). When applied to an IgG1 antibody (trastuzumab), **DvTz** achieved near-complete re-bridging with all four interchain disulfides. However, the subsequent IEDDA functionalisation proceeded with incomplete conversion, which will motivate future optimisation of the reagent and reaction conditions. Collectively, these results establish **DvTz** as an efficient and versatile linchpin for peptide stapling and disulfide re-bridging. Further therapeutically relevant applications of this reagent, including drug conjugates, are of high interest and are currently being explored.

Data availability

The data supporting this article have been included as part of the ESI.

Author contributions

T. Y. was involved in conceptualisation, data curation, formal analysis, investigation, methodology, validation of the chemical, peptidic and bioconjugation parts, visualisation, and writing (original draft and editing). Y. C. was involved in data curation, formal analysis, validation of the biological result, visualisation, and writing (original draft and editing). D. K. W. was involved in investigation and writing (editing). L. Z. was involved in conceptualisation and writing (editing). M. R. H. and D. R. S. were involved in conceptualisation, funding acquisition, supervision and writing (editing). All authors have been involved in proofreading of the manuscript.

Conflicts of interest

There are no conflicts to declare.

Acknowledgements

T. Yang thanks the INEOS Oxford Institute (IOI) for a studentship and financial support. Y. Cui was funded by the David James Trust Fund. D. K. Wanic acknowledges support from the Cambridge Trust (Cambridge International Scholarship). We thank Dr. T. Wharton, Dr. J. Sutro, A. Rowley for proofreading this manuscript. The Spring group acknowledges support from the EPSRC, BBSRC, MRC, UKRI and Cystic Fibrosis Trust UK. For Open Access, the authors have applied a CC BY public copyright licence to any Author Accepted Manuscript (AAM) version arising. Figures and Schemes have been made with use of BioRender.

Notes and references

1 S. B. Gunnoo and A. Madder, *ChemBioChem*, 2016, **17**, 529–553.
2 J. M. Chalker, G. J. L. Bernardes, Y. A. Lin and B. G. Davis, *Chem. Asian J.*, 2009, **4**, 630–640.
3 N. Krall, F. P. da Cruz, O. Boutureira and G. J. L. Bernardes, *Nat. Chem.*, 2016, **8**, 103–113.
4 K. Gavriel and K. Neumann, *Precis. Chem.*, 2026, **4**, 712–727.
5 M. E. B. Smith, F. F. Schumacher, C. P. Ryan, L. M. Tedaldi, D. Papaioannou, G. Waksman, S. Caddick and J. R. Baker, *J. Am. Chem. Soc.*, 2010, **132**, 1960–1965.
6 A. Wall, A. G. Wills, N. Forte, C. Bahou, L. Bonin, K. Nicholls, M. T. Ma, V. Chudasama and J. R. Baker, *Chem. Sci.*, 2020, **11**, 11455–11460.
7 F. F. Schumacher, J. P. M. Nunes, A. Maruani, V. Chudasama, M. E. B. Smith, K. A. Chester, J. R. Baker and S. Caddick, *Org. Biomol. Chem.*, 2014, **12**, 7261–7269.
8 N. Forte, M. Livanos, E. Miranda, M. Morais, X. Yang, V. S. Rajkumar, K. A. Chester, V. Chudasama and J. R. Baker, *Bioconjug. Chem.*, 2018, **29**, 486–492.
9 M. Morais, J. P. M. Nunes, K. Karu, N. Forte, I. Benni, M. E. B. Smith, S. Caddick, V. Chudasama and J. R. Baker, *Org. Biomol. Chem.*, 2017, **15**, 2947–2952.
10 F. Bryden, A. Maruani, H. Savoie, V. Chudasama, M. E. B. Smith, S. Caddick and R. W. Boyle, *Bioconjug. Chem.*, 2014, **25**, 611–617.
11 E. Robinson, J. P. M. Nunes, V. Vassileva, A. Maruani, J. C. F. Nogueira, M. E. B. Smith, R. B. Pedley, S. Caddick, J. R. Baker and V. Chudasama, *RSC Adv.*, 2017, **7**, 9073–9077.
12 I. A. Thanasi, N. Bouloc, C. McMahon, N. Wang, P. A. Szijj, T. Butcher, L. N. C. Rochet, E. A. Love, A. Merritt, J. R. Baker and V. Chudasama, *Chem. Sci.*, 2025, **16**, 2763–2776.
13 A. Maruani, M. E. B. Smith, E. Miranda, K. A. Chester, V. Chudasama and S. Caddick, *Nat. Commun.*, 2015, **6**, 6645.
14 V. Chudasama, M. E. B. Smith, F. F. Schumacher, D. Papaioannou, G. Waksman, J. R. Baker and S. Caddick, *Chem. Commun.*, 2011, **47**, 8781.
15 S. J. Walsh, S. Omarjee, W. R. J. D. Galloway, T. T.-L. Kwan, H. F. Sore, J. S. Parker, M. Hyvönen, J. S. Carroll and D. R. Spring, *Chem. Sci.*, 2019, **10**, 694–700.
16 S. J. Walsh, S. Omarjee, F. M. Dannheim, D.-L. Couturier, D. Bexheti, L. Mendil, G. Cronshaw, T. Fewster, C. Gregg, C. Brodie, J. L. Miller, R. Houghton, J. S. Carroll and D. R. Spring, *Chem. Commun.*, 2022, **58**, 1962–1965.
17 A. R. Hanby, S. J. Walsh, A. J. Counsell, N. Ashman, K. T. Mortensen, J. S. Carroll and D. R. Spring, *Chem. Commun.*, 2022, **58**, 9401–9404.
18 S. Krajcovicova, T. Wharton, C. L. Driscoll, T. A. King, M. R. Howarth and D. R. Spring, *Chem. Sci.*, 2025, **16**, 10602–10609.
19 T. A. King, S. J. Walsh, M. Kapun, T. Wharton, S. Krajcovicova, M. S. Glossop and D. R. Spring, *Chem. Commun.*, 2023, **59**, 9868–9871.
20 R. B. Del Rosario, R. L. Wahl, S. J. Brocchini, R. G. Lawton and R. H. Smith, *Bioconjug. Chem.*, 1990, **1**, 51–59.
21 M. Pabst, W. McDowell, A. Manin, A. Kyle, N. Camper, E. De Juan, V. Parekh, F. Rudge, H. Makwana, T. Kantner, H. Parekh, A. Michelet, X. Sheng, G. Popa, C. Tucker, F. Khayrzad, D. Pollard, K. Kozakowska, R. Resende, A. Jenkins, F. Simoes, D. Morris, P. Williams, G. Badescu, M. P. Baker, M. Bird, M. Frigerio and A. Godwin, *J. Control. Release*, 2017, **253**, 160–164.
22 G. Badescu, P. Bryant, M. Bird, K. Henseleit, J. Swierkosz, V. Parekh, R. Tommasi, E. Pawlisz, K. Jurlewicz, M. Farys, N. Camper, X. Sheng, M. Fisher, R. Grygorash, A. Kyle, A. Abhilash, M. Frigerio, J. Edwards and A. Godwin, *Bioconjug. Chem.*, 2014, **25**, 1124–1136.
23 T. Deingruber, J. S. Gaynord, B. H. Gan, K. A. Kostadinova, T. J. O'Brien, Y. S. Tan, J. S. Parker, T. A. Hunt, J. S. Carroll, M. Welch and D. R. Spring, *Chem. Sci.*, 2025, **16**, 19288–19295.

24 D. A. Richards, S. A. Fletcher, M. Nobles, H. Kossen, L. Tedaldi, V. Chudasama, A. Tinker and J. R. Baker, *Org. Biomol. Chem.*, 2016, **14**, 455–459.
25 J. Iegre, S. Krajcovicova, A. Gunnarsson, L. Wissler, H. Käck, A. Luchniak, S. Tångefjord, F. Narjes and D. R. Spring, *Chem. Sci.*, 2023, **14**, 10800–10805.
26 E. L. Atkinson, J. Iegre, C. D'Amore, P. Brear, M. Salvi, M. Hyvönen and D. R. Spring, *Chem. Commun.*, 2022, **58**, 4791–4794.
27 N. S. Robertson, S. J. Walsh, E. Fowler, M. Yoshida, S. M. Rowe, Y. Wu, H. F. Sore, J. S. Parker and D. R. Spring, *Chem. Commun.*, 2019, **55**, 9499–9502.
28 A. J. Counsell, S. J. Walsh, N. Ashman, M. Park, F. M. Dannheim, T. A. King, T. Wharton, J. S. Carroll and D. R. Spring, *Chem. Sci.*, 2026, **17**, 2722–2731.
29 M. Park, F. M. Dannheim, M. A. Papworth, R. Kay, E. Tsonou, D. Trajkovski, S. J. Walsh, D. Hovdal, T. Wharton, A.-C. Nassoy, J. S. Parker and D. R. Spring, *Chem. Sci.*, 2026, **17**, 13454–13464.
30 A. Chrzastek, I. A. Thanasi, J. A. Irving, V. Chudasama and J. R. Baker, *Chem. Sci.*, 2022, **13**, 11533–11539.
31 S. J. Walsh, J. D. Bargh, F. M. Dannheim, A. R. Hanby, H. Seki, A. J. Counsell, X. Ou, E. Fowler, N. Ashman, Y. Takada, A. Isidro-Llobet, J. S. Parker, J. S. Carroll and D. R. Spring, *Chem. Soc. Rev.*, 2021, **50**, 1305–1353.
32 B. L. Oliveira, Z. Guo and G. J. L. Bernardes, *Chem. Soc. Rev.*, 2017, **46**, 4895–4950.
33 X. He, J. Li, X. Liang, W. Mao, X. Deng, M. Qin, H. Su and H. Wu, *Nat. Commun.*, 2024, **15**, 2831.
34 S. P. Brown and A. B. Smith, *J. Am. Chem. Soc.*, 2015, **137**, 4034–4037.
35 L. Xu, M. Raabe, M. M. Zegota, J. C. F. Nogueira, V. Chudasama, S. L. Kuan and T. Weil, *Org. Biomol. Chem.*, 2020, **18**, 1140–1147.
36 H. Xu, M. Chang, Y. Dong, F. Bi, H. Li and W. Wang, *JACS Au*, 2025, **5**, 4893–4903.
37 K. Hu, Q. Zuo, Q. He, J. Yan, X. Yang, H. Tian, H. Huang, X. Gao, J. Shen, Y. Hu, L. Li, M. Lu and R. Wang, *Research Square*, 2026, preprint, DOI: 10.21203/rs.3.rs-10198979/v1.
38 M. Chang, H. Xu, Y. Dong, G. Gnawali, F. Bi and W. Wang, *ACS Chem. Biol.*, 2025, **20**, 153–161.
39 X. Cheng, C. Li, H. Hong, Z. Zhou and Z. Wu, *RSC Med. Chem.*, 2025, **16**, 3077–3083.
40 H. Javid, M. A. Oryani, N. Rezagholinejad, A. Esparham, M. Tajaldini and M. Karimi-Shahri, *Cancer Med.*, 2024, **13**, e6800.
41 L. Yin, X. Li, R. Wang, Y. Zeng, Z. Zeng and T. Xie, *Int. J. Pept. Res. Ther.*, 2023, **29**, 53.
42 C. Viero, I. Shibuya, N. Kitamura, A. Verkhratsky, H. Fujihara, A. Katoh, Y. Ueta, H. H. Zingg, A. Chvatal, E. Sykova and G. Dayanithi, *CNS Neurosci. Ther.*, 2010, **16**, e138–e156.
43 M. P. Deonarain and Q. Xue, *Antib. Ther.*, 2020, **3**, 237–245.
44 X. Ma, M. Wang, T. Ying and Y. Wu, *Antib. Ther.*, 2024, **7**, 114–122.
45 Z. Li, B.-F. Krippendorff, S. Sharma, A. C. Walz, T. Lavé and D. K. Shah, *MAbs*, 2016, **8**, 113–119.
46 H. Lou and X. Cao, *Cancer Commun.*, 2022, **42**, 804–827.
47 J. T. Heads, R. Adams, L. E. D'Hooghe, M. J. T. Page, D. P. Humphreys, A. G. Popplewell, A. D. Lawson and A. J. Henry, *Protein Science*, 2012, **21**, 1315–1322.
48 S. Puthenveetil, S. Musto, F. Loganzo, L. N. Tumey, C. J. O'Donnell and E. Graziani, *Bioconjug. Chem.*, 2016, **27**, 1030–1039.
49 X. Wang, X. Hou, L. Tan, C. Chen, L. Chang, B. Han, Y. Xing, Z. Zeng, Z. Zhou, Q. Lu, L. Xie, Z. Lu, K. Zhao, B. Cao, T. Liu and Y. Wang, *J. Med. Chem.*, 2026, **69**, 10169–10182.
50 M. El Alaoui, E. Sivado, A.-C. Jallas, L. Mebarki, M. R. Dyson, F. Perrez, S. Valsesia-Wittmann and S. El Alaoui, *Cell Death Discov.*, 2024, **10**, 79.
51 M. P. Deonarain, G. Yahioglu, I. Stamati, B. Edwards, S. Diez-Posada, A. Pomowski, A. Stewart, I. Perez-Castro, L. Bouche, T. Jurgenson, M. Maciuszek, S. Ness, M. Ngiam and Q. Xue, *Cancer Res.*, 2021, **81**, 909–909.
52 A. H. Keeble, P. Turkki, S. Stokes, I. N. A. Khairil Anuar, R. Rahikainen, V. P. Hytönen and M. Howarth, *Proc. Natl. Acad. Sci. U. S. A.*, 2019, **116**, 26523–26533.
53 T. L. Andres and M. E. Kadin, *Am. J. Clin. Pathol.*, 1983, **79**, 546–552.
54 S. A. Tuazon, B. M. Sandmaier, J. J. Orozco, A. K. Gopal, L. A. Holmberg, P. S. Becker, S. J. Lundberg, B. G. Till, M. E. Nartea, T. Gooley, D. R. Fisher, J. G. Rajendran, O. W. Press, W. I. Bensinger and D. J. Green, *Blood*, 2017, **130**, 910–910.
55 R. Mawad, T. A. Gooley, J. G. Rajendran, D. R. Fisher, A. K. Gopal, A. T. Shields, B. M. Sandmaier, M. L. Sorror, H. J. Deeg, R. Storb, D. J. Green, D. G. Maloney, F. R. Appelbaum, O. W. Press and J. M. Pagel, *Biol. Blood Marrow Transplant.*, 2014, **20**, 1363–1368.
56 S. Trivedi, A.-C. Uhlemann, P. Herman-Bausier, S. B. Sullivan, M. G. Sowash, E. Y. Flores, S. D. Khan, Y. F. Dufrêne, and F. D. Lowy, *J. Infect. Dis.*, 2017, **215**, 1846–1854.
57 D. Bousbaine, K. D. Bauman, Y. E. Chen, P. V. Lalgudi, T. T. D. Nguyen, J. M. Swenson, V. K. Yu, E. Tsang, S. Conlan, D. B. Li, A. Jbara, A. Zhao, A. Naziripour, A. Veinbachs, Y. E. Lee, J. L. Phung, A. Dimas, S. Jain, X. Meng, T. P. T. Pham, M. I. McLaughlin, L. J. Barkal, I. Gribonika, K. K. A. Van Rompay, H. H. Kong, J. A. Segre, Y. Belkaid, C. O. Barnes and M. A. Fischbach, *Nature*, 2025, **638**, 1054–1064.
58 G. D. Miteu, *Discov. Appl. Sci.*, 2025, **7**, 1148.
59 S. S. Matikonda, R. McLaughlin, P. Shrestha, C. Lipshultz and M. J. Schnermann, *Bioconjug. Chem.*, 2022, **33**, 1241–1253.
60 E. Ferraro, J. Z. Drago and S. Modi, *Breast Cancer Res.*, 2021, **23**, 84.

61 O. Koniev, I. Dovgan, B. Renoux, A. Ehkirch, J. Eberova, S. Cianférani, S. Kolodych, S. Papot and A. Wagner, *MedChemComm*, 2018, **9**, 827–830.

Table of Contents

1. Experimental Procedures

1.1. General Information

All reagents were of reagent grade and used as received. Solvents and chemicals were purchased from Sigma-Aldrich, Fluorochem or Iris Biotech. Ethyl acetate, methanol, dichloromethane, and acetonitrile were distilled from calcium hydride. Diethyl ether was distilled from a mixture of lithium aluminium hydride and calcium hydride. Petroleum ether (PE) refers to the fraction obtained between 40–60 °C upon distillation. Software used: chemical structures (ChemDraw), NMR (MestReNova), UV-LCMS (MassLynx), figures (MS PowerPoint), citations (Mendeley)

Reactions were monitored by thin layer chromatography (TLC) or liquid chromatography mass spectrometry (LCMS). TLC was performed using glass plates precoated with Merck silica gel 60 F254 and visualised by quenching of UV fluorescence (λ_{max} = 254 nm) or by staining with potassium permanganate. Retention factors (R_f) are quoted to two decimal places.

Reactions were conducted under a stream of dry nitrogen using oven-dried glassware. Temperature of 0 °C was maintained using an ice-water bath.

1.2. Instrumentation

UV-LCMS analysis

Liquid chromatography mass spectroscopy (LCMS) was carried out using a Waters ACQUITY HClass UPLC with an ESI Multi-Mode Ionisation Waters SQ Detector 2 spectrometer; ESI refers to the electrospray ionisation technique; LC system: solvent A: 2 mM NH_4OAc in H_2O/MeCN (95:5); solvent B: MeCN; solvent C: 2% formic acid (aq.); column: ACQUITY UPLC CSH C18 (2.1 mm × 50 mm, 1.7 µm, 130 Å) at 40 °C; gradient: 5–95 % B with constant 5% C, over 1 minute at a flow rate of 0.6 mL/minute; detector: PDA eλ Detector 220–800 nm, interval 1.2 nm

Analytical HPLC

Analysis was carried out using an Agilent 1260 Infinity II system with a reversed-phase Eclipse Plus C18 column (150 mm × 4.6 mm, 3.5 µm) eluting with a linear gradient system (solvent A: 0.05% TFA in water (v/v), solvent B: 0.05% TFA in MeCN (v/v)) over 15 minutes, at a flow rate of 1 mL/min. Analytical HPLC was monitored by UV absorbance at 220 nm.

Preparative HPLC

Purification was carried out on an Agilent 1260 Infinity using a Supelcosil ABZ+PLUS column (250 mm × 21.2 mm, 5 µm), eluting with a linear gradient system with mobile phases (A) 0.1% TFA in water (v/v) and (B) 0.05% TFA in MeCN (v/v) over 20 min at a flow rate of 20 mL/min

Mass directed HPLC

Analysis was carried out on a Waters Mass Directed Autopurification System with an ESI Multi-Mode Ionisation Waters SQ Detector 2 spectrometer and XSelect® CSH column (C18, 5 µm, 19 x 150 mm) eluting with a linear gradient 5–100% B (solvent A: 0.1% formic acid in water (v/v); solvent B: 0.1% formic acid in MeCN (v/v)) over 14 min at a flow rate of 1.2 mL/min. Abosrbance was detected in the range of 210–650 nm.

NMR Spectra

Proton nuclear magnetic resonance (^{1}H NMR) spectra were recorded at ambient temperature (unless otherwise stated) on a Bruker TXO Cryo Probe (700 MHz). ^{1}H NMR chemical shifts are reported in parts per million (ppm), to the nearest 0.01 ppm and are referenced to the residual non-deuterated solvent peak ($CDCl_3$: 7.260, CD_3OD: 3.310, CD_3CN: 1.940, DMSO-d_6: 2.500).[1] Coupling constants (*J*) are reported in Hertz (Hz) to the nearest 0.1 Hz. Data are reported as follows: chemical shift, multiplicity (s = singlet; d = doublet; t = triplet; q = quartet; qn = quintet; m = multiplet; br = broad; or as a combination of these), coupling constant(s), integration, and assignment. Carbon NMR (^{13}C NMR) spectra were recorded at ambient temperature on a Bruker TXO Cryo Probe (176 MHz). Chemical shifts are quoted in ppm, to the nearest 0.1 ppm, and are referenced to the residual non-deuterated solvent peak ($CDCl_3$: 77.16, CD_3OD: 49.00, CD_3CN: 1.320, 118.26, DMSO-d_6: 39.52).[1]

HRMS Analysis

Analysis was performed on a Xevo G2-S TOF mass spectrometer coupled to an Acquity UPLC system using Electrospray ionisation (ESI) techniques.

Protein LC-MS

Analysis was performed on a Xevo G2-S TOF mass spectrometer coupled to an Acquity UPLC system using an Acquity UPLC BEH300 C4 column (1.7 µm, 2.1 × 50 mm). 0.1% Formic acid (aq.) (solvent A) and 95% MeCN with 5% 0.1% formic acid (aq.) (solvent B) were used as the mobile phase at a flow rate of 0.2 mL/min. The gradient was programmed as follows: 95% A for 0.93 min, then a linear gradient to 100% B over 4.28 min, then 100% B for 1.04 minutes, then a linear gradient to 95% A over 1.04 min. The electrospray source S-5 was operated with a capillary voltage of 2.0 kV and a cone voltage of 190 V. Nitrogen was used as the desolvation gas at a total flow rate of 850 L/h. Total mass spectra were reconstructed from the ion series using the MaxEnt 1 algorithm preinstalled on MassLynx 4.2 software according to the manufacturer's instructions. Trastuzumab samples were deglycosylated with PNGase F (New England Biolabs) prior to LC-MS analysis. Only the region of each total ion chromatogram (TIC) containing protein signals was analysed.[2] All calculated values for the masses of trastuzumab conjugates are based on the observed mass ion of native trastuzumab under the same preparation and ionisation conditions (145,171 Da)

Protein Concentration

Analysis was carried out using UV-vis spectrometry on a NanoDrop One spectrophotometer. Sample buffer was used as the blank for baseline correction. Extinction coefficients from Expasy ProtParam. https://web.expasy.org/protparam/

SDS-PAGE

Analysis was carried out using freshly made plates of 12% polyacrylamide running gel with a 4% polyacrylamide stacking gel. The analytes (15 µL sample of 0.67 µM final concentration with a reducing Coomassie brilliant blue loading dye (with 2-mercaptoethanol) or non-reducing (without additives)) were denatured by heating the sample to 90 °C for 5 min immediately before loading. Each gel was run with a 10-200 kDa molecular weight marker ladder (5 µL, New England BioLabs). Gels were run at 200 V for 65 min in Laemmli running buffer (LRB). All gels were stained with Coomassie Blue dye and imaged on a Syngene gel imaging system.

1.3. DvTz synthesis (Figure S1)

Modified from literature procedures:[3,4]

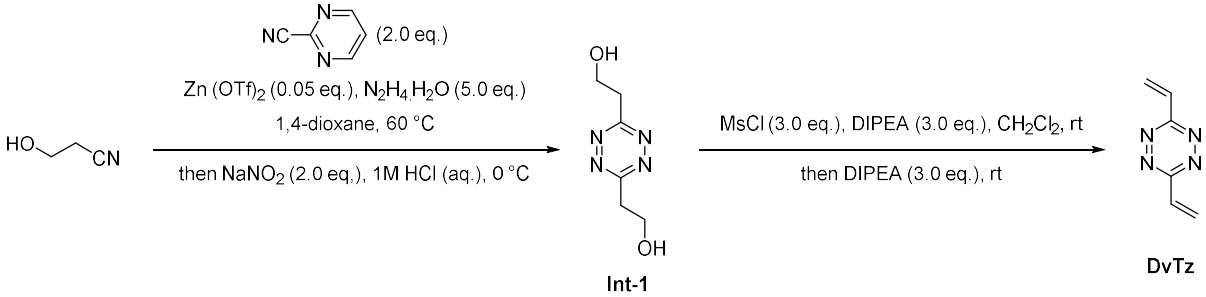

Figure S1 Two-step synthesis for 3,6-divinyl-1,2,4,5-tetrazine (DvTz)

2,2'-(1,2,4,5-tetrazine-3,6-diyl)bis(ethan-1-ol) (Int-1):

To a mixture of 3-hydroxypropionitrile (325 µL, 4.76 mmol. 1.0 eq.) and 2-pyrimidinecarbonitrile (100 mg, 0.95 mmol, 0.2 eq.) in dioxane (2 mL) were added $Zn(OTf)_2$ (86 mg, 0.24 mmol, 0.05 eq.) and hydrazine hydrate (1.16 mL, 24.8 mmol, 5.0 eq.). The mixture was stirred at 60 °C overnight. The reaction was then cooled to 0 °C and a solution of sodium nitrite (656 mg, 9.51 mmol, 2.0 equiv.) in H_2O (5 mL) was added. The mixture was acidified to pH <3 by dropwise addition of 1M aqueous HCl. The mixture was then extracted with EtOAc (6 × 100 mL). The organic layers were combined, washed with brine (200 mL), dried over Na_2SO_4 and concentrated *in vacuo*. The mixture was purified by flash column chromatography (SiO_2, 3% MeOH in EtOAc) to afford 2,2'-(1,2,4,5-tetrazine-3,6-diyl)bis(ethan-1-ol) (**Int-1**) as a pink solid (176 mg, 43%).

R_f = 0.32 (SiO_2, 3% MeOH in EtOAc).

^{1}H NMR (700 MHz, $CDCl_3$) δ/ppm 4.27 (t, *J* = 5.8 Hz, 4H), 3.59 (t, *J* = 5.8 Hz, 4H), 2.37 (s, 2H).
^{13}C NMR (176 MHz, $CDCl_3$) δ/ppm 169.0, 60.1, 37.6.
Data in accordance with literature.[3]

3,6-divinyl-1,2,4,5-tetrazine (DvTz):

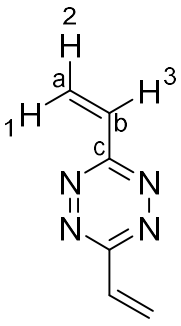

A solution of **Int-1** (82 mg, 0.48 mmol, 1 eq.) and DIPEA (252 µL, 1.45 mmol, 3.0 eq.) in CH_2Cl_2 (2 mL) was cooled to 0 °C. MsCl (252 µL, 1.45 mmol, 3.0 eq.) was added dropwise and the mixture was stirred at room temperature for 1 hour. The reaction was monitored by TLC. After the complete consumption of **Int-1**, DIPEA (252 µL, 1.45 mmol, 3.0 eq.) was added and the mixture was further stirred at room temperature for 1 hour. The reaction was then quenched by the addition of sat. aq. $NaHCO_3$ (20 mL) and the mixture was extracted with CH_2Cl_2 (4 × 40 mL). The combined organic layers were washed with brine (100 mL), dried over Na_2SO_4 and concentrated *in vacuo*. The mixture was purified by flash column chromatography (SiO_2, 20% Et_2O in 40-60 PE) to afford 3,6-divinyl-1,2,4,5-tetrazine as a pink oil (50 mg, 77%).

R_f = 0.48 (20% Et_2O in PE).

^{1}H NMR (700 MHz, DMSO-d_6) δ/ppm 7.19 (2H, dd, *J* = 17.5, 10.9 Hz, H3), 6.87 (2H, dd, *J* = 17.5, 1.1 Hz, H1), 6.12 (2H, dd, *J* = 10.9, 1.1 Hz, H2).

^{13}C NMR (176 MHz, DMSO-d_6) δ/ppm 163.1 (C_c), 130.7 (C_b), 127.5 (C_a).
The compound was stored and used as MeCN or DMSO stock solutions.

2,2'-(1,2,4,5-tetrazine-3,6-diyl)bis(ethan-1-ol) (Int-1):

^{1}H NMR (700 MHz, $CDCl_3$)

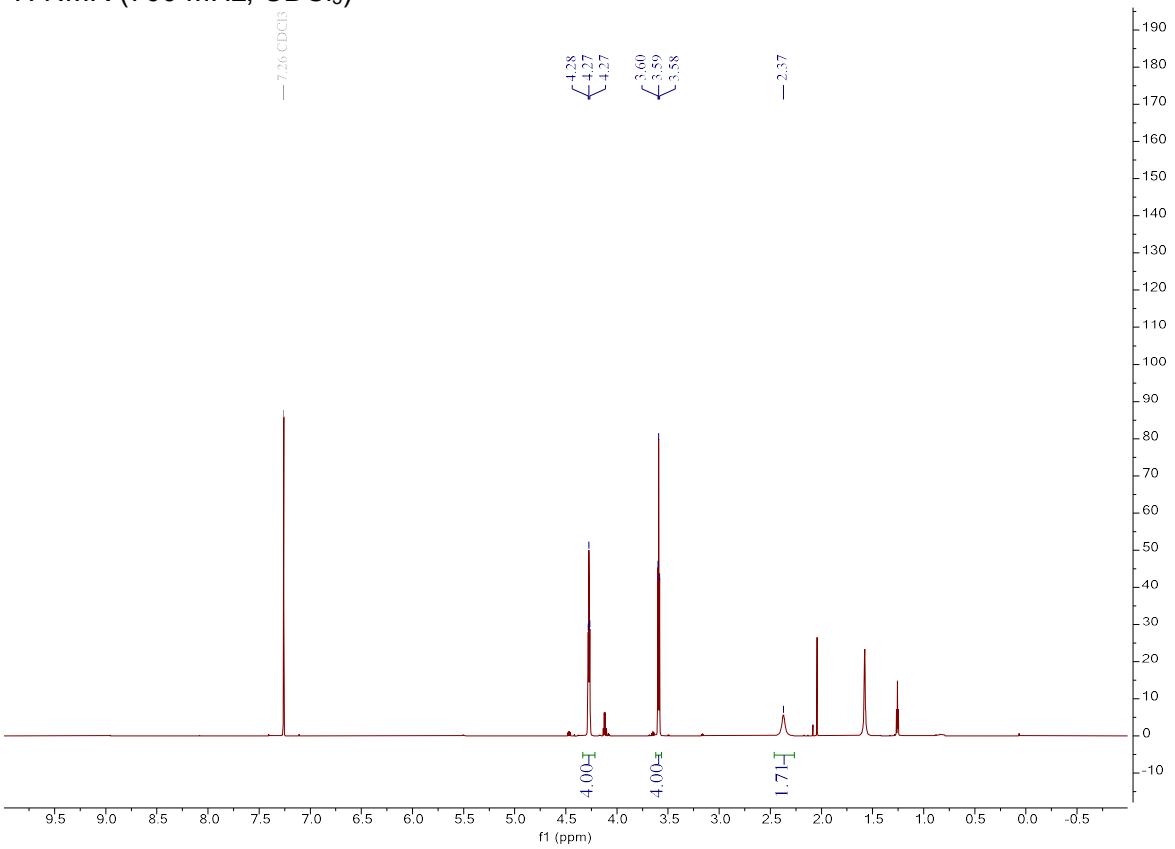

^{13}C NMR (176 MHz, $CDCl_3$)

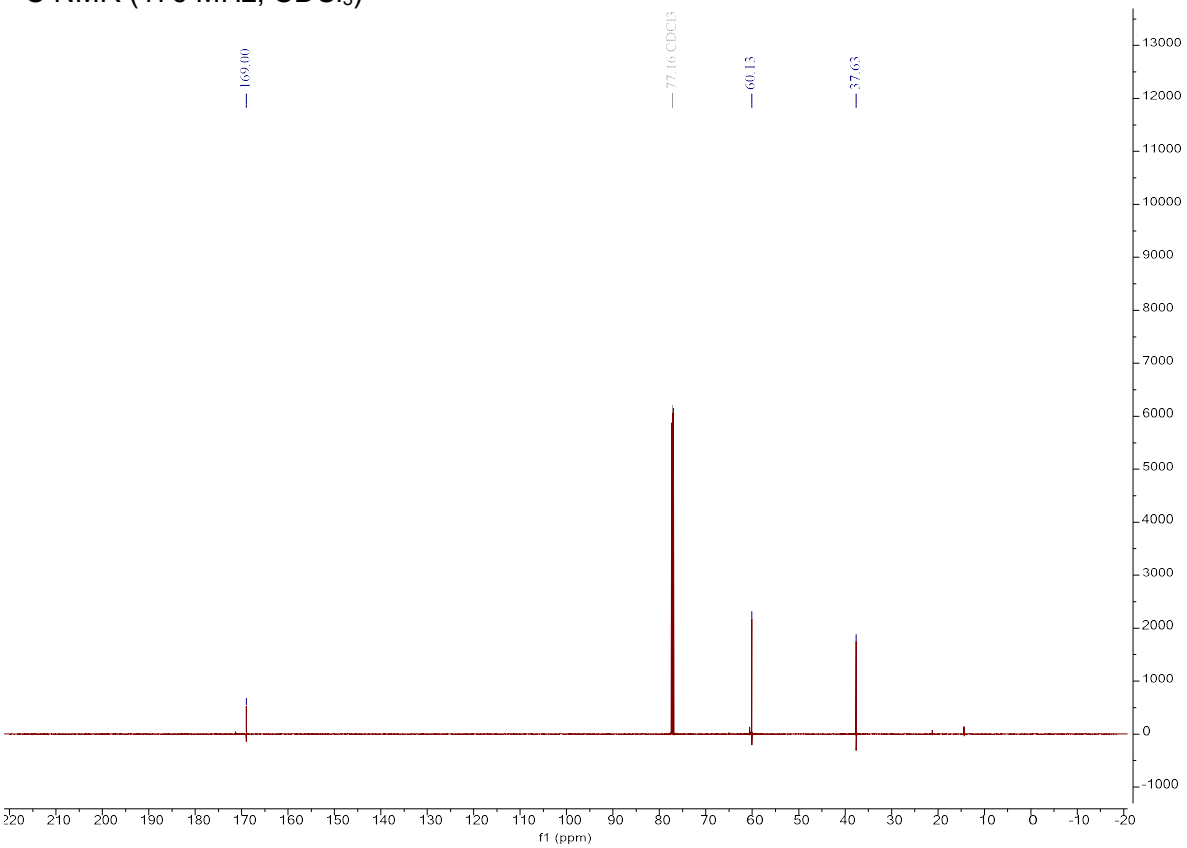

3,6-divinyl-1,2,4,5-tetrazine (DvTz):

^{1}H NMR (700 MHz, DMSO-d_6)

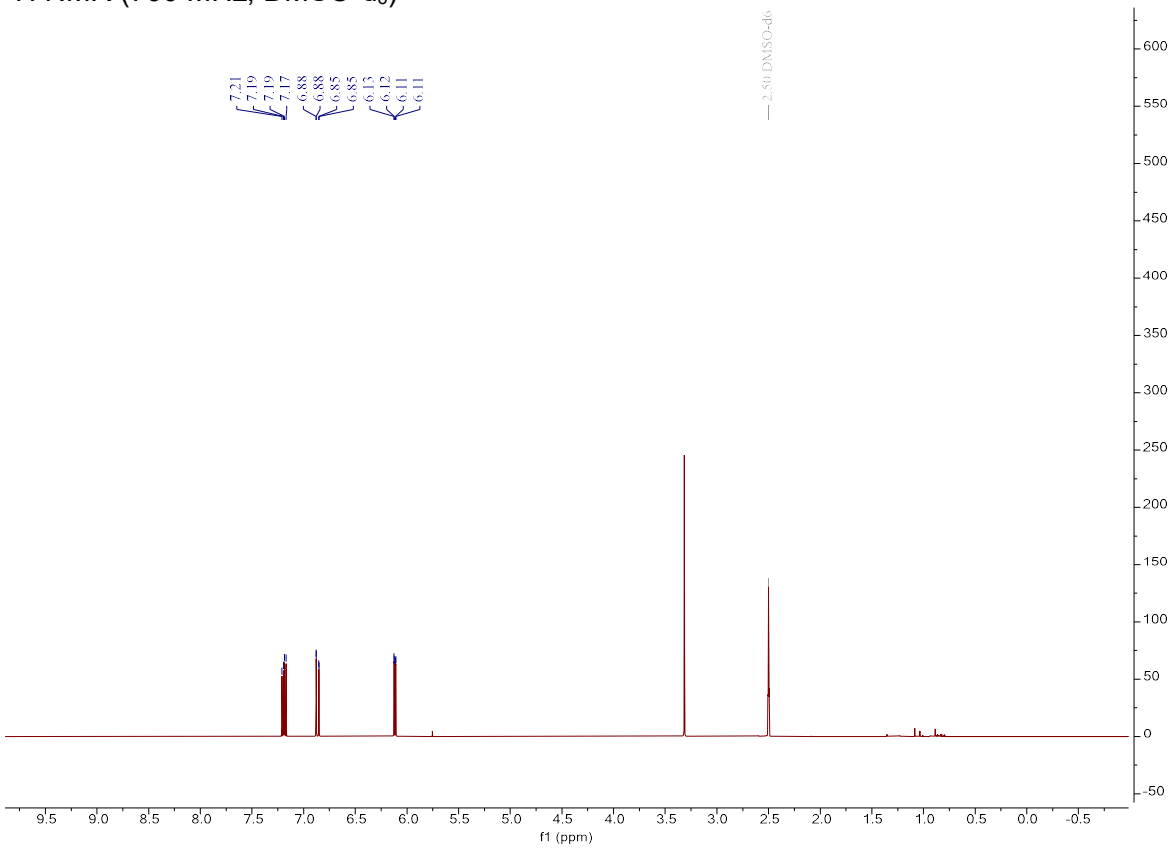

^{13}C NMR (176 MHz, DMSO-d_6)

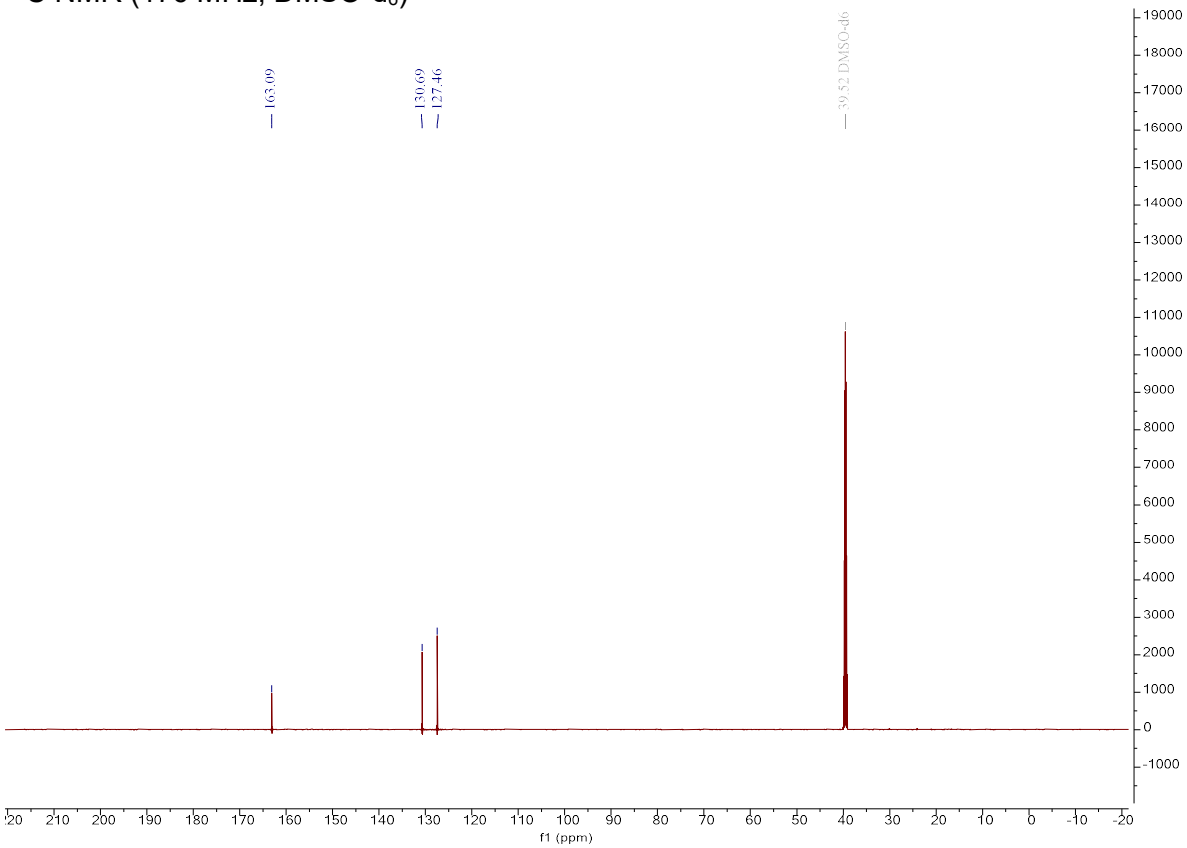

COSY NMR

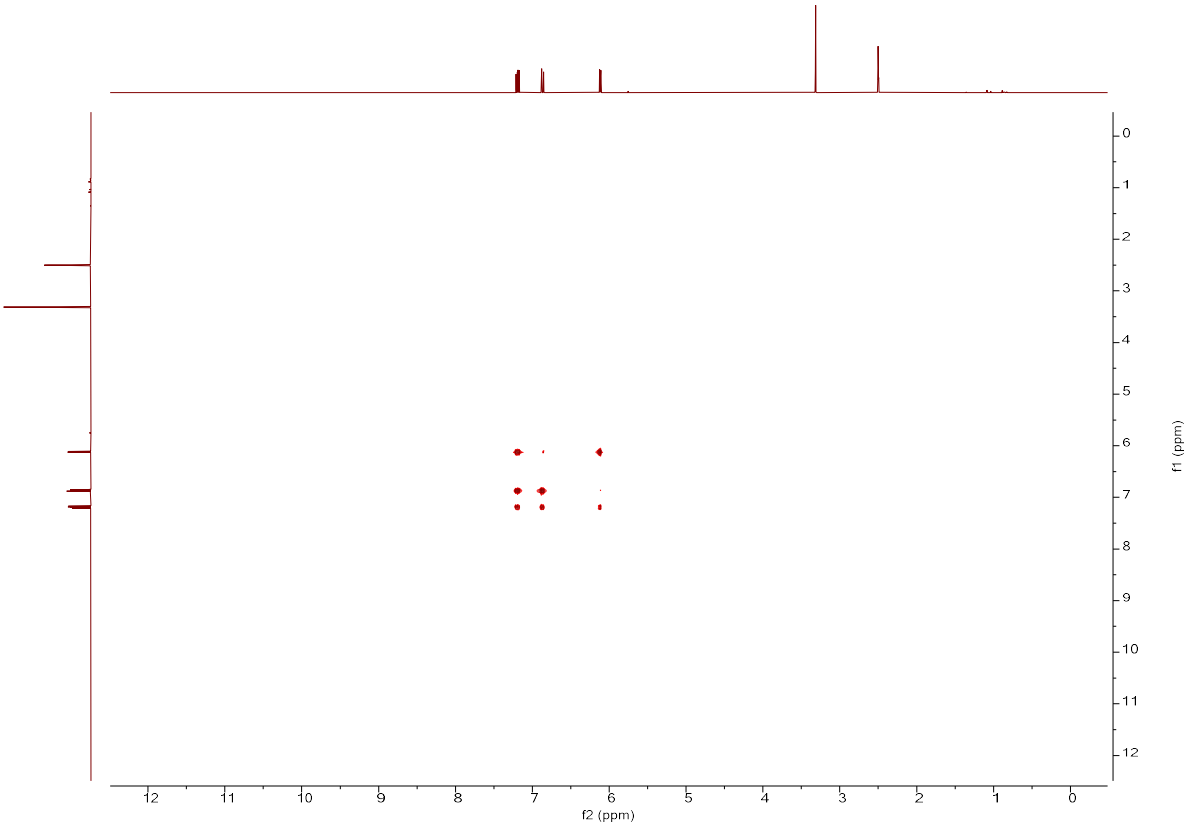

HSQC NMR

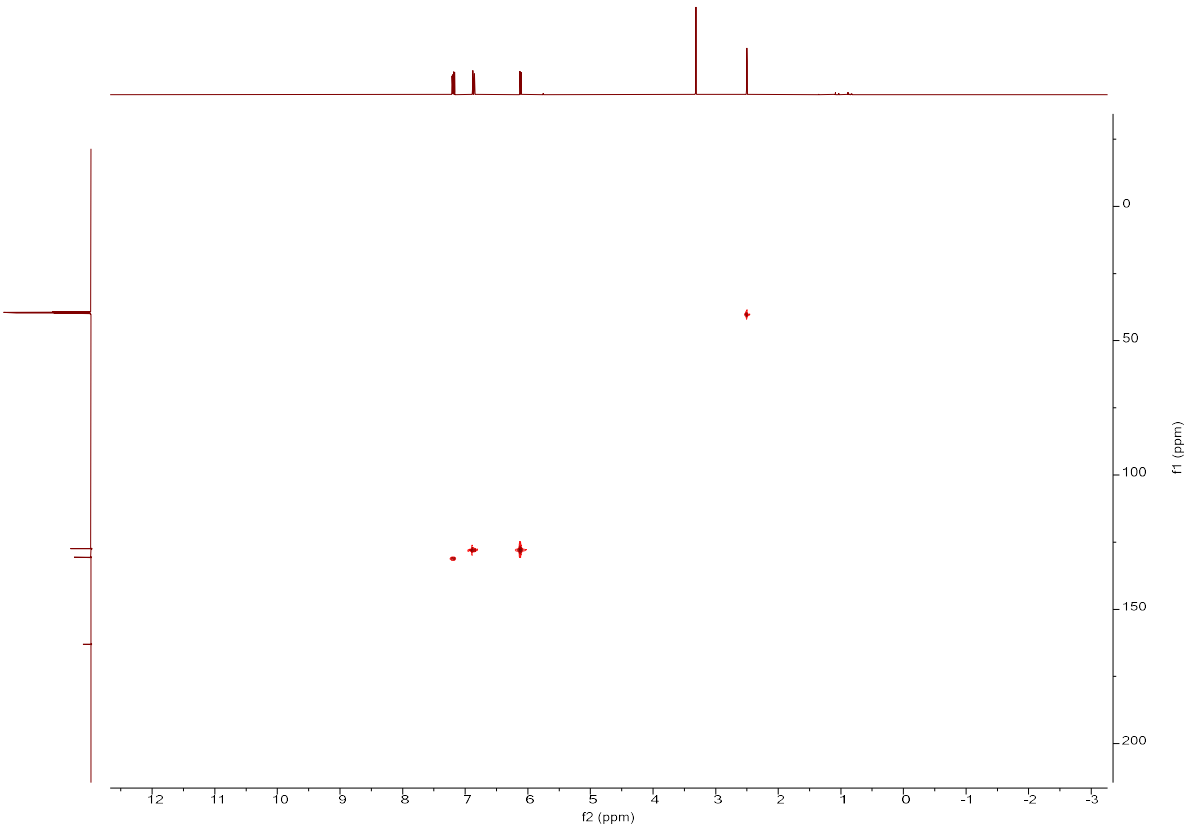

2. Peptide Stapling

2.1. General Procedure A: Manual Solid Phase Peptide Synthesis (SPPS)

All peptides were prepared following this protocol:

Setup:
12 mL Luer-lock syringe with frit (20 µm, Sigma-Aldrich) and 250 mg of Rink Amide MBHA resin HL (loading 0.753 mmol/g, Sigma-Aldrich), resin mixed with nitrogen bubbling

Preparation:
Swell the resin in DMF for 20 min
Prepare stock solutions in DMF according to the sequence (note double coupling):
a. Fmoc- and side-chain-protected amino acids: (0.2 M; use 3 mL for each step)
b. Oxyma Pure: (7.1 g in 100 mL DMF; use 1.5 mL for each step)
c. DIC: (7.5 mL in 100 mL DMF; use 2 mL for each step)

Solid Phase Peptide Synthesis: all steps under heating at 60 °C
1. Add 6 mL 20% piperidine in DMF and remove solution after 1 min using vacuum (Fmoc deprotection)
2. Add 6 mL 20% piperidine in DMF and remove solution after 4 min using vacuum (Fmoc deprotection)
3. While waiting, pre-activate amino acid by mixing 3 mL of 0.2 M amino acid solution in DMF; then 1.5 mL of Oxyma Pure solution in DMF; last 2 mL of DIC solution in DMF
4. Wash the resin with 5 × 6 mL DMF
5. Add the pre-activated amino acid solution and remove solution after 8 min using vacuum (Coupling)
6. While waiting, pre-activate amino acid by mixing 3 mL of 0.2 M amino acid solution in DMF; then 1.5 mL of Oxyma Pure solution in DMF; last 2 mL of DIC solution in DMF
7. Wash the resin with 3 × 6 mL DMF
8. Add the pre-activated amino acid solution and remove solution after 8 min using vacuum (Coupling)
9. Wash the resin with 3 × 6 mL DMF
10. Repeat until the sequence is finished

Cleavage:
1. Wash resin with methanol × 3 and dry under vacuum
2. Transfer to a new 12 mL syringe with PE frit (20 µm, Sigma-Aldrich) and PTFE tap
3. Prepare cleavage mixture: 94% TFA (5.64 mL); 2% TIPS (0.12 mL); 2% H_2O (0.12 mL); 2% DODT (0.12 mL)
4. Pour and shake at rt for 3h
5. Add an additional 30 min per Arg residue, up to a maximum of 6 h
6. Precipitate in cold diethyl ether
7. Purify using Preparative HPLC

Note:
For Arg coupling 2 × 10 min at 50 °C
For His coupling 2 × 10 min at 50 °C

Side chain protecting groups used during solid-phase peptide synthesis: *t*-Bu (Glu, Asp, Tyr, Ser, Thr); Trt (His, Asn, Cys, Gln); Boc (Lys, Trp); Pbf (Arg); All peptide sequences are displayed from *N*- to *C*- terminus

2.2. General Procedure B: Peptide Stapling

2.0 equivalents of **DvTz** were added to peptide dissolved in 30% MeCN and NaPi buffer (20 mM, pH 8.0) mixture at 0.1 mM and incubated at 37 °C on a thermal shaker at 400 rpm for 15 minutes.

2.3. Reaction Optimisation of Peptide Stapling (Table S1)

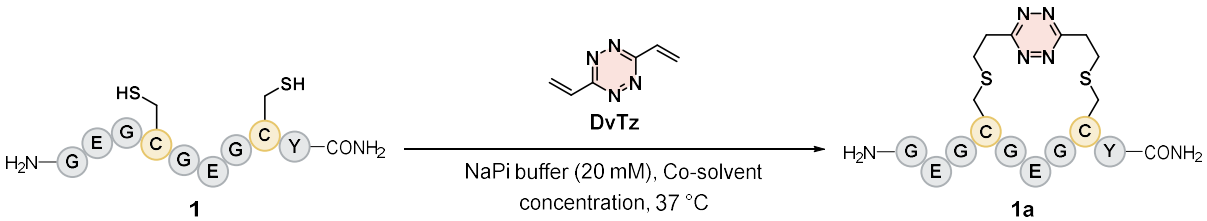

1 **1a**

Entry	Co-solvent (v/v)	NaPi Buffer pH	Conc. (mM)	DvTz eq.	Time (min)	Yield (%)*
1	30% MeCN	8.0	5	1.2	240	44
2	30% MeCN	8.0	2	1.2	240	52
3	30% MeCN	8.0	1	1.2	240	55
4	30% MeCN	8.0	0.5	1.2	240	60
5	30% MeCN	8.0	0.2	1.2	240	63
6	30% MeCN	8.0	0.1	1.2	240	64
7	30% MeCN	8.0	0.05	1.2	240	63
8	30% MeCN	8.0	0.1	1	240	48
9	30% MeCN	8.0	0.1	1.1	240	53
10	30% MeCN	8.0	0.1	1.2	240	60
11	30% MeCN	8.0	0.1	1.5	240	82
12	30% MeCN	8.0	0.1	2	240	91
13	30% MeCN	8.0	0.1	2.2	240	88
14	30% MeCN	8.0	0.1	2.5	240	84
15	30% MeCN	8.0	0.1	3	240	82
16	10% MeCN	8.0	0.1	2	240	88
17	30% MeCN	8.0	0.1	2	240	90
18	50% MeCN	8.0	0.1	2	240	92
19	70% MeCN	8.0	0.1	2	240	92
20	1% DMSO	8.0	0.1	2	240	89
21	5% DMSO	8.0	0.1	2	240	88
22	10% DMSO	8.0	0.1	2	240	87
23	15% DMSO	8.0	0.1	2	240	85
24	20% DMSO	8.0	0.1	2	240	86
25	30% DMSO	8.0	0.1	2	240	83
26	30% MeCN	6.5	0.1	2	240	86
27	30% MeCN	7.0	0.1	2	240	90
28	30% MeCN	7.4	0.1	2	240	90
29	30% MeCN	7.8	0.1	2	240	91
30	5% DMSO	6.5	0.1	2	240	81
31	5% DMSO	7.0	0.1	2	240	86
32	5% DMSO	7.4	0.1	2	240	90

Continued

Entry	Co-solvent	NaPi Buffer pH	Conc. (mM)	DvTz eq.	Time (min)	Yield (%)*
33	5% DMSO	7.8	0.1	2	240	90
34	30% EtOH	8.0	0.1	2	240	88
35	30% ^{i}PrOH	8.0	0.1	2	240	89
36	10% DMF	8.0	0.1	2	240	65
37	30% MeCN	8.0	0.1	2.0	15	93 (89[a], 75[b])
38	30% MeCN	8.0	0.1	2.0	30	93
39	30% MeCN	8.0	0.1	2.0	60	93

Table S1. Reaction conditions for the optimisation of peptide stapling. Peptide **1** was dissolved in NaPi buffer and the corresponding co-solvent at the indicated concentration, followed by the addition of **DvTz** at the specified equivalents and incubated at 37 °C with a thermal shaker at 400 rpm; *LC-estimated yields based on the UV absorption of peptides in HPLC-UV analysis (220 nm) of reaction mixtures; [a]Yield determined using aspirin as internal standard with calibration curve established; [b]Isolated yield;

Selected HPLC-UV absorption trace (220 nm)

Analytical HPLC: C18 column eluting with a linear gradient system 5–95% MeCN/H_2O with constant 0.05% TFA

Peptide **1**:

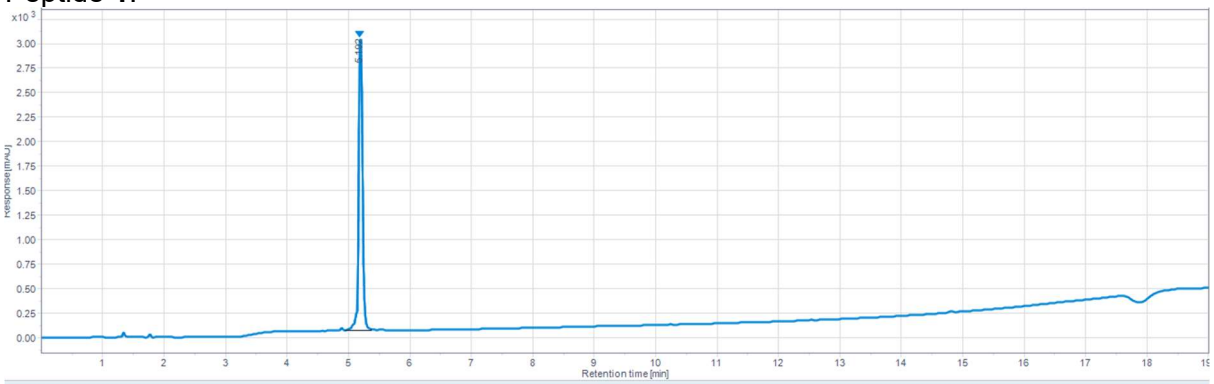

Injection Results

Peaks | Summary

Name	Signal description	RT (min)	Area (mAU·s)	Area%	Height (mAU)	Height%	Amount	Concentration	Start time (min)	End time (min)
1	DAD1A,Sig=220,4 Ref=360,100	5.192	13477.739	100.000	2971.301	100.00			4.949	5.379

Product **1a**:

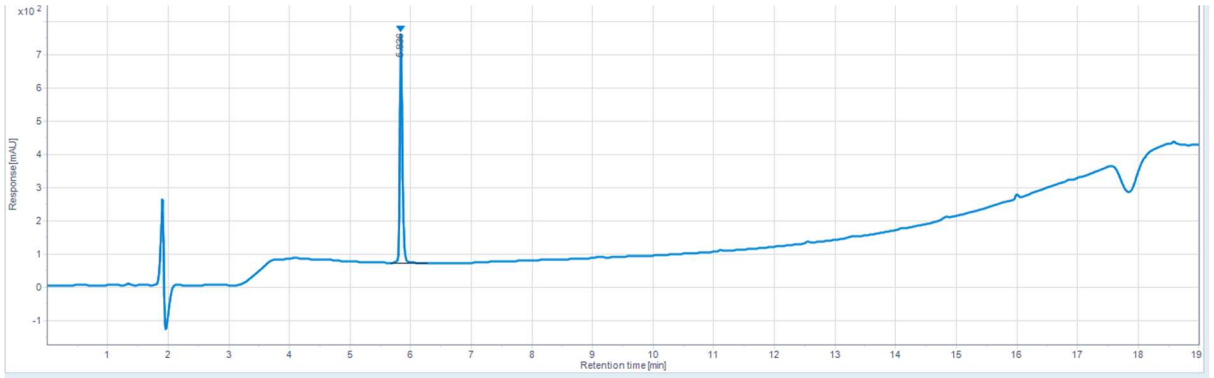

Injection Results

Peaks | Summary

#	Name	Signal description	RT (min)	Area (mAU·s)	Area%	Height (mAU)	Height%	Amount	Concentration	Start time (min)	End time (min)
1		DAD1A,Sig=220,4 Ref=360,100	5.836	1994.862	100.000	692.311	100.00			5.680	6.28

DvTz:

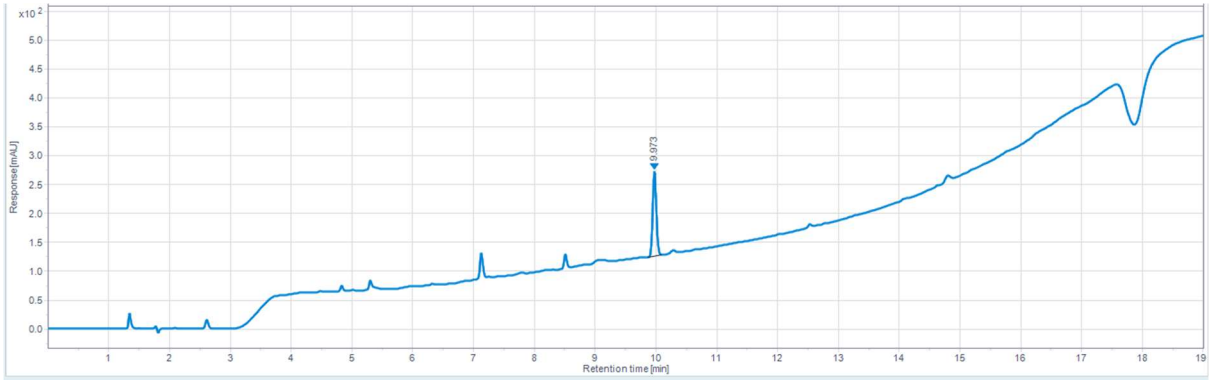

Injection Results

Peaks | Summary

	Name	Signal description	RT (min)	Area (mAU·s)	Area%	Height (mAU)	Height%	Amount	Concentration	Start time (min)	End time (min)
1		DAD1A,Sig=220,4 Ref=360,100	9.973	596.200	100.000	146.519	100.00			9.876	10.091

Table S1 Entry 3:

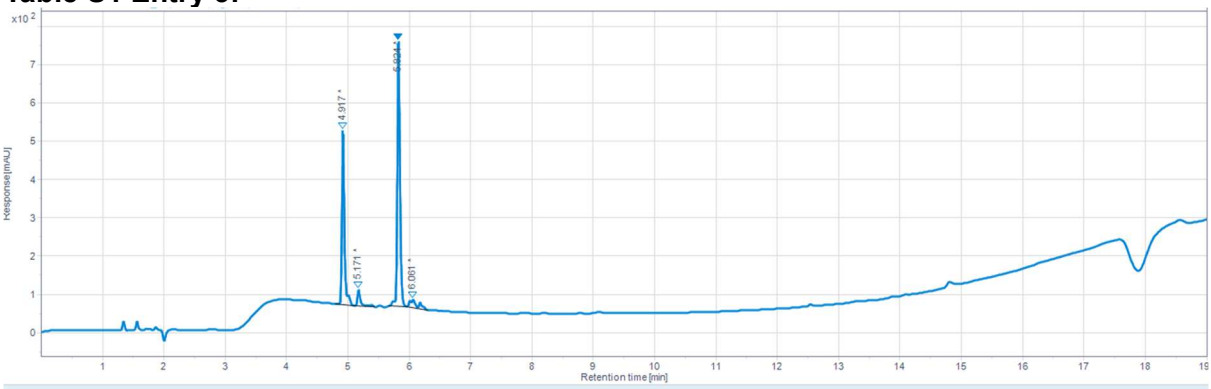

Injection Results

Peaks | Summary

	Name	Signal description	RT (min)	Area (mAU·s)	Area%	Height (mAU)	Height%	Amount	Concentration	Start time (min)	End time (min)
1		DAD1A,Sig=220,4 Ref=360,100	4.917	1252.260	35.134	455.303	37.46			4.805	5.106
2		DAD1A,Sig=220,4 Ref=360,100	5.171	158.388	4.444	43.202	3.55			5.106	5.442
3		DAD1A,Sig=220,4 Ref=360,100	5.824	1966.048	55.161	693.943	57.10			5.676	5.965
4		DAD1A,Sig=220,4 Ref=360,100	6.061	187.529	5.261	22.956	1.89			5.965	6.312

Table S1 Entry 37:

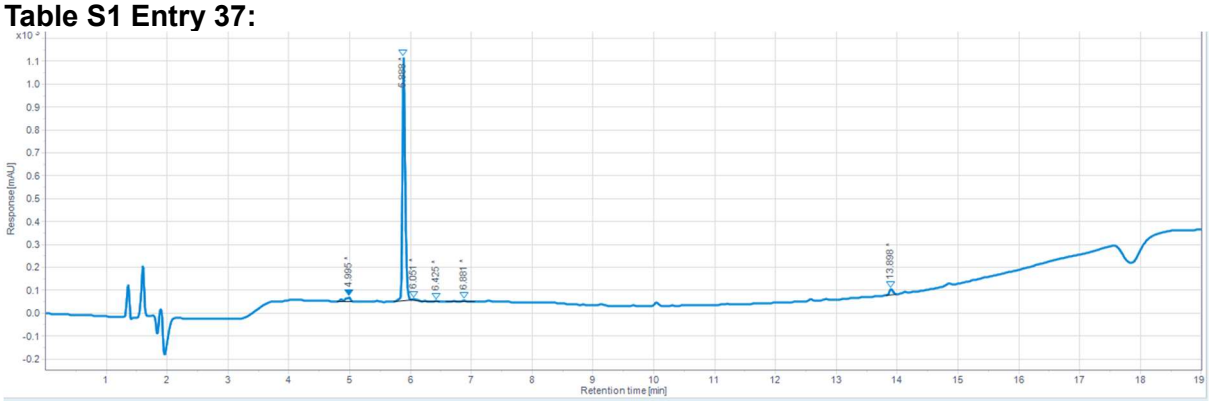

Injection Results

Peaks | Summary

	#	Name	Signal description	RT (min)	Area (mAU·s)	Area%	Height (mAU)	Height%	Amount	Concentration	Start time (min)	End time (min)
1			DAD1A,Sig=220,4 Ref=360,100	4.995	130.245	3.592	18.275	1.61			4.806	5.05
2			DAD1A,Sig=220,4 Ref=360,100	5.888	3289.498	90.730	1065.829	94.14			5.728	6.02
3			DAD1A,Sig=220,4 Ref=360,100	6.051	33.839	0.933	7.978	0.70			6.022	6.20
4			DAD1A,Sig=220,4 Ref=360,100	6.425	20.224	0.558	5.973	0.53			6.200	6.49
5			DAD1A,Sig=220,4 Ref=360,100	6.881	46.136	1.272	6.953	0.61			6.595	7.06
6			DAD1A,Sig=220,4 Ref=360,100	13.898	105.657	2.914	27.203	2.40			13.824	13.99

2.4. Calibration Curve for Peptide Stapling (Figure S2)

Samples containing different concentrations of product **1a** and aspirin in 30% MeCN and NaPi buffer (20 mM, pH 8.0) with total volume of 200 µL were prepared following the table below:

Sample	1	2	3	4	5
Product **1a** concentration (mM)	0.1	0.1	0.1	0.1	0.1
Aspirin concentration (mM)	0.05	0.1	0.2	0.4	0.6
Total volume (µL)	200	200	200	200	200

These samples were analysed using analytical HPLC with a linear gradient system 5–95% MeCN/H_2O with constant 0.05% TFA. The injection volume was fixed at 10 µL. The corresponding absorption peaks at 220 nm were integrated (aspirin peak retention time: 8.00–8.20; **1a** peak retention time 5.65–6.04). The results are summarised below:

Sample	1	2	3	4	5
Concentration ratio (**1a** / aspirin)	2	1	0.5	0.25	0.16667
Absorption peak area ratio (**1a** / aspirin)	3.223	1.573	0.788	0.421	0.317
ε ratio (**1a** / aspirin)	1.593				

Since

$$\frac{Absorption\ peak\ area\ (\mathbf{1a})}{Absorption\ peak\ area\ (Aspirin)} = \frac{\varepsilon\ (\mathbf{1a})}{\varepsilon\ (Aspirin)} \times \frac{Conc.\ (\mathbf{1a})}{Conc.\ (Aspirin)}$$

A calibration curve was established:

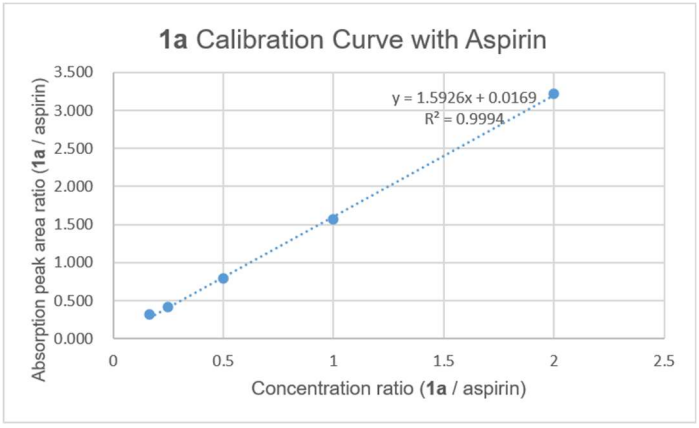

Figure S2. Calibration curve for **1a** using aspirin as an internal standard

Stapling reaction of peptide **1** was conducted following General Procedure A. This step was followed by the addition of 5 µL of 4.1 mM aspirin stock solution in 30% MeCN and NaPi buffer (20 mM, pH 8.0) (giving a final aspirin concentration of 0.1 mM in the reaction mixture). This sample was analysed using analytical HPLC under the conditions described above.

Therefore, the yield of **1a** was then determined based on the corresponding absorption peaks integration at 220 nm were (Aspirin peak retention time: 8.00–8.20; **1a** peak retention time 5.65–6.04). The results are summarised below:

Reaction with internal standard	
Absorption peak area (aspirin) (mAU.s)	2442.847
Absorption peak area (**1a**)(mAU.s)	3448.214
Absorption peak area ratio (**1a** / aspirin)	1.412
Concentration ratio (**1a** / aspirin)	0.886
Aspirin concentration (mM)	0.100
1a concentration (mM)	0.089
Expected **1a** concentration (mM)	0.1
Yield	**89%**

HPLC-UV absorption Trace (220 nm)
Analytical HPLC: C18 column eluting with a linear gradient system 5–95% MeCN/H_2O with constant 0.05% TFA

Aspirin:

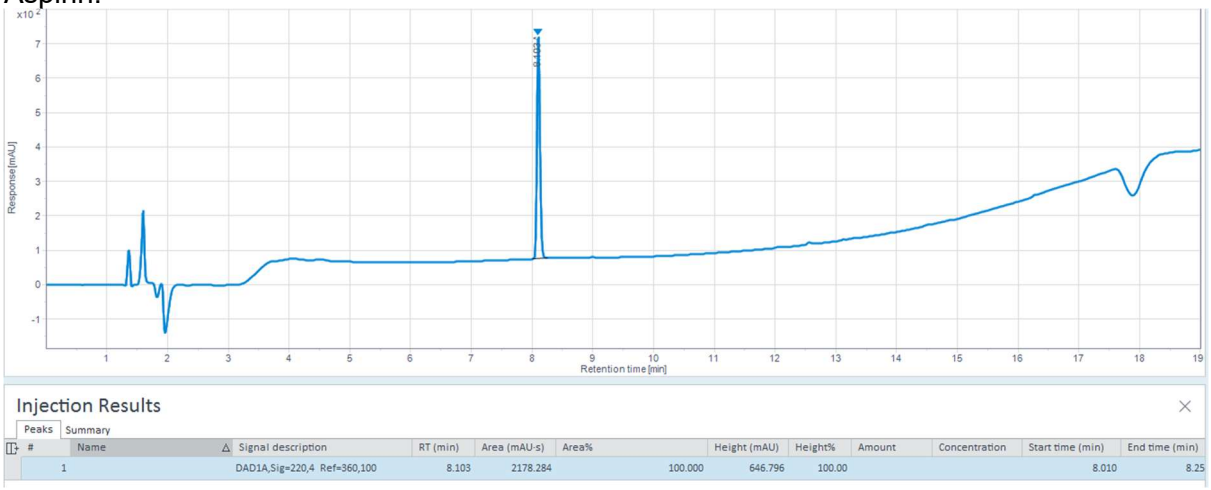

Injection Results

Peaks | Summary

#	Name	Signal description	RT (min)	Area (mAU·s)	Area%	Height (mAU)	Height%	Amount	Concentration	Start time (min)	End time (min)
1		DAD1A,Sig=220,4 Ref=360,100	8.103	2178.284	100.000	646.796	100.00			8.010	8.25

1a:

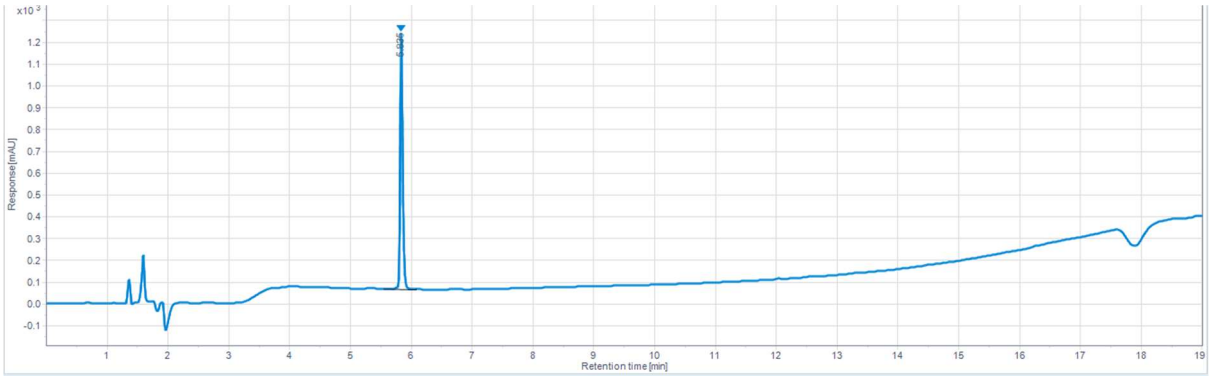

Injection Results

Peaks | Summary

#	Name	Signal description	RT (min)	Area (mAU·s)	Area%	Height (mAU)	Height%	Amount	Concentration	Start time (min)	End time (min)
1		DAD1A,Sig=220,4 Ref=360,100	5.835	3357.370	100.000	1178.540	100.00			5.552	6.08

Reaction of **1** and **DvTz** with aspirin as internal standard:

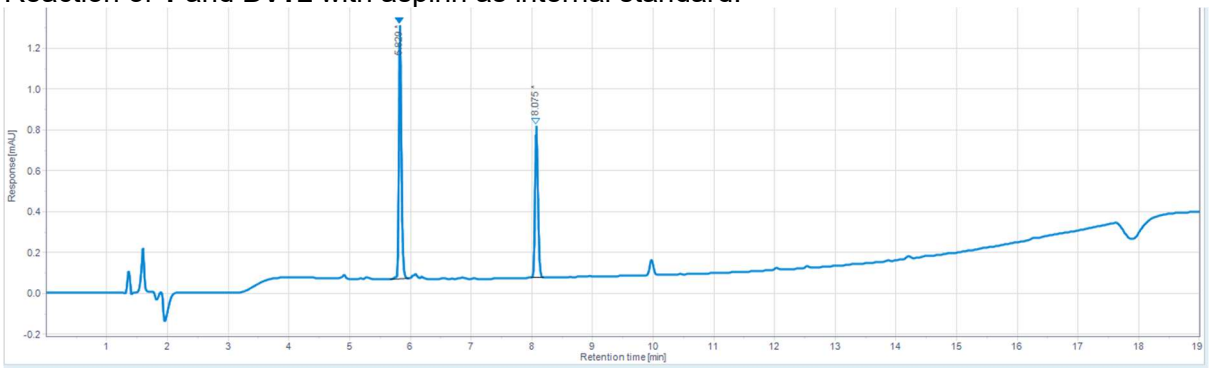

Injection Results

Peaks | Summary

#	Name	Signal description	RT (min)	Area (mAU·s)	Area%	Height (mAU)	Height%	Amount	Concentration	Start time (min)	End time (min)
1		DAD1A,Sig=220,4 Ref=360,100	5.829	3448.214	58.533	1244.439	62.52			5.669	5.98
2		DAD1A,Sig=220,4 Ref=360,100	8.075	2442.847	41.467	746.144	37.48			8.000	8.19

2.5. Isolated Yield of 1a

Peptide **1** (6.4 mg) was dissolved in 64.9 mL of 30% MeCN and NaPi buffer (20 mM, pH 8.0) mixture, followed by the addition of 2.0 eq. **DvTz**. The mixture was stirred at 37 °C for 15 min. Then the reaction mixture was lyophilised and the crude product was purified by preparative HPLC and lyophilised to obtain 5.44 mg of **1a** (75 %).

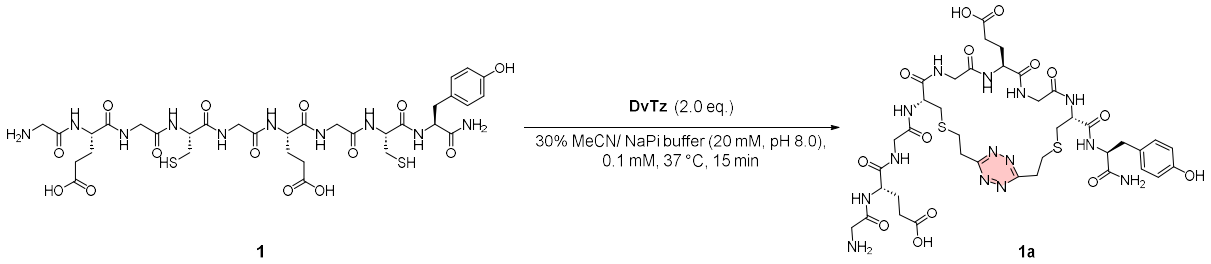

1 1a

1 was obtained following General Procedure A and was purified using preparative HPLC.

Analytical HPLC R_t = 5.19 min (5–95% B over 15 min)

HRMS calcd. for $C_{33}H_{48}N_{10}O_{14}S_2$ *m/z* 873.2866 $[M+H]^+$, found 873.2825

1a

Analytical HPLC R_t = 5.84 min (5–95% B over 15 min); 7.10 min (5–60% B over 15 min); 8.76 min (5–40% B over 15 min); 7.94 min (10–30% B over 15 min)

HRMS calcd. for $C_{39}H_{54}N_{14}O_{14}S_2$ *m/z* 1007.3459 $[M+H]^+$, found 1007.3478

2.6. Peptide Stapling Scope

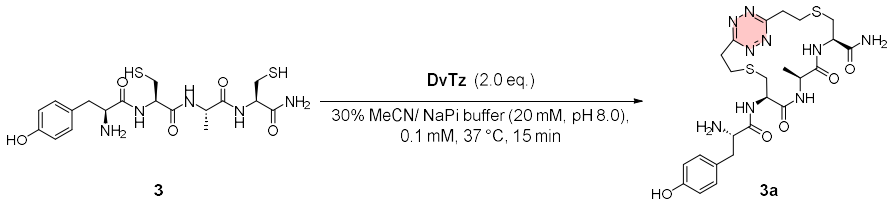

3 3a

3 was obtained following General Procedure A and was purified using preparative HPLC.

Analytical HPLC R_t = 5.57 min (1–99% B over 15 min); 5.01 min (5–95% B over 15 min); 5.60 min (5–60% B over 15 min); 6.29 min (5–40% B over 15 min); 7.87 min (5–20% B over 15 min)

HRMS calcd. for $C_{18}H_{27}N_5O_5S_2$ *m/z* 458.1527 $[M+H]^+$, found 458.1501

3a was obtained following General Procedure B. 73% yield was estimated based on the UV absorption of peptides in HPLC-UV analysis (220 nm) of the reaction mixture

LCMS R_t = 1.24 min (5–95% B over 3 min with constant 5% C over 1 min)

LRMS calcd. for $C_{24}H_{33}N_9O_5S_2$ m/z 592.2 $[M+H]^+$, found 592.3

Analytical HPLC R_t = 6.36 min (1–99% B over 15 min)

HRMS calcd. for $C_{24}H_{33}N_9O_5S_2$ *m/z* 592.2119 $[M+H]^+$, found 592.2117

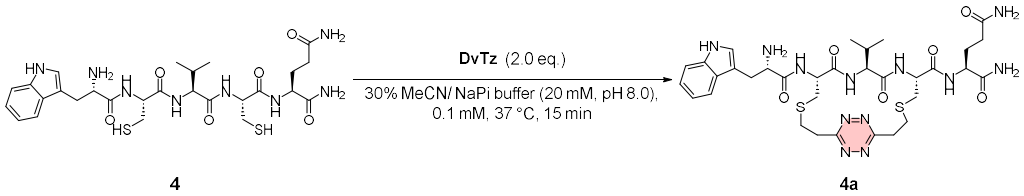

4 4a

4 was obtained following General Procedure A and was purified using preparative HPLC.

Analytical HPLC R_t = 7.13 min (1–99% B over 15 min); 6.75 min (5–95% B over 15 min); 8.47 min (5–60% B over 15 min); 10.47 min (5–40% B over 15 min);

HRMS calcd. for $C_{27}H_{40}N_8O_6S_2$ *m/z* 637.2585 $[M+H]^+$, found 637.2621

4a was obtained following General Procedure B. 81% yield was estimated based on the UV absorption of peptides in HPLC-UV analysis (220 nm) of the reaction mixture

LCMS R_t = 1.39 min (5–95% B over 3 min with constant 5% C over 1 min)

LRMS calcd. for $C_{33}H_{46}N_{12}O_6S_2$ m/z 771.3 $[M+H]^+$, found 771.6

Analytical HPLC R_t = 7.36 min (1–99% B over 15 min)

HRMS calcd. for $C_{33}H_{46}N_{12}O_6S_2$ *m/z* 771.3178 $[M+H]^+$, found 771.3179

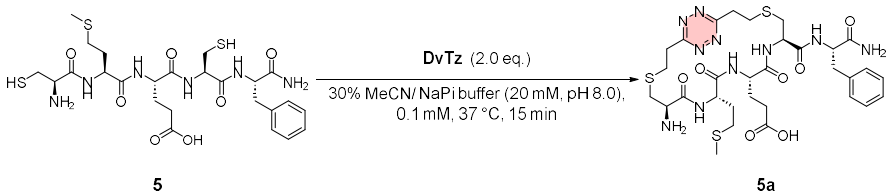

5 5a

5 was obtained following General Procedure A and was purified using preparative HPLC.

Analytical HPLC R_t = 6.72 min (5–95% B over 15 min)

HRMS calcd. for $C_{25}H_{38}N_6O_7S_3$ *m/z* 631.2037 $[M+H]^+$, found 631.2015

5a was obtained following General Procedure B. 67% yield was estimated based on the UV absorption of peptides in HPLC-UV analysis (220 nm) of the reaction mixture

LCMS R_t = 1.38 min (5–95% B over 3 min with constant 5% C over 1 min)

LRMS calcd. for $C_{31}H_{44}N_{10}O_7S_3$ m/z 765.3 $[M+H]^+$, found 765.5

Analytical HPLC R_t = 7.46 min (5–95% B over 15 min)

HRMS calcd. for $C_{31}H_{44}N_{10}O_7S_3$ *m/z* 765.2630 $[M+H]^+$, found 765.2628

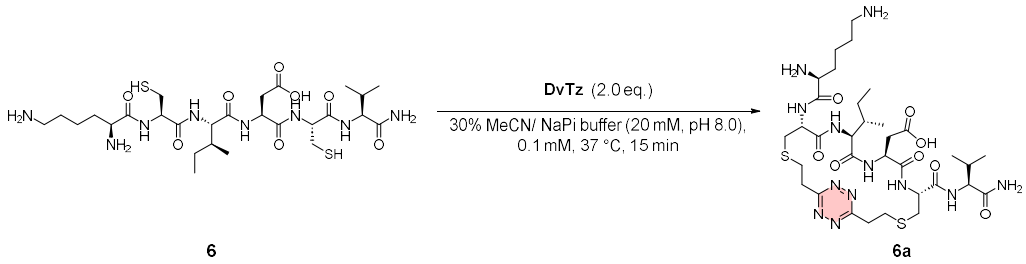

6 **6a**

6 was obtained following General Procedure A and was purified using preparative HPLC.

Analytical HPLC R_t = 6.32 min (1–99% B over 15 min); 5.85 min (5–95% B over 15 min); 8.73 min (5–40% B over 15 min); 13.53 min (5–20% B over 15 min);

HRMS calcd. for $C_{27}H_{50}N_8O_8S_2$ *m/z* 679.3266 $[M+H]^+$, found 679.3229

6a was obtained following General Procedure B. 71% yield was estimated based on the UV absorption of peptides in HPLC-UV analysis (220 nm) of the reaction mixture

LCMS R_t = 1.25 min (5–95% B over 3 min with constant 5% C over 1 min)

LRMS calcd. for $C_{33}H_{56}N_{12}O_8S_2$ m/z 813.4 $[M+H]^+$, found 813.7

Analytical HPLC R_t = 6.71 min (1–99% B over 15 min)

HRMS calcd. for $C_{33}H_{56}N_{12}O_8S_2$ *m/z* 813.3859 $[M+H]^+$, found 813.3803

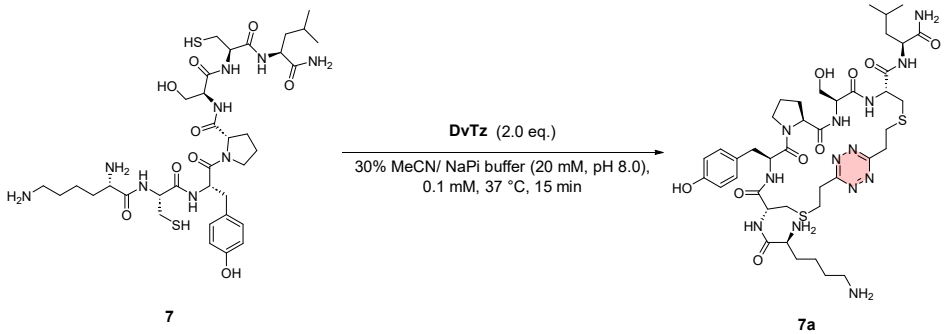

7 **7a**

7 was obtained following General Procedure A and was purified using preparative HPLC.

Analytical HPLC R_t = 6.38 min (5–95% B over 15 min); 8.01 min (5–60% B over 15 min); 10.15 min (5–40% B over 15 min);

HRMS calcd. for $C_{35}H_{57}N_9O_9S_2$ *m/z* 812.3794 $[M+H]^+$, found 812.3772

7a was obtained following General Procedure B. 83% yield was estimated based on the UV absorption of peptides in HPLC-UV analysis (220 nm) of the reaction mixture

LCMS R_t = 1.30 min (5–95% B over 5 min with constant 5% C over 1 min)

LRMS calcd. for $C_{41}H_{63}N_{13}O_9S_2$ m/z 946.4 $[M+H]^+$, found 946.6

Analytical HPLC R_t = 6.71 min (5–95% B over 15 min)

HRMS calcd. for $C_{41}H_{63}N_{13}O_9S_2$ *m/z* 946.4386 $[M+H]^+$, found 946.4434

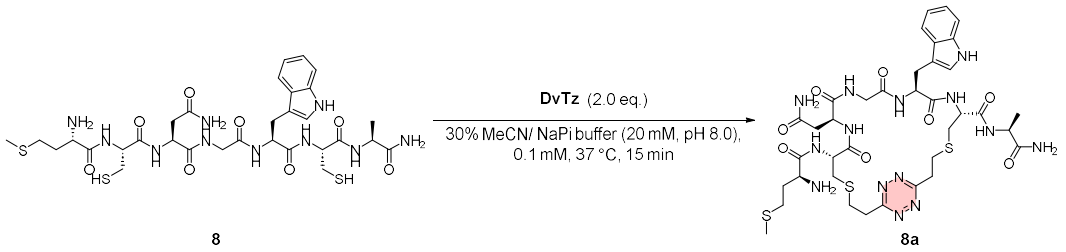

8 8a

8 was obtained following General Procedure A and was purified using preparative HPLC.

Analytical HPLC R_t = 6.75 min (5–95% B over 15 min); 8.49 min (5–60% B over 15 min); 10.79 min (5–40% B over 15 min);

HRMS calcd. for $C_{31}H_{46}N_{10}O_8S_3$ *m/z* 783.2735 $[M+H]^+$, found 783.2709

8a was obtained following General Procedure B. 81% yield estimated based on the UV absorption of peptides in HPLC-UV analysis (220 nm) of the reaction mixture

LCMS R_t = 1.28 min (5–95% B over 3 min with constant 5% C over 1 min)

LRMS calcd. for $C_{37}H_{52}N_{14}O_8S_3$ m/z 917.3 $[M+H]^+$, found 917.7

Analytical HPLC R_t = 7.07 min (5–95% B over 15 min)

HRMS calcd. for $C_{37}H_{52}N_{14}O_8S_3$ *m/z* 917.3328 $[M+H]^+$, found 917.3339

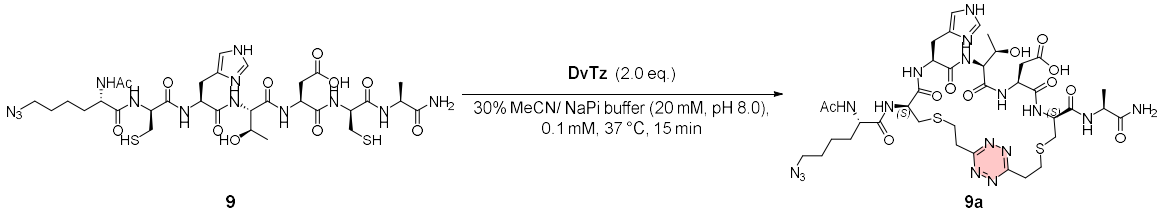

9 9a

9 was obtained following General Procedure A and was purified using preparative HPLC.

Analytical HPLC R_t = 6.95 min (5–95% B over 15 min); 8.81 min (5–60% B over 15 min); 11.24 min (5–40% B over 15 min);

HRMS calcd. for $C_{31}H_{49}N_{13}O_{10}S_2$ *m/z* 844.3189 $[M+H]^+$, found 844.3190

9a was obtained following General Procedure B. 67% yield was estimated based on the UV absorption of peptides in HPLC-UV analysis (220 nm) of the reaction mixture

LCMS R_t = 1.44 min (5–95% B over 5 min with constant 5% C over 1 min)

LRMS calcd. for $C_{37}H_{55}N_{17}O_{11}S_2$ m/z 978.4 $[M+H]^+$, found 978.5

Analytical HPLC R_t = 7.58 min (5–95% B over 15 min)

HRMS calcd. for $C_{37}H_{55}N_{17}O_{11}S_2$ *m/z* 978.3782 $[M+H]^+$, found 978.3734

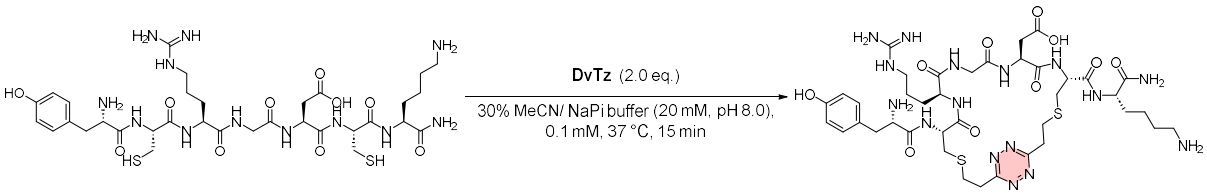

10 10a

10 was obtained following General Procedure A and was purified using preparative HPLC.

Analytical HPLC R_t = 4.96 min (1–99% B over 15 min); 4.37 min (5–95% B over 15 min); 5.10 min (5–40% B over 15 min); 5.97 min (5–20% B over 15 min);

LCMS R_t = 0.32 min (5–95% B over 3 min with constant 5% C over 1 min)

LRMS calcd. for $C_{33}H_{54}N_{12}O_{10}S_2$ m/z 422.2 $[M+2H]^{2+}$, found 422.4

10a was obtained following General Procedure B. 79% yield was estimated based on the UV absorption of peptides in HPLC-UV analysis (220 nm) of the reaction mixture

LCMS R_t = 1.00 min (5–95% B over 3 min with constant 5% C over 1 min)

LRMS calcd. for $C_{39}H_{60}N_{16}O_{10}S_2$ m/z 489.2 $[M+2H]^{2+}$, found 489.5

Analytical HPLC R_t = 4.90 min (1–99% B over 15 min)

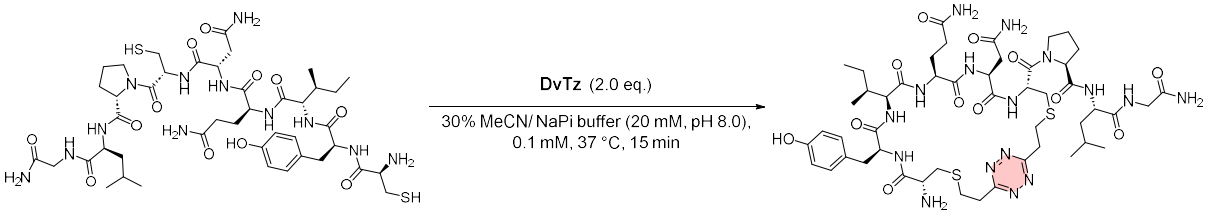

11 11a

11 was obtained following General Procedure A and was purified using preparative HPLC.

Analytical HPLC R_t = 7.01 min (5–95% B over 15 min); 8.54 min (15–40% B over 15 min);

HRMS calcd. for $C_{43}H_{68}N_{12}O_{12}S_2$ *m/z* 1009.4594 $[M+H]^+$, found 1009.4549

11a was obtained following General Procedure B. 76% yield was estimated based on the UV absorption of peptides in HPLC-UV analysis (220 nm) of the reaction mixture

LCMS R_t = 6.46 min (5–95% B over 17.5 min with constant 5% C over 1 min)

LRMS calcd. for $C_{49}H_{74}N_{16}O_{12}S_2$ m/z 1143.52 $[M+H]^+$, found 1143.66

Analytical HPLC R_t = 7.28 min (5–95% B over 15 min)

HRMS calcd. for $C_{49}H_{74}N_{16}O_{12}S_2$ m/z 1143.5187 $[M+H]^+$, found 1143.5214

3. IEDDA Functionalisation

3.1. Procedure for IEDDA functionalisation of DvTz-stapled peptide

2.0 equivalents of **2** were added to stapled peptide dissolved in a 5% DMSO and NaPi buffer (20 mM, pH 8.0) mixture at 0.1 mM and incubated at 37 °C on a thermal shaker at 400 rpm for 2 h.

3.2. IEDDA of peptide 1a (Figure S3)

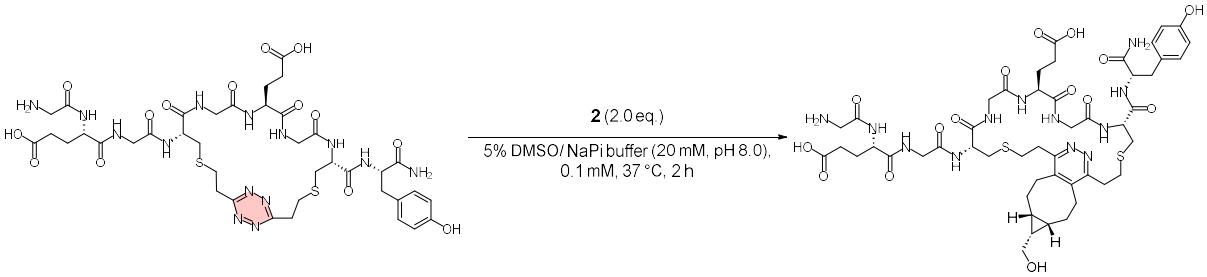

1a **1b**

Reaction after 30 min:

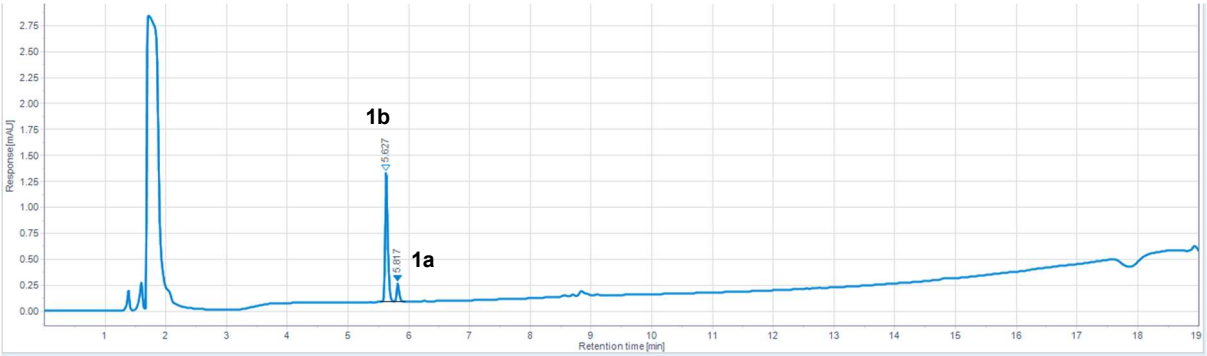

Injection Results

Peaks | Summary

#	Name	Signal description	RT (min)	Area (mAU·s)	Area%	Height (mAU)	Height%	Amount	Concentration	Start time (min)	End time (min)
1		DAD1A,Sig=220,4 Ref=360,100	5.627	3680.591	88.144	1248.767	87.38			5.534	5.76
2		DAD1A,Sig=220,4 Ref=360,100	5.817	495.049	11.856	180.412	12.62			5.761	5.94

Reaction after 2 h:

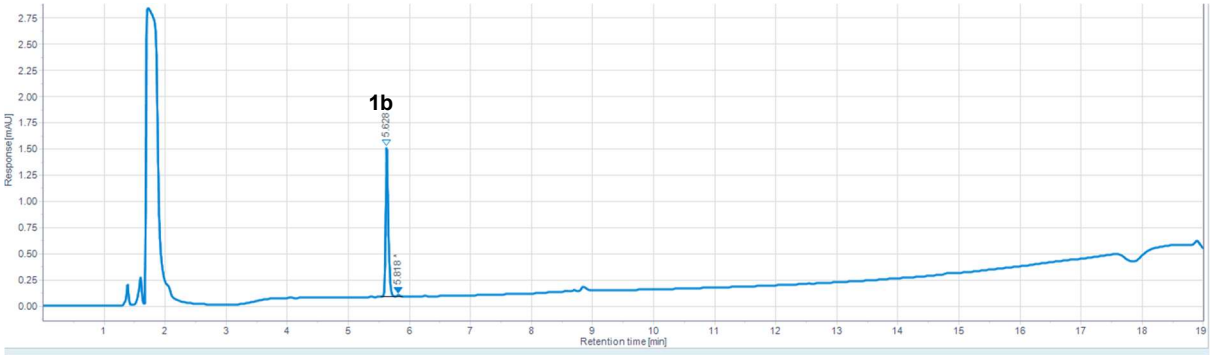

Injection Results

Peaks | Summary

#	Name	Signal description	RT (min)	Area (mAU·s)	Area%	Height (mAU)	Height%	Amount	Concentration	Start time (min)	End time (min)
1		DAD1A,Sig=220,4 Ref=360,100	5.628	4239.440	98.643	1432.056	98.58			5.541	5.77
2		DAD1A,Sig=220,4 Ref=360,100	5.818	58.319	1.357	20.618	1.42			5.771	5.89

Figure S3. HPLC-UV absorption trace (220 nm) of the IEDDA reaction of **1a** with 2.0 eq. of **2.** Analytical HPLC: C18 column eluting with a linear gradient system 5–95% MeCN/H_2O with constant 0.05% TFA Reaction reached completion after 2 hours.

3.3. *General Procedure C* :One-pot peptide stapling and functionalisation

2.0 equivalents of **DvTz** were added to peptide dissolved in a 5% DMSO and NaPi buffer (20 mM, pH 8.0) mixture at 0.1 mM and incubated at 37 °C on a thermal shaker at 400 rpm for 15 minutes. This was followed by the addition of 2.0 equivalents of **2** and incubated at 37 °C on a thermal shaker at 400 rpm for 2 hours

3.4. Characterisation of 1b

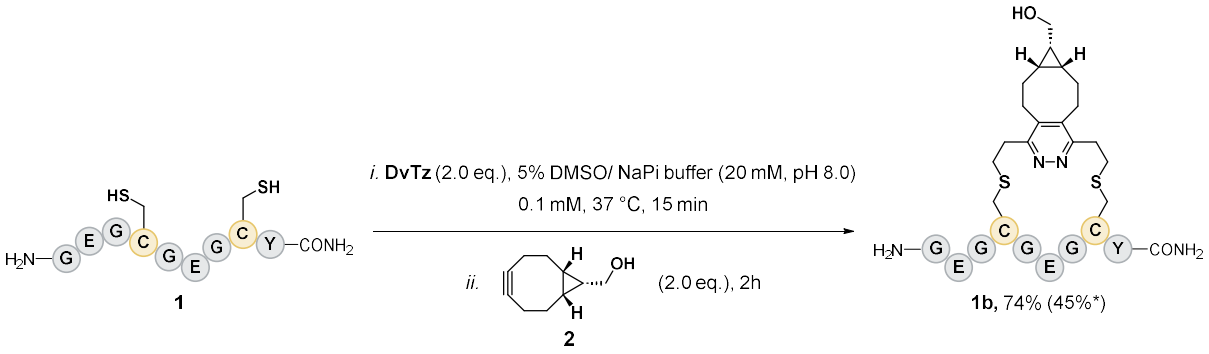

Peptide **1** (7.3 mg) was dissolved in 74 mL of 5% DMSO and NaPi buffer (20 mM, pH 8.0), followed by the addition of 2.0 eq. **DvTz**. The mixture was stirred at 37 °C for 15 minutes. Then 2.0 eq. of **2** was added and the reaction for a further 2 hours at 37 °C. The reaction mixture was lyophilised and the product was purified by preparative HPLC and lyophilised to obtain **1b** (4.1 mg, 45%).

1b

Analytical HPLC R_t = 5.65 min (5–95% B over 15 min); 6.83 min (5–60% B over 15 min); 8.41min (5–40% B over 15 min);

HRMS calcd. for $C_{49}H_{68}N_{12}O_{15}S_2$ *m/z* 1129.4442 $[M+H]^+$, found 1129.4485

Selected HPLC-UV absorption Trace (220 nm)

1 with 2.0 eq. **DvTz** after 15 min:

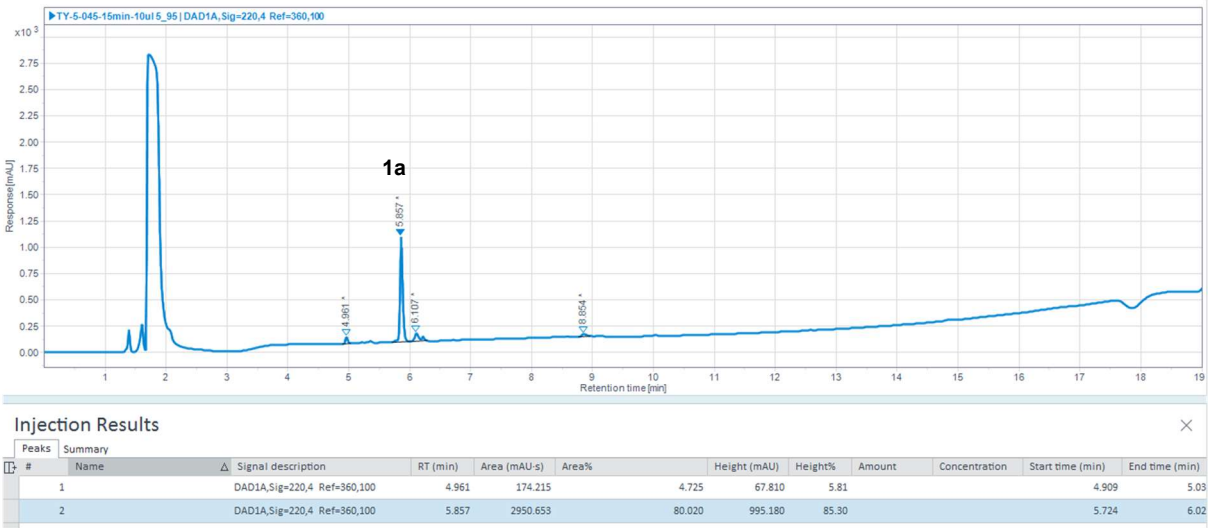

#	Name	Signal description	RT (min)	Area (mAU·s)	Area%	Height (mAU)	Height%	Amount	Concentration	Start time (min)	End time (min)
1		DAD1A,Sig=220,4 Ref=360,100	4.961	174.215	4.725	67.810	5.81			4.909	5.03
2		DAD1A,Sig=220,4 Ref=360,100	5.857	2950.653	80.020	995.180	85.30			5.724	6.02

C18 column eluting with a linear gradient system 5–95% MeCN/H_2O with constant 0.05% TFA

2 h after the addition of 2.0 eq. of **2** :

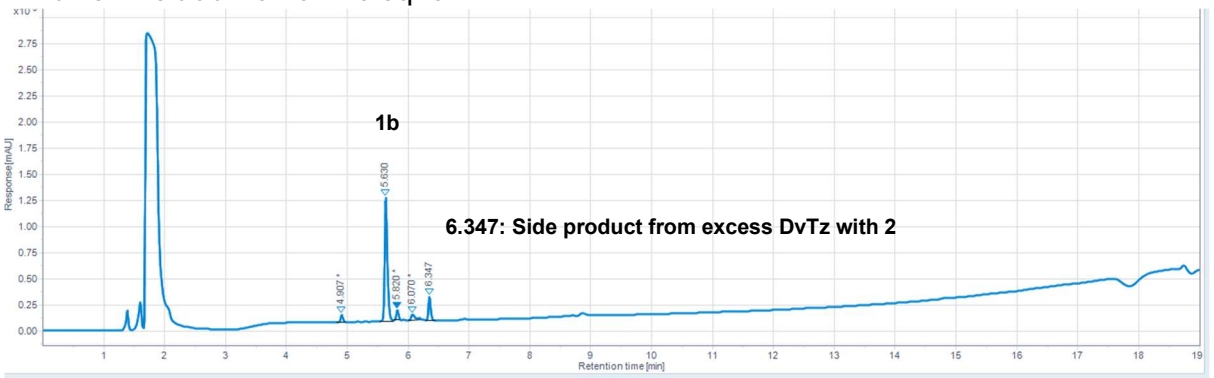

Injection Results

Peaks | Summary

#	Name	Signal description	RT (min)	Area (mAU·s)	Area%	Height (mAU)	Height%	Amount	Concentration	Start time (min)	End time (min)
1		DAD1A,Sig=220,4 Ref=360,100	4.907	178.038	3.692	73.943	4.48			4.824	4.97
2		DAD1A,Sig=220,4 Ref=360,100	5.630	3570.165	74.034	1188.471	72.02			5.540	5.76
3		DAD1A,Sig=220,4 Ref=360,100	5.820	234.945	4.872	99.174	6.01			5.783	5.87
4		DAD1A,Sig=220,4 Ref=360,100	6.070	258.232	5.355	58.521	3.55			6.014	6.20
5		DAD1A,Sig=220,4 Ref=360,100	6.347	580.924	12.047	230.074	13.94			6.297	6.45

C18 column eluting with a linear gradient system 5–95% MeCN/H_2O with constant 0.05% TFA

1b

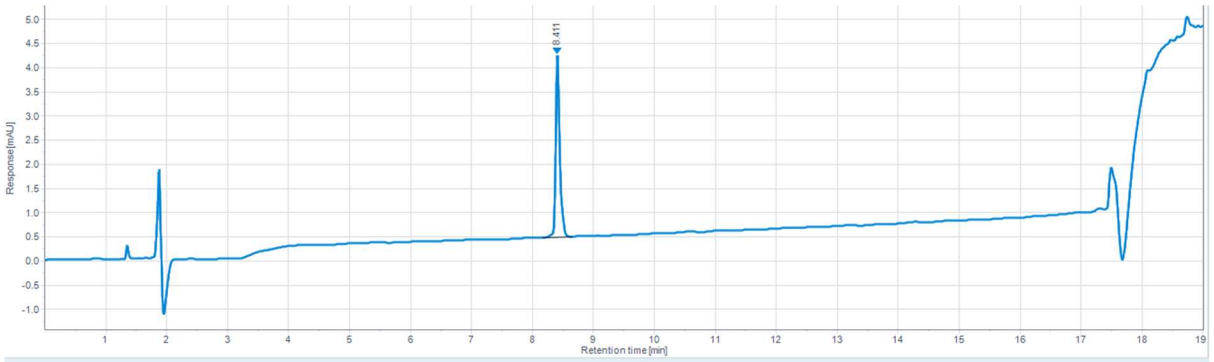

Injection Results

Peaks | Summary

#	Name	Signal description	RT (min)	Area (mAU·s)	Area%	Height (mAU)	Height%	Amount	Concentration	Start time (min)	End time (min)
1		DAD1A,Sig=220,4 Ref=360,100	8.411	1738.175	100.000	376.858	100.00			8.168	8.66

C18 column eluting with a linear gradient system 5–40% MeCN/H_2O with constant 0.05% TFA

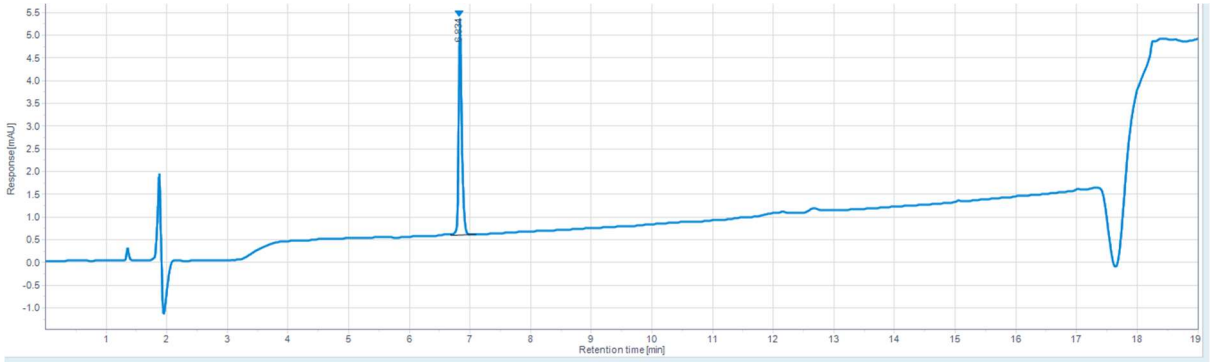

Injection Results

Peaks | Summary

#	Name	Signal description	RT (min)	Area (mAU·s)	Area%	Height (mAU)	Height%	Amount	Concentration	Start time (min)	End time (min)
1		DAD1A,Sig=220,4 Ref=360,100	6.834	1723.799	100.000	478.132	100.00			6.687	7.10

C18 column eluting with a linear gradient system 5–60% MeCN/H_2O with constant 0.05% TFA

4. Analytical HPLC Spectra and UV-LCMS Spectra

Peptide **1**

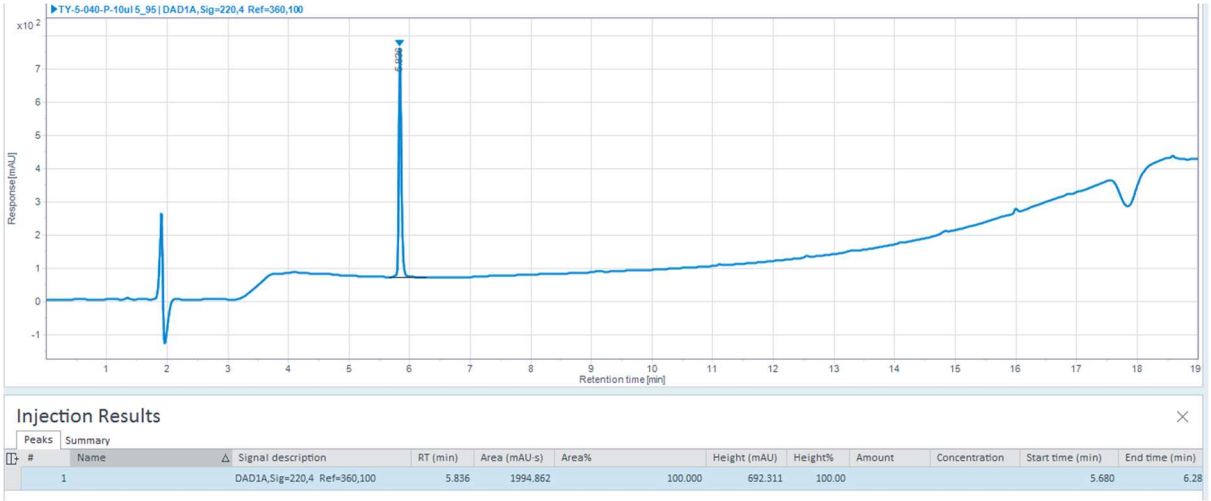

Analytical HPLC: Linear gradient system 5–95% MeCN/H_2O with constant 0.05% TFA

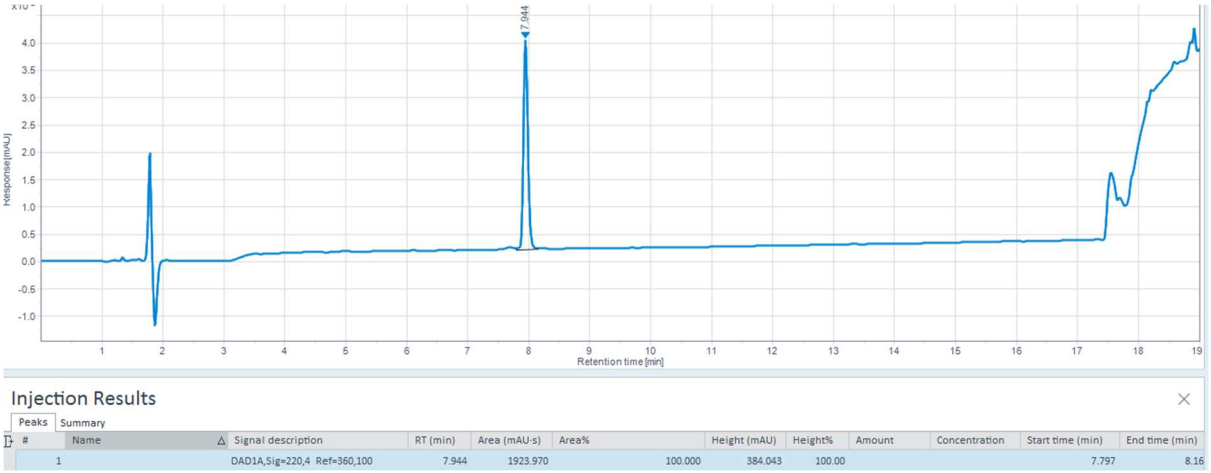

Analytical HPLC: Linear gradient system 10–30% MeCN/H_2O with constant 0.05% TFA

Peptide **3**

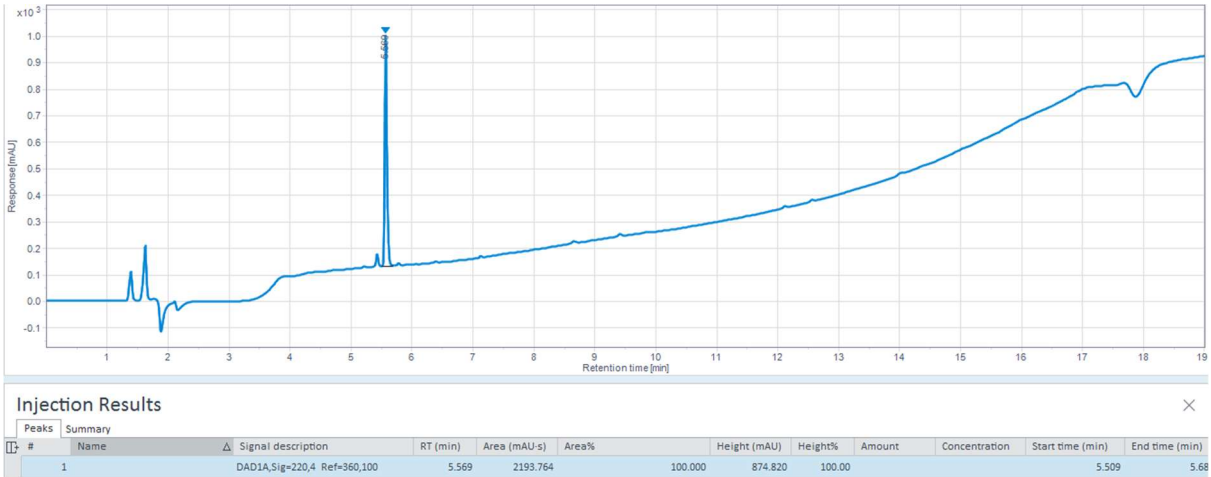

Analytical HPLC: Linear gradient system 1–99% MeCN/H_2O with constant 0.05% TFA

Peptide **3a**

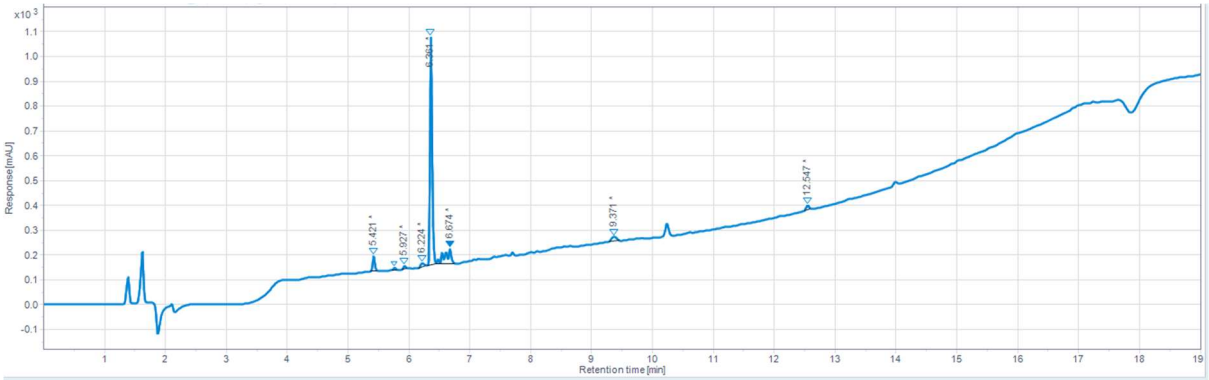

Injection Results

Peaks | Summary

#	Name	Signal description	RT (min)	Area (mAU·s)	Area%	Height (mAU)	Height%	Amount	Concentration	Start time (min)	End time (min)
1		DAD1A,Sig=220,4 Ref=360,100	5.421	145.434	4.745	61.537	5.52			5.375	5.47
2		DAD1A,Sig=220,4 Ref=360,100	5.764	22.307	0.728	9.684	0.87			5.728	5.80
3		DAD1A,Sig=220,4 Ref=360,100	5.927	27.748	0.905	12.032	1.08			5.896	5.96
4		DAD1A,Sig=220,4 Ref=360,100	6.224	59.198	1.931	15.493	1.39			6.159	6.27
5		DAD1A,Sig=220,4 Ref=360,100	6.361	2230.581	72.776	922.474	82.68			6.307	6.44

Analytical HPLC: Linear gradient system 1–99% MeCN/H_2O with constant 0.05% TFA

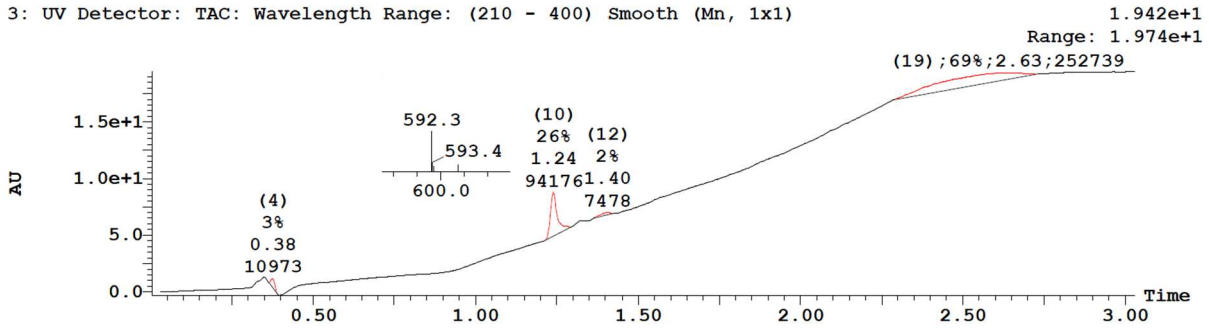

UV-LCMS: 5–95% B over 3 min with constant 5% C over 1 min

Peptide **4**

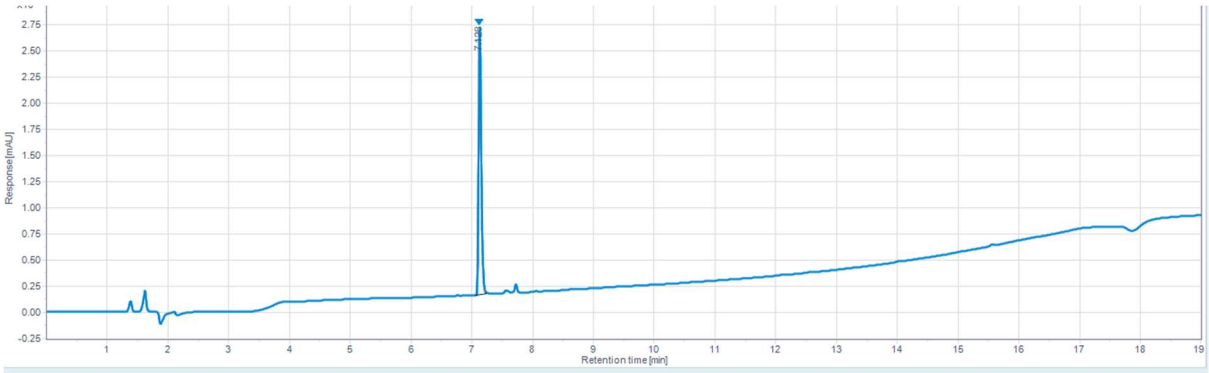

Injection Results

Peaks | Summary

#	Name	Signal description	RT (min)	Area (mAU·s)	Area%	Height (mAU)	Height%	Amount	Concentration	Start time (min)	End time (min)
1		DAD1A,Sig=220,4 Ref=360,100	7.128	7786.510	100.000	2567.204	100.00			7.071	7.24

Analytical HPLC: Linear gradient system 1–99% MeCN/H_2O with constant 0.05% TFA

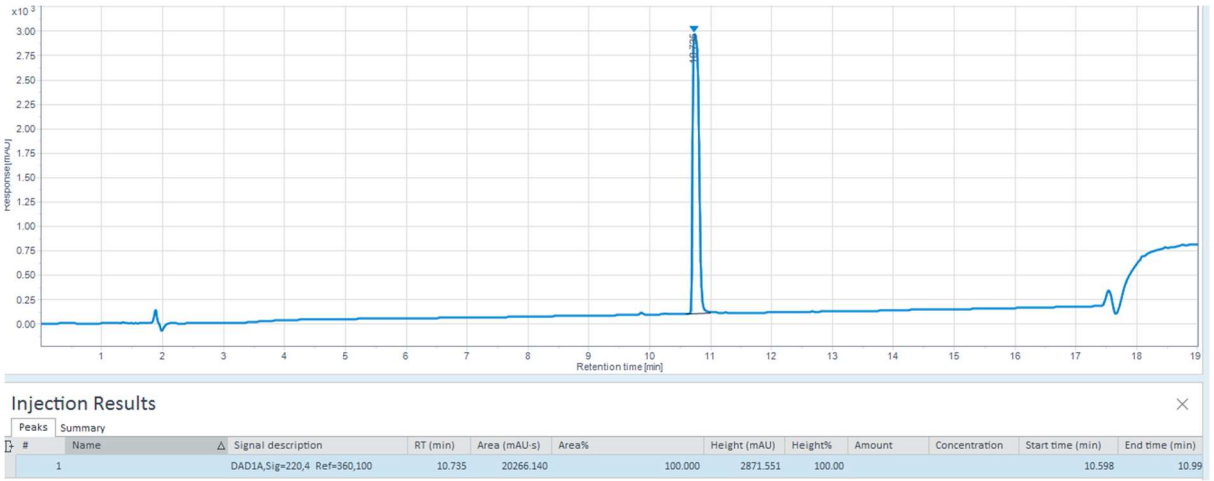

Injection Results

Peaks | Summary

#	Name	Signal description	RT (min)	Area (mAU·s)	Area%	Height (mAU)	Height%	Amount	Concentration	Start time (min)	End time (min)
1		DAD1A,Sig=220,4 Ref=360,100	10.735	20266.140	100.000	2871.551	100.00			10.598	10.99

Analytical HPLC: Linear gradient system 5–40% MeCN/H_2O with constant 0.05% TFA

Peptide **4a**

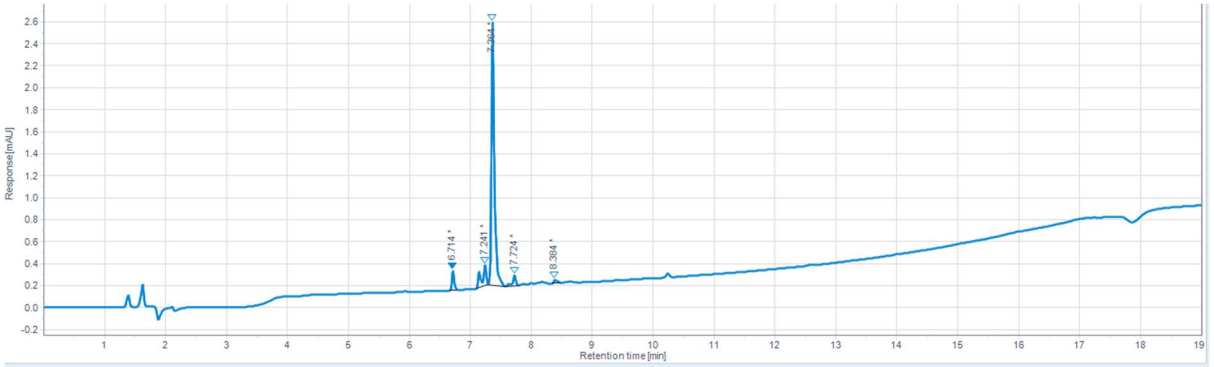

Injection Results

Peaks | Summary

#	Name	Signal description	RT (min)	Area (mAU·s)	Area%	Height (mAU)	Height%	Amount	Concentration	Start time (min)	End time (min)
1		DAD1A,Sig=220,4 Ref=360,100	6.714	426.612	4.449	177.446	6.14			6.663	6.78
2		DAD1A,Sig=220,4 Ref=360,100	7.241	908.326	9.473	189.473	6.55			7.101	7.29
3		DAD1A,Sig=220,4 Ref=360,100	7.364	7812.437	81.479	2394.323	82.82			7.293	7.57
4		DAD1A,Sig=220,4 Ref=360,100	7.724	327.265	3.413	98.818	3.42			7.574	7.79
5		DAD1A,Sig=220,4 Ref=360,100	8.384	113.620	1.185	31.016	1.07			8.357	8.47

Analytical HPLC: Linear gradient system 1–99% MeCN/H_2O with constant 0.05% TFA

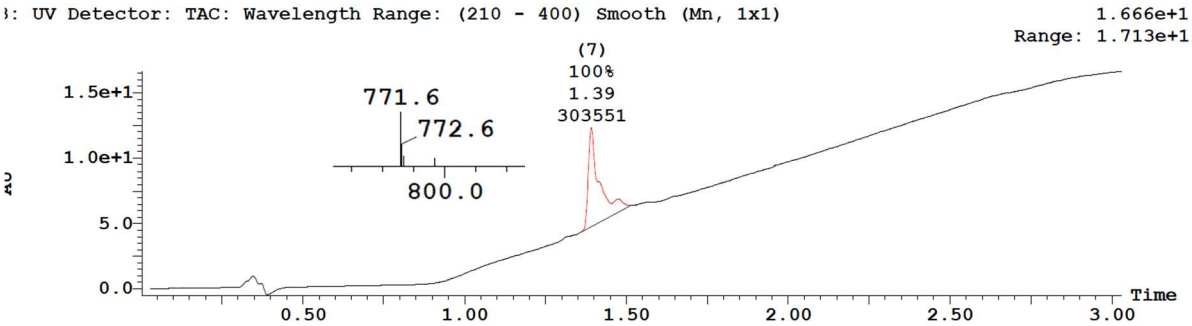

LCMS: 5–95% B over 3 min with constant 5% C over 1 min

Peptide **5**

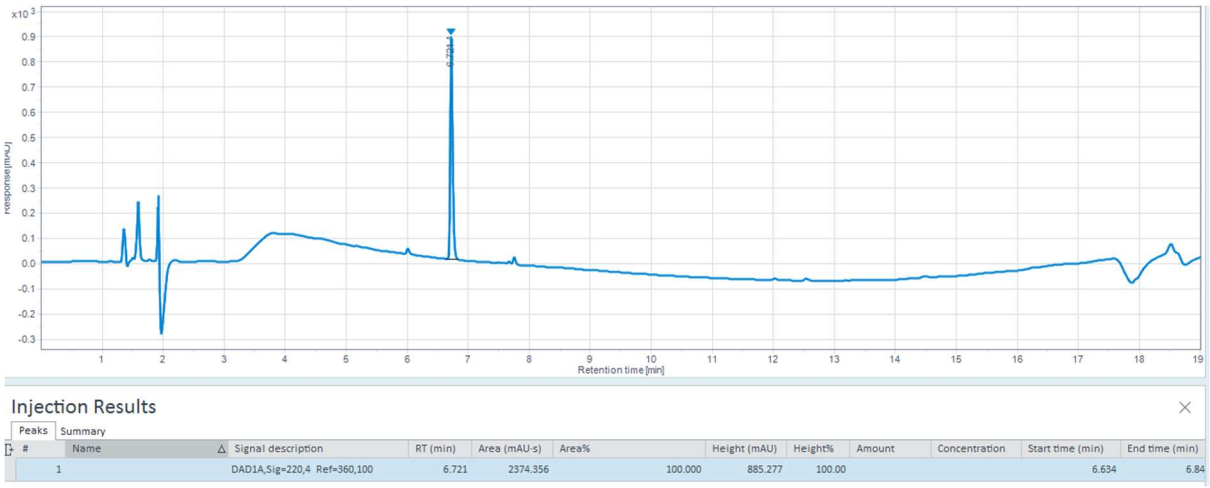

Analytical HPLC: Linear gradient system 5–95% MeCN/H_2O with constant 0.05% TFA

Peptide **5a**

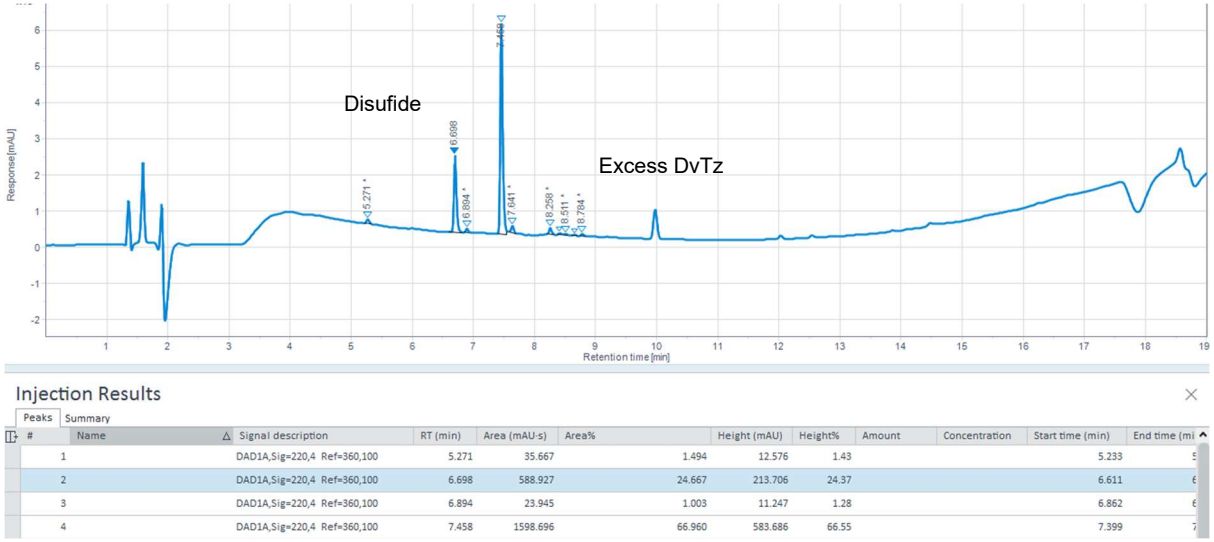

Analytical HPLC: Linear gradient system 5–95% MeCN/H_2O with constant 0.05% TFA

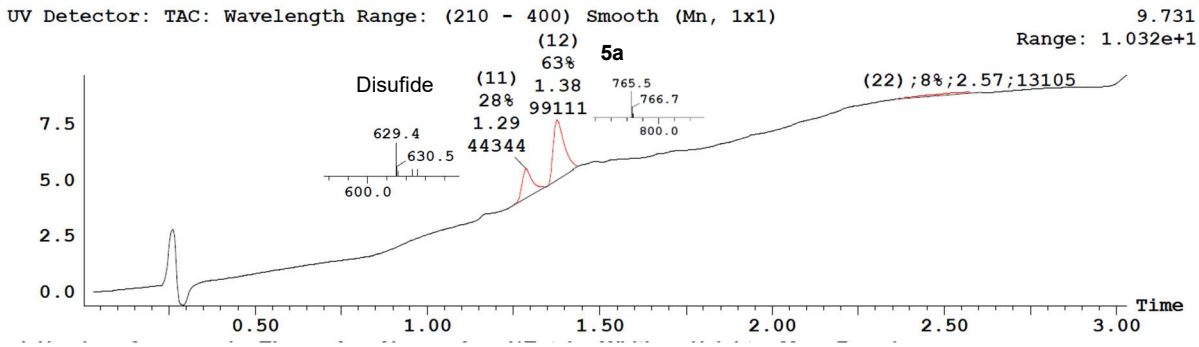

LCMS: 5–95% B over 3 min with constant 5% C over 1 min

Peptide **6**

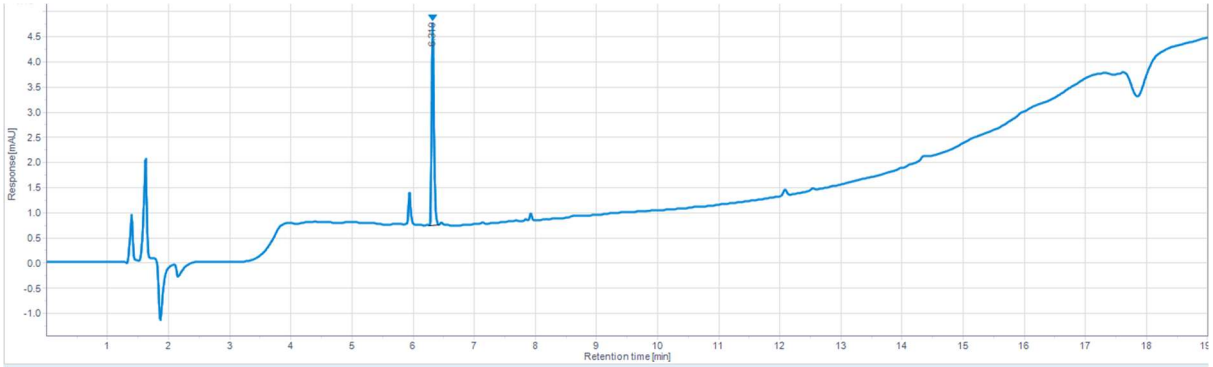

Injection Results

Peaks | Summary

#	Name	Signal description	RT (min)	Area (mAU·s)	Area%	Height (mAU)	Height%	Amount	Concentration	Start time (min)	End time (min)
1		DAD1A,Sig=220,4 Ref=360,100	6.319	1012.453	100.000	404.624	100.00			6.269	6.4

Analytical HPLC: Linear gradient system 1–99% MeCN/H_2O with constant 0.05% TFA

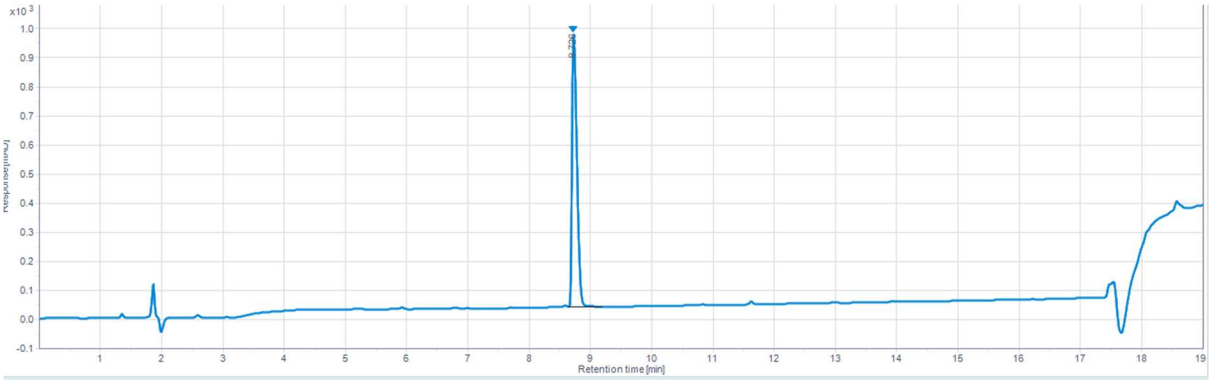

Injection Results

Peaks | Summary

#	Name	Signal description	RT (min)	Area (mAU·s)	Area%	Height (mAU)	Height%	Amount	Concentration	Start time (min)	End time (min)
1		DAD1A,Sig=220,4 Ref=360,100	8.726	5258.813	100.000	941.227	100.00			8.649	9.18

Analytical HPLC: Linear gradient system 5–40% MeCN/H_2O with constant 0.05% TFA

Peptide **6a**

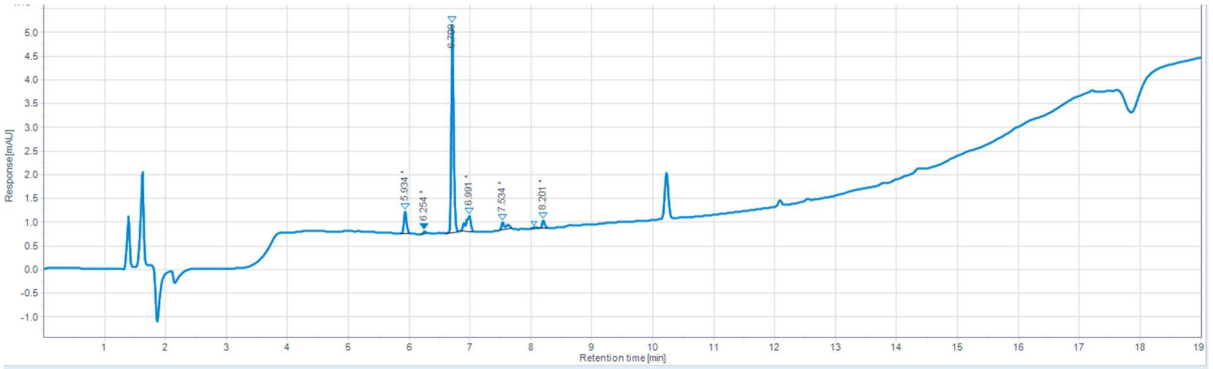

Injection Results

Peaks | Summary

#	Name	Signal description	RT (min)	Area (mAU·s)	Area%	Height (mAU)	Height%	Amount	Concentration	Start time (min)	End time (min)
1		DAD1A,Sig=220,4 Ref=360,100	5.934	137.403	8.421	47.508	8.41			5.859	6.01
2		DAD1A,Sig=220,4 Ref=360,100	6.254	12.119	0.743	5.523	0.98			6.198	6.28
3		DAD1A,Sig=220,4 Ref=360,100	6.708	1154.337	70.744	440.971	78.04			6.608	6.80

Analytical HPLC: Linear gradient system 1–99% MeCN/H_2O with constant 0.05% TFA

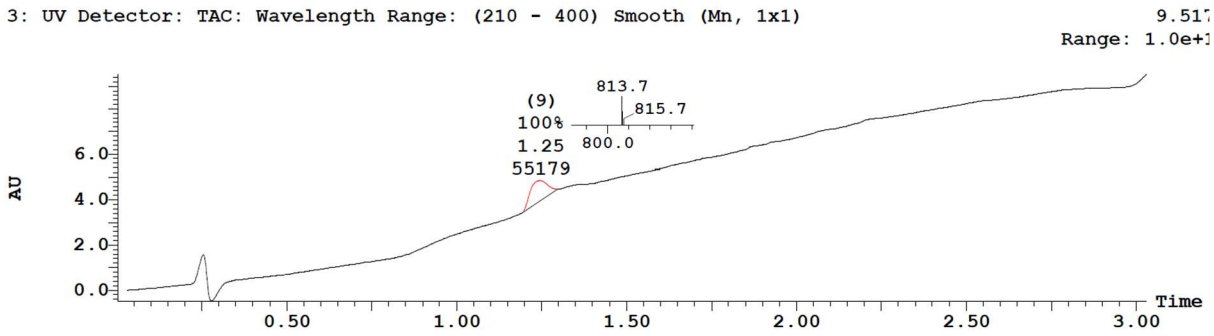

LCMS: 5–95% B over 3 min with constant 5% C over 1 min

Peptide **7**

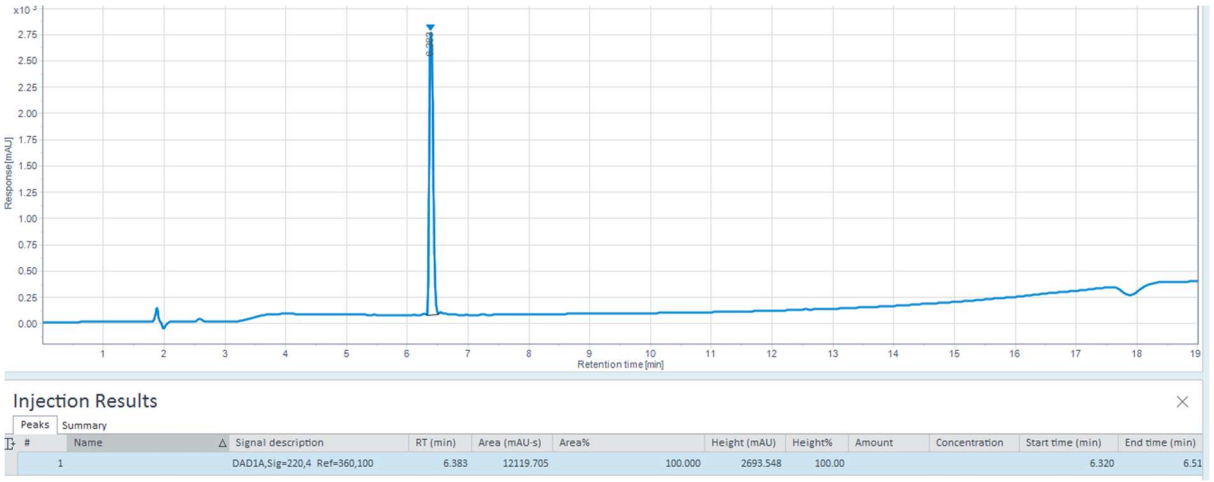

Analytical HPLC: Linear gradient system 5–95% MeCN/H_2O with constant 0.05% TFA

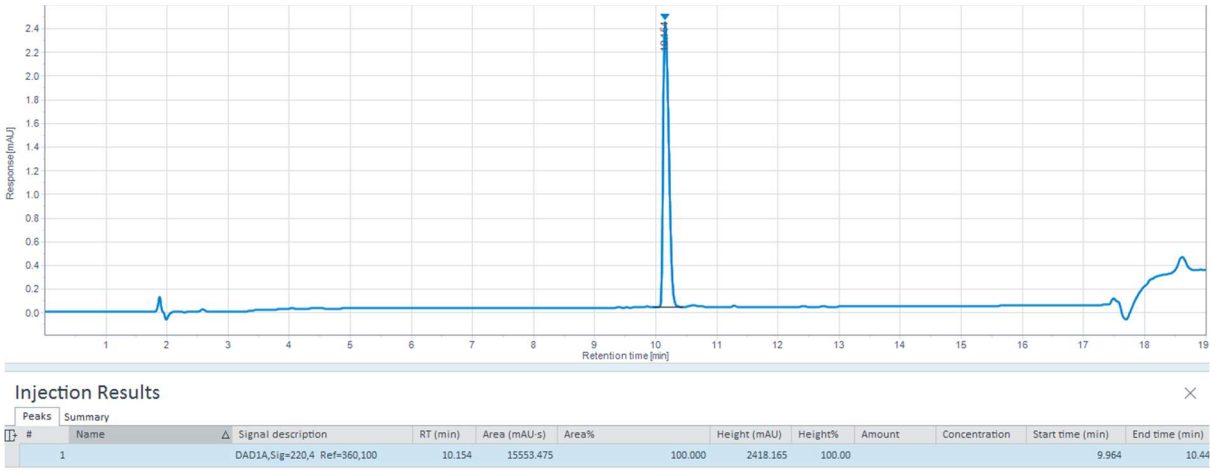

Analytical HPLC: Linear gradient system 5–40% MeCN/H_2O with constant 0.05% TFA

Peptide **7a**

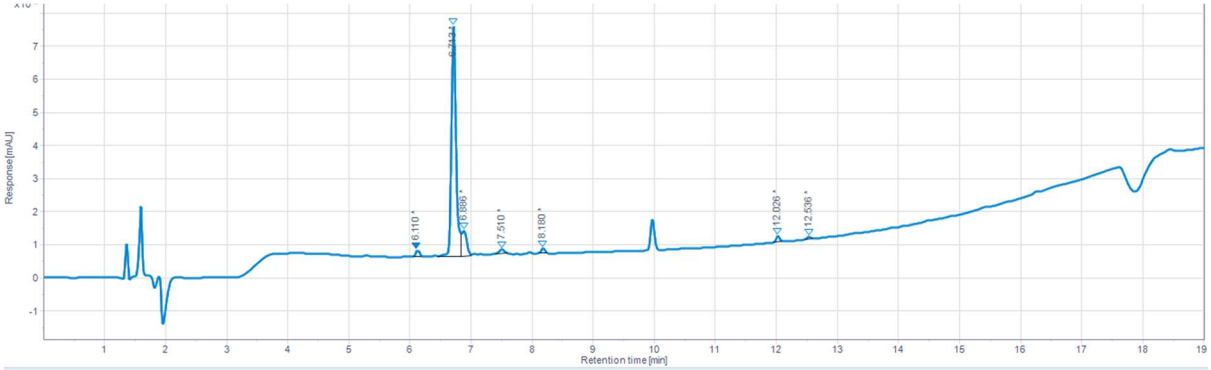

Injection Results

Peaks | Summary

#	Name	Signal description	RT (min)	Area (mAU·s)	Area%	Height (mAU)	Height%	Amount	Concentration	Start time (min)	End time (min)
1		DAD1A,Sig=220,4 Ref=360,100	6.110	77.560	1.774	17.651	2.09			6.064	6.19
2		DAD1A,Sig=220,4 Ref=360,100	6.713	3634.244	83.118	697.247	82.74			6.466	6.83

Analytical HPLC: Linear gradient system 5–95% MeCN/H_2O with constant 0.05% TFA

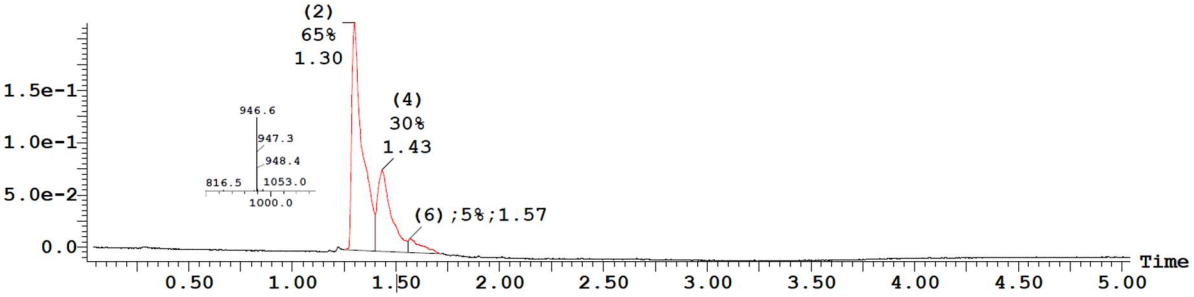

LCMS: 5–95% B over 5 min with constant 5% C over 1 min

Peptide **8**

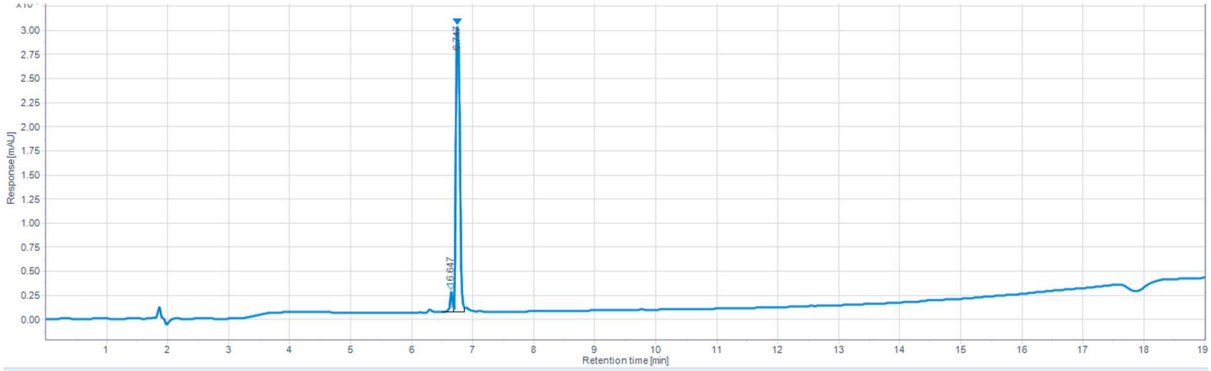

Injection Results

Peaks | Summary

#	Name	Signal description	RT (min)	Area (mAU·s)	Area%	Height (mAU)	Height%	Amount	Concentration	Start time (min)	End time (min)
1		DAD1A,Sig=220,4 Ref=360,100	6.647	600.088	4.272	211.847	6.66			6.501	6.69
2		DAD1A,Sig=220,4 Ref=360,100	6.747	13446.197	95.728	2970.691	93.34			6.694	6.87

Analytical HPLC: Linear gradient system 5–95% MeCN/H_2O with constant 0.05% TFA

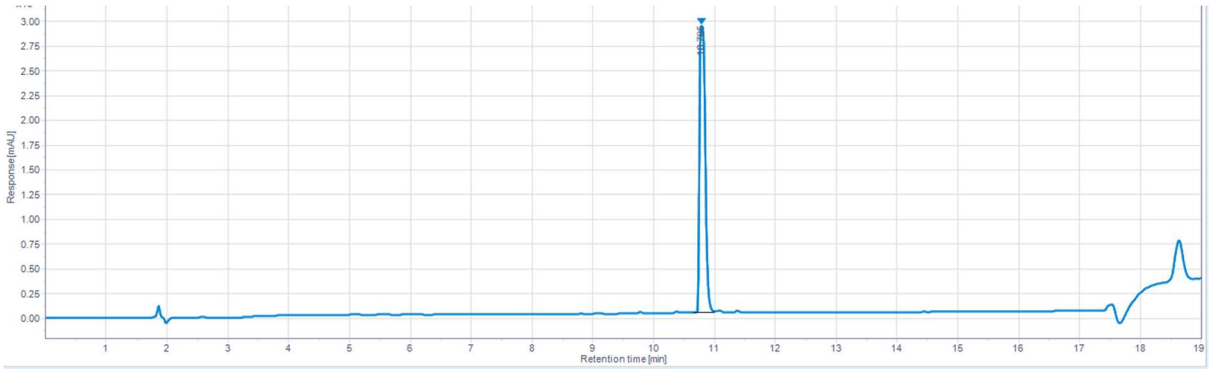

Injection Results

Peaks | Summary

#	Name	Signal description	RT (min)	Area (mAU·s)	Area%	Height (mAU)	Height%	Amount	Concentration	Start time (min)	End time (min)
1		DAD1A,Sig=220,4 Ref=360,100	10.785	19048.965	100.000	2902.766	100.00			10.652	10.99

Analytical HPLC: Linear gradient system 5–40% MeCN/H_2O with constant 0.05% TFA

Peptide **8a**

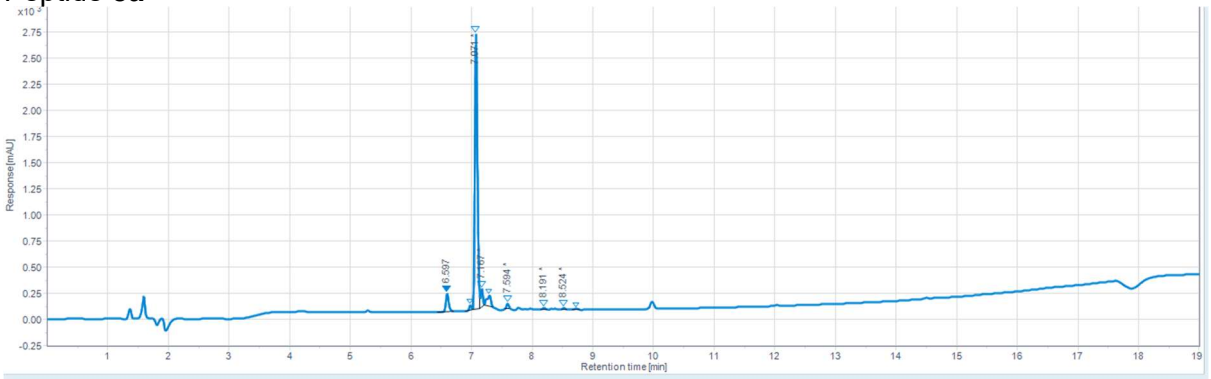

Injection Results

Peaks | Summary

#	Name	Signal description	RT (min)	Area (mAU·s)	Area%	Height (mAU)	Height%	Amount	Concentration	Start time (min)	End time (min)
1		DAD1A,Sig=220,4 Ref=360,100	6.597	576.726	5.954	179.065	5.51			6.447	6.70
2		DAD1A,Sig=220,4 Ref=360,100	6.977	113.673	1.174	53.233	1.64			6.903	7.01
3		DAD1A,Sig=220,4 Ref=360,100	7.071	7878.934	81.344	2637.415	81.21			7.018	7.14

Analytical HPLC: Linear gradient system 5–95% MeCN/H_2O with constant 0.05% TFA

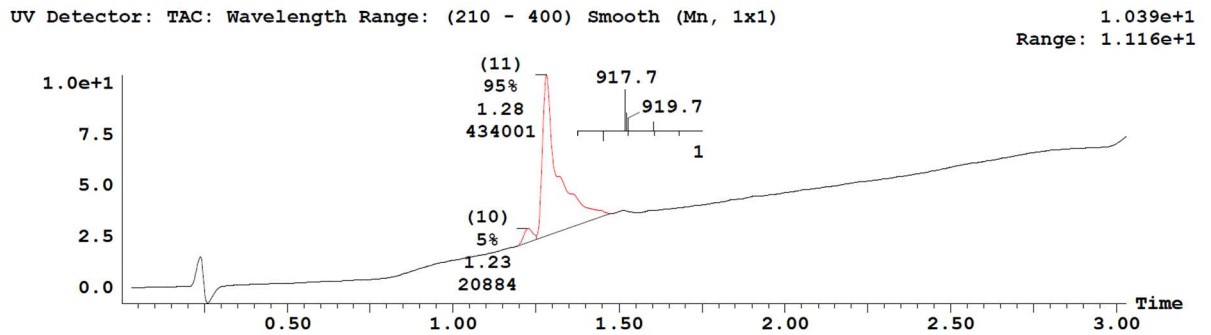

LCMS: 5–95% B over 3 min with constant 5% C over 1 min

Peptide **9**

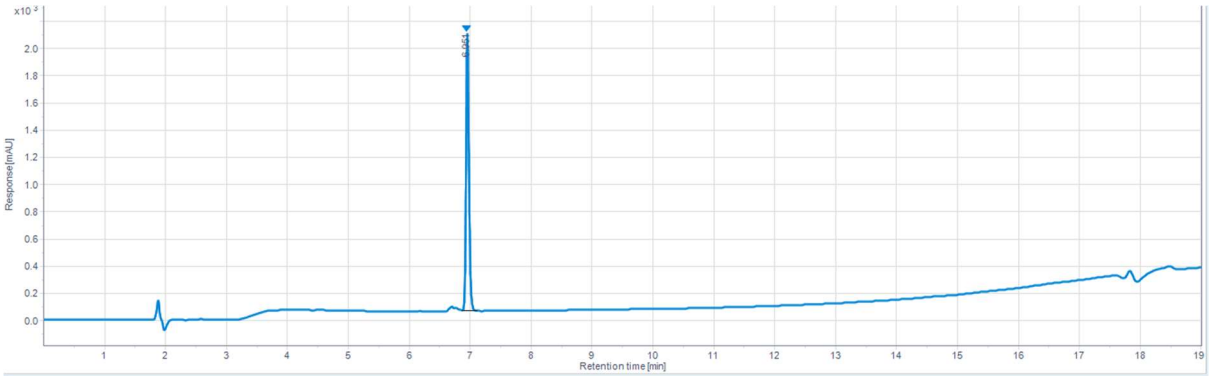

Injection Results

Peaks | Summary

#	Name	Signal description	RT (min)	Area (mAU·s)	Area%	Height (mAU)	Height%	Amount	Concentration	Start time (min)	End time (min)
1		DAD1A,Sig=220,4 Ref=360,100	6.951	6679.809	100.000	2041.459	100.00			6.868	7.12

Analytical HPLC: Linear gradient system 5–95% MeCN/H_2O with constant 0.05% TFA

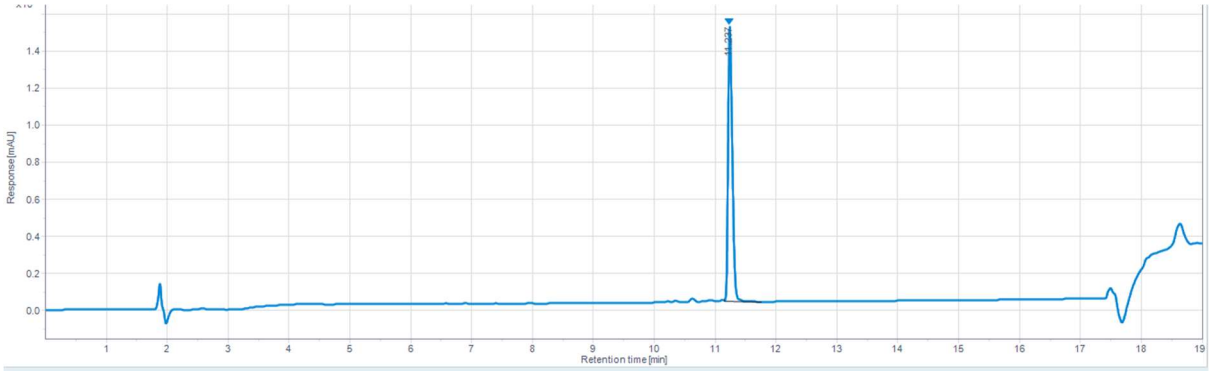

Injection Results

Peaks | Summary

#	Name	Signal description	RT (min)	Area (mAU·s)	Area%	Height (mAU)	Height%	Amount	Concentration	Start time (min)	End time (min)
1		DAD1A,Sig=220,4 Ref=360,100	11.237	7163.162	100.000	1488.624	100.00			11.154	11.76

Analytical HPLC: Linear gradient system 5–40% MeCN/H_2O with constant 0.05% TFA

Peptide **9a**

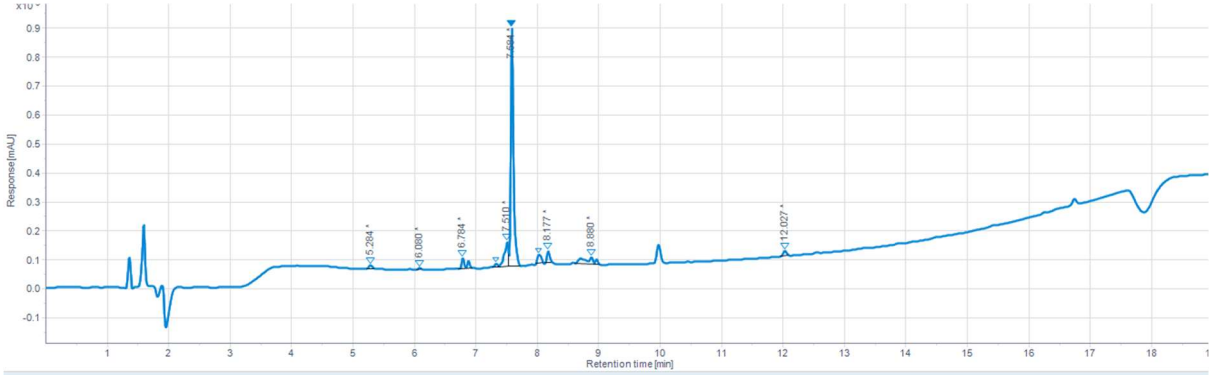

Injection Results

Peaks | Summary

#	Name	Signal description	RT (min)	Area (mAU·s)	Area%	Height (mAU)	Height%	Amount	Concentration	Start time (min)	End time (mi
1		DAD1A,Sig=220,4 Ref=360,100	5.284	39.944	1.069	11.845	1.09			5.227	
2		DAD1A,Sig=220,4 Ref=360,100	6.080	13.907	0.372	6.021	0.55			6.041	
3		DAD1A,Sig=220,4 Ref=360,100	6.784	163.839	4.385	36.992	3.39			6.720	
4		DAD1A,Sig=220,4 Ref=360,100	7.334	43.415	1.162	12.936	1.19			7.263	
5		DAD1A,Sig=220,4 Ref=360,100	7.510	376.151	10.066	85.728	7.86			7.377	
6		DAD1A,Sig=220,4 Ref=360,100	7.584	2486.620	66.546	824.637	75.59			7.534	

Analytical HPLC: Linear gradient system 5–95% MeCN/H_2O with constant 0.05% TFA

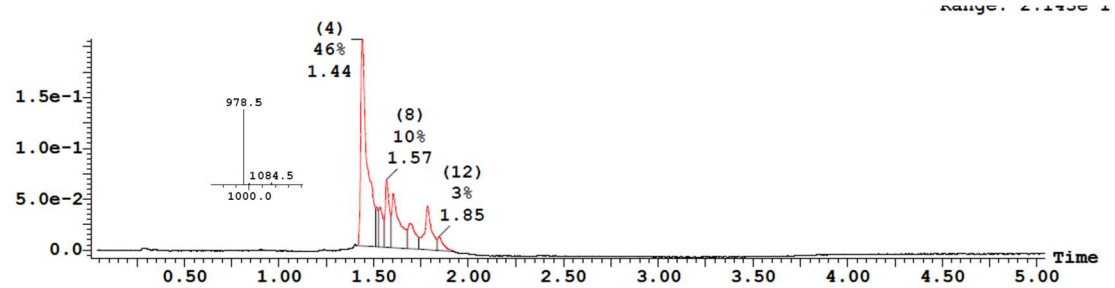

LCMS: 5–95% B over 5 min with constant 5% C over 1 min

Peptide **10**

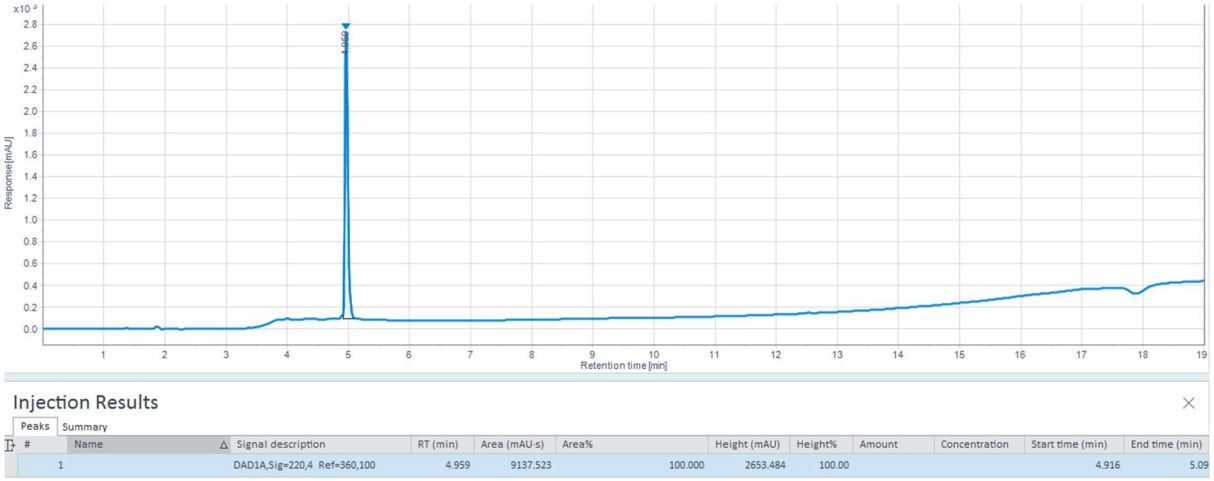

Analytical HPLC: Linear gradient system 1–99% MeCN/H_2O with constant 0.05% TFA

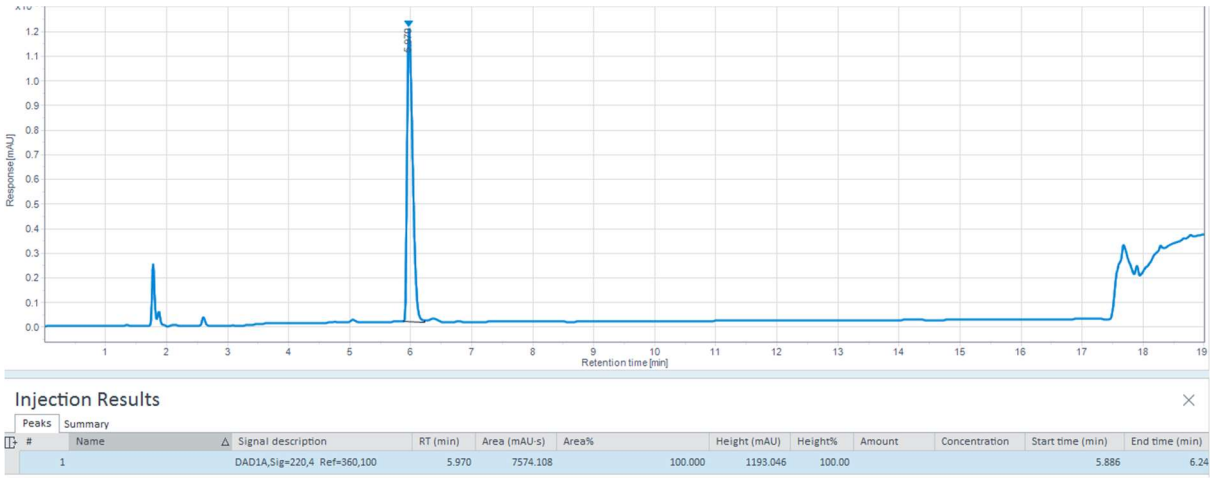

Analytical HPLC: Linear gradient system 5–20% MeCN/H_2O with constant 0.05% TFA

Peptide **10a**

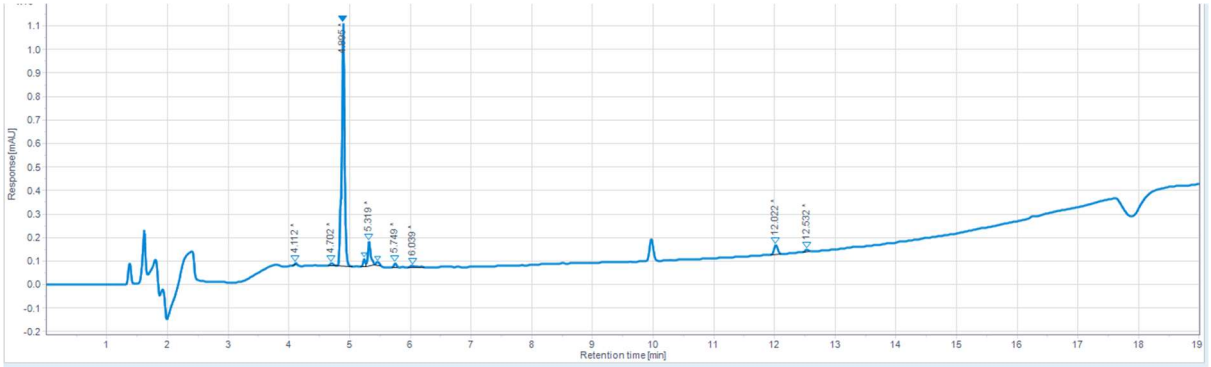

Injection Results

Peaks | Summary

#	Name	Signal description	RT (min)	Area (mAU·s)	Area%	Height (mAU)	Height%	Amount	Concentration	Start time (min)	End time (mi
1		DAD1A,Sig=220,4 Ref=360,100	4.112	8.172	0.203	6.974	0.54			4.060	4
2		DAD1A,Sig=220,4 Ref=360,100	4.702	40.288	1.001	10.472	0.82			4.649	4
3		DAD1A,Sig=220,4 Ref=360,100	4.895	3194.994	79.355	1034.917	80.62			4.802	5

Analytical HPLC: Linear gradient system 1–99% MeCN/H_2O with constant 0.05% TFA

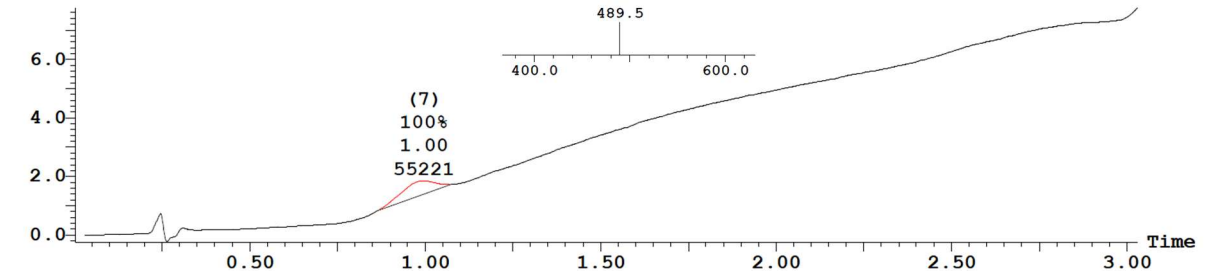

LCMS: 5–95% B over 3 min with constant 5% C over 1 min

Peptide **11**

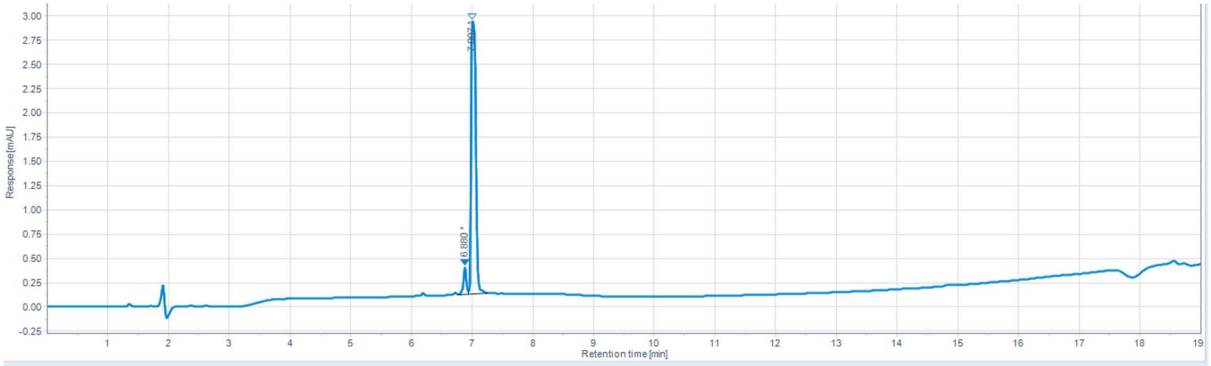

Injection Results

Peaks | Summary

#	Name	Signal description	RT (min)	Area (mAU·s)	Area%	Height (mAU)	Height%	Amount	Concentration	Start time (min)	End time (min)
1		DAD1A,Sig=220,4 Ref=360,100	6.880	875.022	5.541	280.270	9.05			6.770	6.94
2		DAD1A,Sig=220,4 Ref=360,100	7.007	14915.876	94.459	2816.170	90.95			6.944	7.25

Analytical HPLC: Linear gradient system 5–95% MeCN/H_2O with constant 0.05% TFA

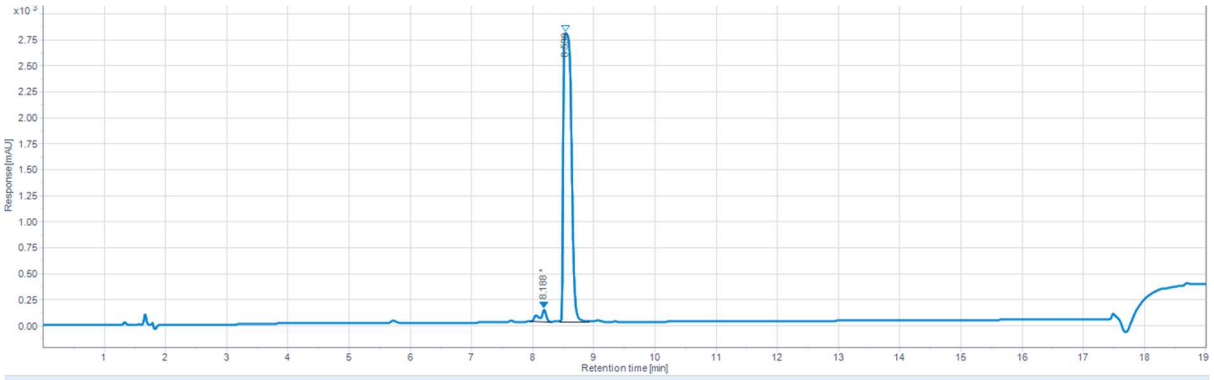

Injection Results

Peaks | Summary

#	Name	Signal description	RT (min)	Area (mAU·s)	Area%	Height (mAU)	Height%	Amount	Concentration	Start time (min)	End time (min)
1		DAD1A,Sig=220,4 Ref=360,100	8.188	848.846	3.234	121.191	4.17			7.965	8.30
2		DAD1A,Sig=220,4 Ref=360,100	8.538	25402.583	96.766	2782.364	95.83			8.451	8.93

Analytical HPLC: Linear gradient system 15–40% MeCN/H_2O with constant 0.05% TFA

Peptide **11a**

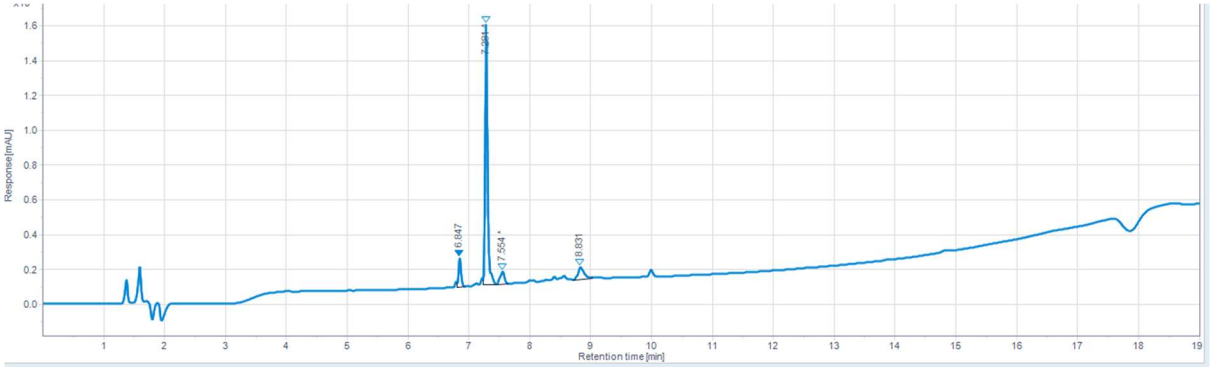

Injection Results

Peaks | Summary

#	Name	Signal description	RT (min)	Area (mAU·s)	Area%	Height (mAU)	Height%	Amount	Concentration	Start time (min)	End time (min)
1		DAD1A,Sig=220,4 Ref=360,100	6.847	464.496	8.505	169.696	9.37			6.811	6.94
2		DAD1A,Sig=220,4 Ref=360,100	7.281	4128.280	75.590	1493.058	82.40			7.237	7.45

Analytical HPLC: Linear gradient system 5–95% MeCN/H_2O with constant 0.05% TFA

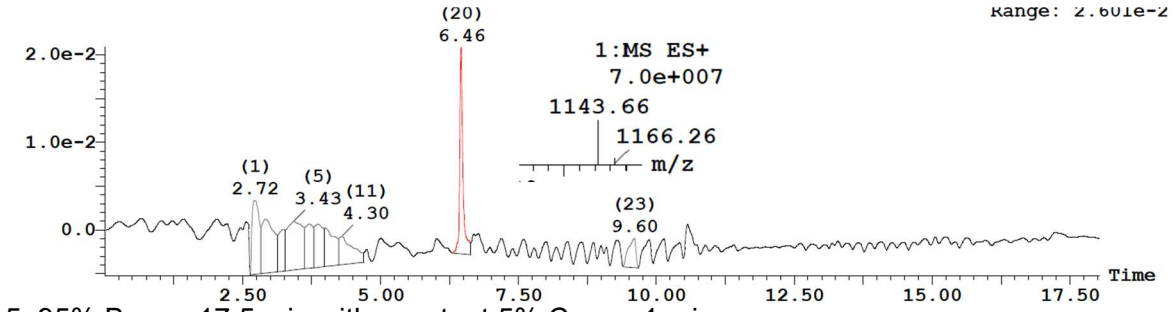

5–95% B over 17.5 min with constant 5% C over 1 min

5. Protein information

5.1. General Infomation

Trastuzumab was acquired from F. Hoffmann-La Roche AG. Human HER2-HisTag was acquired from Acro BIOSYSTEMS (Catalog No. HE2-H5225).

5.2. αHER2 Fab preparation

Following literature procedure:[5]

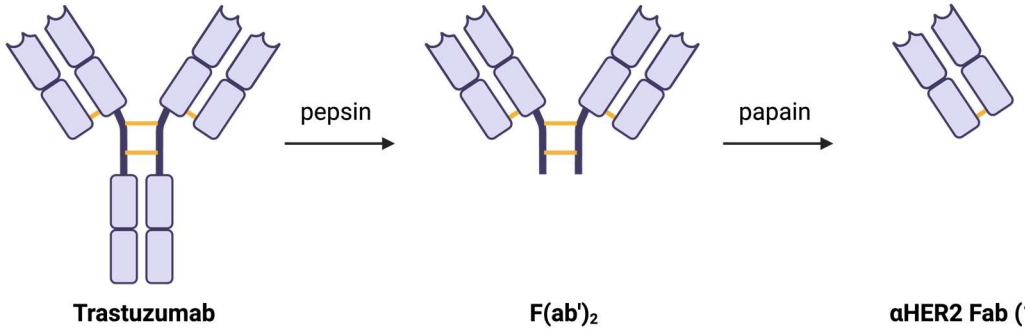

Immobilised pepsin (Thermo Scientific, Cat. No. 20343; 150 µL) was transferred to an enzyme column and washed with Digest Buffer 1 (20 mM NaOAc, pH 3.1; 4 × 200 µL). Trastuzumab (5 mg) was dissolved in Digest Buffer 1 (500 µL) and added to the immobilised pepsin. The mixture was shaken on a thermal shaker at 900 rpm and 37 °C for 16 h.

The resin was separated from the filtrate by centrifugation (1G, 1 min) and washed with Digest Buffer 2 (4 × 200 µL; 50 mM NaPi, 150 mM NaCl, 1 mM EDTA, pH 6.8). The filtrates were combined and subjected to membrane filtration five times with Digest Buffer 2 *via* an Amicon-Ultra 15 diafiltration spin-concentrator (10,000 MW cut-off, Merck Millipore).

Immobilised papain (Thermo Scientific, Cat. No. 20341; 500 µL) was isolated in an enzyme column, washed with Digest Buffer 2 (2 × 500 µL), and activated with dithiothreitol (DTT) (500 µL, 10 mM) at 37 °C for 1.5 h. The resin was separated from the DTT solution and washed with Digest Buffer 2 (4 × 500 µL). The antibody fragment solution was added to the resin and incubated on a thermal shaker at 900 rpm and 37 °C for 16 h. The resin was then isolated and washed with TBS (25 mM Tris-HCl, 25 mM NaCl, 0.5 mM EDTA, pH 8.0; 4 × 500 µL), and the combined filtrates were subjected to repeated membrane filtration with TBS five times *via* an Amicon-Ultra 15 diafiltration spin-concentrator (10,000 MW cut-off, Merck Millipore) to yield a solution of the antibody Fab in TBS.

5.3. Recombinant protein expression and purification for αCD45 Fab, αSdrF Fab, and SdrF antigen

αCD45 Fab was derived from anti-CD45 antibody BC8;[6] αSdrF Fab was derived from humanized anti-SdrF monoclonal antibody HU108-36 (Patent No. WO2003076470A1). αCD45 Fab and αSdrF Fab constructs were encoded using the pcDNA3.1 vector backbone and expressed in Expi293F cells (Thermo Fisher, A14635), which were cultured under humidified conditions at 37 °C and 8% (v/v) CO_2 in Expi293 Expression Medium (Thermo Fisher). Cells were transfected using the ExpiFectamine 293 Transfection Kit (Thermo Fisher

Scientific). After approximately 16-18 h, ExpiFectamine 293 Transfection Enhancers 1 and 2 were added. Cell supernatants were collected after 5-7 days by centrifuging for 4,000g at 4 °C for 10 min and were passed through a 0.45 µm filter and then a 0.22 µm filter (Starlab).

SdrF belongs to the MSCRAMM (Microbial Surface Components Recognizing Adhesive Matrix Molecules) family.[7] Structurally, the N2N3 domain is the core component for the protein's functional binding.[7] AviTag-SdrF N2N3 was encoded using the pET28a vector backbone. pET28a-AviTag-SdrF N2N3 was transformed in to *Escherichia coli* BL21(DE3) cells (Agilent) and grown on LB-Agar plates with 50 µg/ml kanamycin for 16 h at 37 °C. A single colony was added in 10 ml of LB medium containing 50 µg/ml kanamycin and grown for 16 h at 37 °C with shaking at 200 rpm. This starter culture was then amplified in 1L of LB containing 50 µg/ml kanamycin and incubated at 37 °C and with 200 rpm shaking until optical density $(OD)_{600}$ =0.6. Cultures were induced with 0.42 mM isopropyl β-d-1-thiogalactopyranoside and grown at 18 °C with shaking at 200 rpm for 16 h. Cultures were pelleted by centrifugation at 4,000g.
Cell pellets were resuspended in 20 ml of 50 mM Tris-HCl, 300 mM NaCl, pH 7.8, supplemented with 0.1 mg/ml lysozyme, 1 mg/ml cOmplete mini EDTA-free protease inhibitor (Roche) and 1 mM phenylmethanesulfonyl fluoride. The lysate was incubated at 4 °C for 45 min. An Ultrasonic Processor equipped with a microtip (Cole-Parmer) was used to perform sonication on ice (four times for 60 s, 50% duty-cycle). Cell debris was cleaded by centrifugation at 35,000g for 45 min at 4 °C.

All proteins from mammalian cell supernatant or from cleared bacterial lysates were purified by nickel–nitrilotriacetic acid (Ni–NTA) affinity chromatography, with all purification steps performed at 4 °C as described in the previous study.[8] AviTag-SdrF N2N3 was biotinylated using GST–BirA following a published site-specific biotinylation protocol.[9] Proteins were aliquoted and stored at - 70 °C before use.

5.4. Protein sequences

αCD45 Fab (**13**):
Heavy chain:
MGILPSPGMPALLSLVSLLSVLLMGCVAEVKLLESGGGLVQPGGSLKLSCAASGFDFSRYW
MSWVRQAPGKGLEWIGEINPTSSTINFTPSLKDKVFISRDNAKNTLYLQMSKVRSEDTALYY
CARGNYYRYGDAMDYWGQGTSVTVSSAKTTPPSVYPLAPGSAAQTNSMVTLGCLVKGYF
PEPVTVTWNSGSLSSGVHTFPAVLQSDLYTLSSSVTVPSSTWPSETVTCNVAHPASSTKVD
KKIVPRDCGSGRGVPHIVMVDAYKRYKGHHHHHH*
Light chain:
MGILPSPGMPALLSLVSLLSVLLMGCVADIALTQSPASLAVSLGQRATISCRASKSVSTSGYS
YLHWYQQKPGQPPKLLIYLASNLESGVPARFSGSGSGTDFTLNIHPVEEEDAATYYCQHSR
ELPFTFGSGTKLEIKRADAAPTVSIFPPSSEQLTSGGASVVCFLNNFYPKDINVKWKIDGSER
QNGVLNSWTDQDSKDSTYSMSSTLTLTKDEYERHNSYTCEATHKTSTSPIVKSFNRNEC*

αSdrF Fab (**14**):
Heavy chain:
MGILPSPGMPALLSLVSLLSVLLMGCVAQVTLRESGPGILKPSQTLSLTCTFSGFSLSTSGM
GVTWIRQPSGKGLEWLANIYWDDDKRYNPSLKSRLTISKANSRNQVFLKITSVDPVDTATYY
CTRPNYLGTVYWYFDVWGQGTMVTVSSAKTTPPSVYPLAPGSAAQTNSMVTLGCLVKGY
FPEPVTVTWNSGSLSSGVHTFPAVLQSDLYTLSSSVTVPSSTWPSETVTCNVAHPASSTKV
DKKIVPRDCGSGRGVPHIVMVDAYKRYKGHHHHHH*

Light chain:
MGILPSPGMPALLSLVSLLSVLLMGCVAEIVLTQSPATMSASPGERVTMSCSASSSVSYMYW
YQQKPGQSPRVLIYDTSNLASGVPSRFSGSGSGTSYSLTISSMEPEDAATYYCQQWNGYP
PTFGGGTKLEVKRADAAPTVSIFPPSSEQLTSGGASVVCFLNNFYPKDINVKWKIDGSERQ
NGVLNSWTDQDSKDSTYSMSSTLTLTKDEYERHNSYTCEATHKTSTSPIVKSFNRNEC*

AviTag-SdrF N2N3:
MRGSHHHHHHGSGLNDIFEAQKIEWHEGSGPNSGKNVNDKVKITNPTLSLNKSNNHANNVI
WPTSNEQFNLKANYELDDSIKEGDTFTIKYGQYIRPGGLELPAIKTQLRSKDGSIVANGVYDK
TTNTTTYTFTNYVDQYQNITGSFDLIATPKRETAIKDNQNYPMEVTIANEVVKKDFIVDYGNK
KDNTTTAAVANVDNVNNKHNEVVYLNQNNQNPKYAKYFSTVKNGEFIPGEVKVYEVTDTNA
MVDSFNPDLNSSNVKDVTSQFAPKVSADGTRVDINFARSMANGKKYIVTQAVRPTGTGNVY
TEYWLTRDGTTNTNDFYRGTKSTTVTYLNGSSTAQGDNP*

6. Bioconjugation and biology

6.1. General Procedure D: Fab disulfide re-bridging and IEDDA functionalisation via DvTz

To a 10 μM solution of Fab in TBS buffer (25 mM Tris-HCl, 25 mM NaCl, 0.5 mM EDTA, pH 8.0, 100 μL) was added tris(2-carboxyethyl)phosphine hydrochloride (TCEP, 10 eq.) and the solution was incubated for 1 h at 37 °C on a thermal shaker at 400 rpm. **DvTz** (20 eq., stock solution in MeCN) was subsequently added in MeCN (10% of the total reaction volume), and the solution was incubated at 37 °C for a further 1h. The reaction was filtered through a Zeba™ spin desalting column (equilibrated into phosphate-buffered saline (PBS, 1x, pH 7.4), 7,000 MW cut-off, Thermo-Fisher Scientific) and buffer-exchanged into PBS *via* an Amicon-Ultra 15 diafiltration spin-concentrator (10,000 MW cut-off, Merck Millipore) to yield the Fab-DvTz.

To a 10 μM solution of Fab-DvTz in PBS was added **2** (Fig.2, 20 eq.) in DMSO (10% of the reaction volume), and the reaction was incubated for 2 h at 37 °C on a thermal shaker at 400 rpm. The reaction was filtered through a Zeba™ spin desalting column (equilibrated into PBS, 7,000 MW cut-off, Thermo-Fisher Scientific) and concentrated *via* an Amicon-Ultra 15 diafiltration spin-concentrator (10,000 MW cut-off, Merck Millipore) to yield the Fab-DvTz-BCN.

6.2. Optimisation on αHER2 Fab (Figure S4)

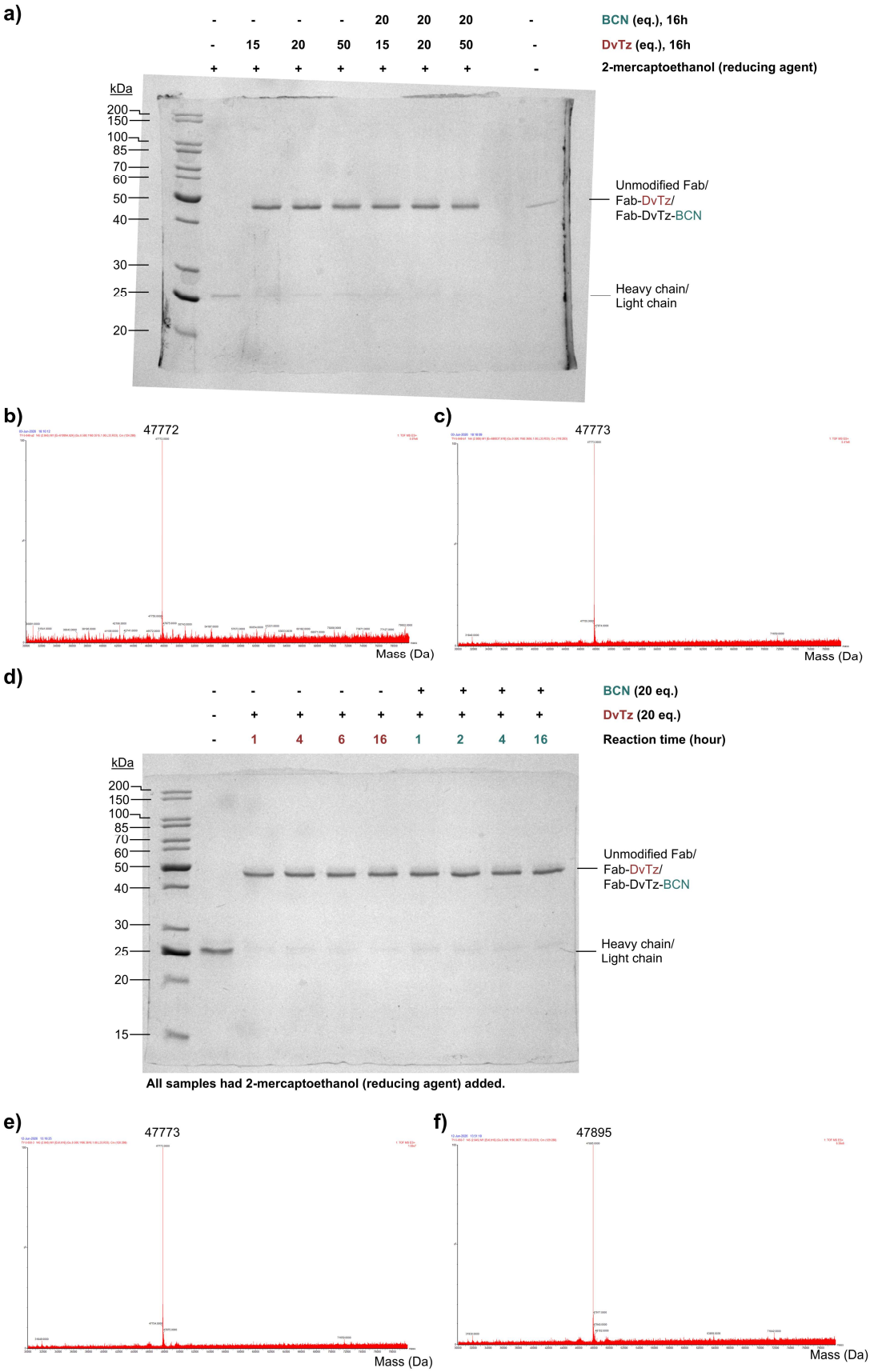

Figure S4: Optimisation of αHER2 Fab conjugation, including **DvTz** eq and reaction time. **a)** SDS–PAGE analysis of the **DvTz** re-bridging titration. Unmodified αHER2 Fab (**12**) is shown

alongside Fab treated under identical reduction and reaction conditions with increasing equivalents of **DvTz** incubated at 37 °C in 10% MeCN/TBS buffer mixture to give αHER2 Fab–DvTz (**12a**); **12a** was subsequently treated with 20 eq. BCN incubated at 37 °C in 10% DMSO and PBS mixture to give αHER2 Fab–DvTz–BCN (**12b**). **12**, **12a,** and **12b** on 12% acrylamide gel with samples prepared using a loading dye with or without reducing agent 2-mercaptoethanol as labelled, followed by Coomassie Blue staining. **b)** Deconvoluted MS (1500–4000 m/z) of **12a** formed with 15 eq. **DvTz**. Peak height referenced to most intense signal. Expected 47772 Da, observed 47772 Da. **c)** Deconvoluted MS (1500–4000 m/z) of **12a** with 20 eq. **DvTz**. Peak height referenced to most intense signal. Expected 47773 Da, observed 47772 Da. **d)** SDS–PAGE analysis of the re-bridging and IEDDA functionalization at different reaction time points. Unmodified αHER2 Fab (**12**) was shown alongside Fab incubated with 20 eq. **DvTz** at 37 °C in 10% MeCN and TBS buffer mixture at different reaction time points to give αHER2 Fab–DvTz (**12a**); **12a** was subsequently treated with 20 eq. BCN and incubated at 37 °C in 10% DMSO and PBS mixture at different reaction time points to give αHER2 Fab–DvTz–BCN (**12b**). **12**, **12a** and **12b** on 12% acrylamide gel with samples prepared using a loading dye with reducing agent 2-mercaptoethanol as labelled, followed by Coomassie Blue staining. **e)** Deconvoluted MS (1500–4000 m/z) of **12a** formed with 20 eq. DvTz after 1 hour reaction from **12**. Peak height referenced to most intense signal. Expected 47772 Da, observed 47773 Da. **f)** Deconvoluted MS (1500–4000 m/z) of **12b** formed with 20 eq. BCN after 2-hour reaction from **12a**. Peak height referenced to most intense signal. Expected 47894 Da, observed 47895 Da.

6.3. General method for BLI

Binding kinetics were measured using an Octet-RED 96 BLI system (ForteBio). Assays were performed at 30 °C with shaking at 1,000 rpm in PBS, pH 7.4, containing 0.05% (v/v) Tween-20. Samples were prepared in 96-well plates (Greiner Bio-One, 655209) at 200 µL per well.

To measure the binding kinetics of anti-SdrF Fabs (**14**, **14a**, **14b**) to biotinylated SdrF, Octet SA biosensors (Sartorius, 18-5019) were hydrated in running buffer for at least 15 min before use. Biotinylated SdrF was then immobilised on streptavidin biosensors at 5 µg/mL. Loaded biosensors were exposed to Fab analytes at 10, 3.3, 1.1, 0.37, 0.12 and 0 nM. An unloaded biosensor exposed to 10 nM Fab analyte was included as a control for non-specific binding.

To measure the binding kinetics of anti-HER2 Fabs (**12**, **12a**, **12b**) and anti-HER2 IgGs (**15**, **15a**, **15b**) to human HER2-HisTag, Octet HIS1K Biosensors (Sartorius, 18-5120) were hydrated in running buffer for at least 15 min before use. Human HER2-HisTag was then immobilised on HIS1K biosensors at 5 µg/mL. Loaded biosensors were exposed to Fab analytes at 100, 50, 25, 12.5, 6.25, 3.125 and 0 nM. Loaded biosensors were exposed to IgG analytes at 100, 33.3, 11.1, 3.7, 1.2 and 0 nM. An unloaded biosensor exposed to 100 nM Fab analyte was included as a control for non-specific binding.

Association and dissociation were monitored as changes in wavelength shift over time. The equilibrium dissociation constant (K_d) was determined by globally fitting the data to a 1:1 binding model. Data were collected using Octet Data Acquisition software (version 11.0.0.64; ForteBio) and analysed using ForteBio Data Analysis software (version 11.0).

6.4. αHER2 Fab conjugate analysis (Figure S5)

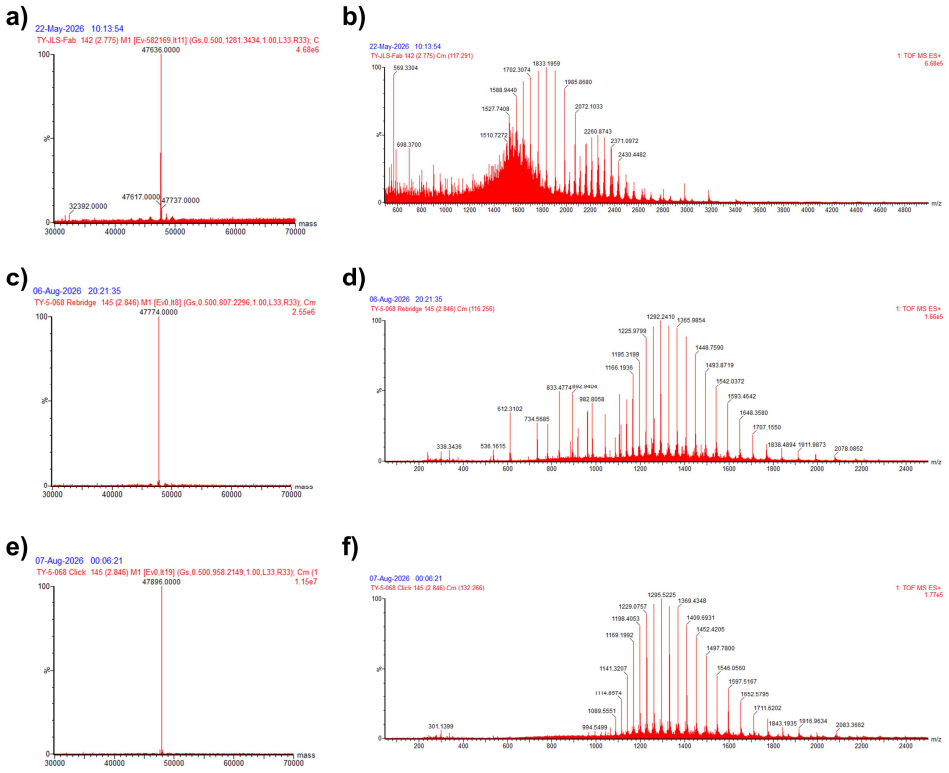

Figure S5: Analytical data for **12**, **12a** and **12b**. **a)** Deconvoluted MS (1500–4000 m/z) of **12**. Peak height is referenced to most intense signal. Expected 47638 Da, observed 47636 Da. **b)** Raw MS of **12**; intensity vs. m/z. **c)** Deconvoluted MS (1500–4000 m/z) of **12a**. Peak height referenced to most intense signal. Expected 47772 Da, observed 47774 Da. **d)** Raw MS of **12a**; intensity vs. m/z. **e)** Deconvoluted MS (1500–4000 m/z) of **12b**. Peak height referenced to most intense signal. Expected 47894 Da, observed 47896 Da. **f)** Raw MS of **12b**; intensity vs. m/z.

6.5. αCD45 Fab conjugate analysis (Figure S6)

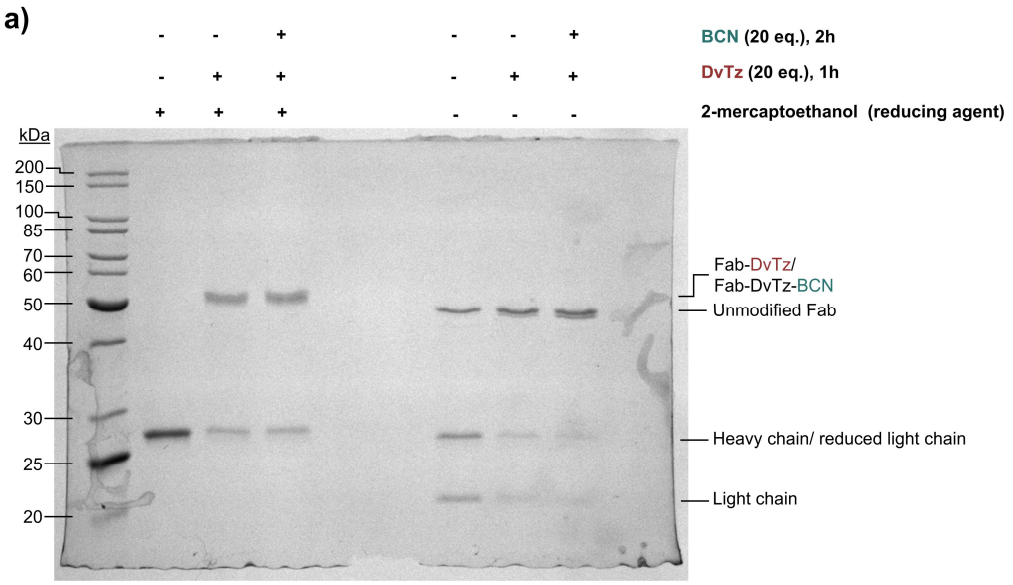

(The αCD45 Fab was prone to incomplete disulfide bond formation, with free light and heavy chains detected in the absence of reducing agent.)

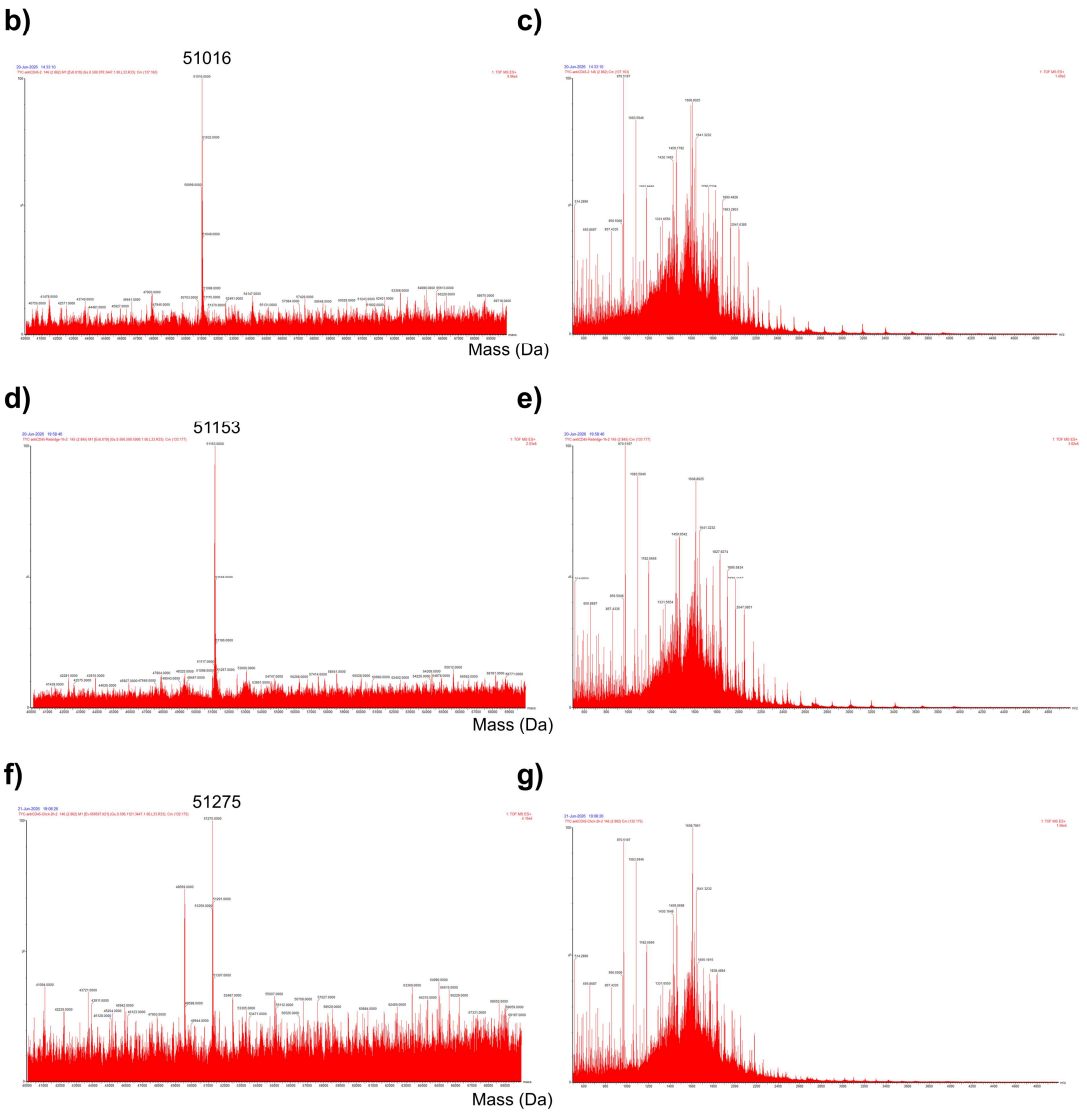

Figure S6: Analytical data for αCD45 Fab (**13**), αCD45 Fab-DvTz (**13a**) and αCD45 Fab-DvTz-BCN (**13b**). **a)** SDS-PAGE analysis of **13**, **13a** and **13b** on 12% acrylamide gel with samples prepared using a loading dye with or without reducing agent 2-mercaptoethanol as labelled, followed by Coomassie Blue staining. **b)** Deconvoluted MS (1500–4000 m/z) of **13**. Peak height is referenced to most intense signal. Expected 51016 Da, observed 51016 Da. **c)** Raw MS of **13**; intensity vs. m/z. **d)** Deconvoluted MS (1500–4000 m/z) of **13a**. Peak height is referenced to most intense signal. Expected 51152 Da, observed 51153 Da. **e)** Raw MS of **13a**; intensity vs m/z. **f)** Deconvoluted MS (1500–4000 m/z) of **13b**. Peak height is referenced to most intense signal. Expected 51274 Da, observed 51275 Da. **g)** Raw MS of **13b**; intensity vs. m/z.

6.6. αSdrF Fab conjugate analysis (Figure S7)

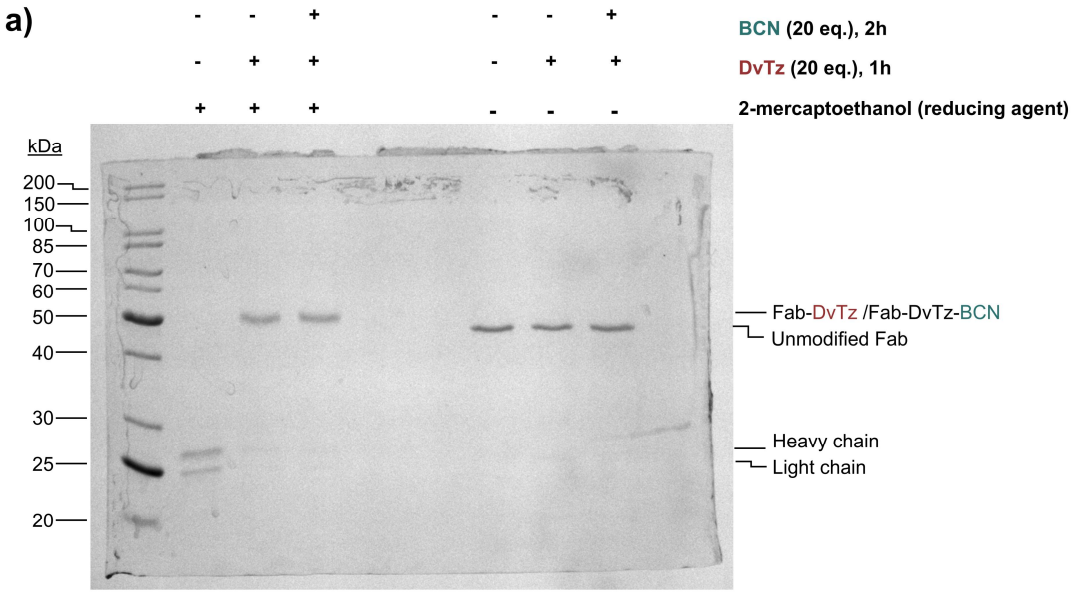

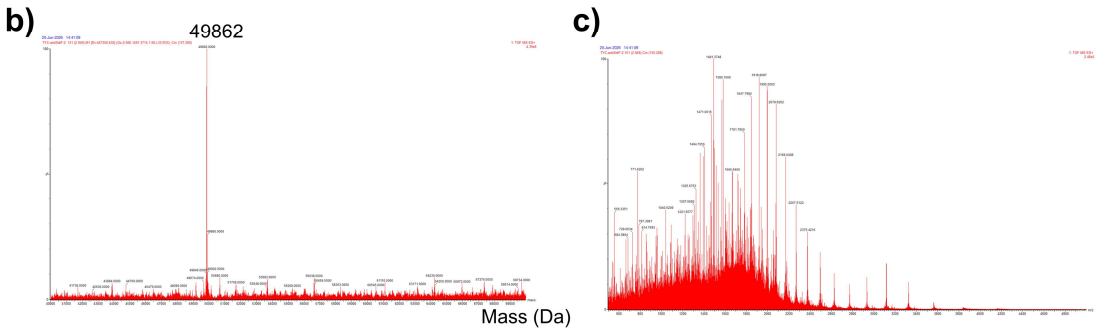

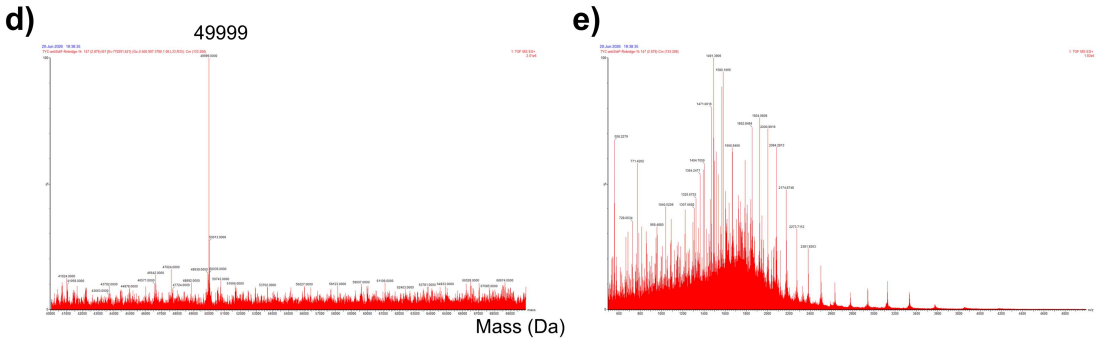

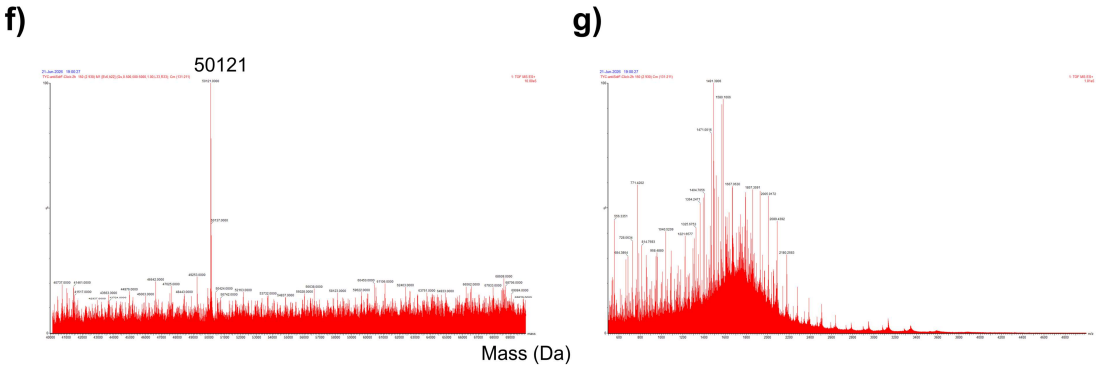

Figure S7: Analytical data for αSdrF Fab (**14**), αSdrF Fab-DvTz (**14a**) and αSdrF Fab-DvTz-BCN (**14b**). **a)** Uncropped SDS-PAGE gel from Figure 4C. **14**, **14a** and **14b** on 12% acrylamide gel with samples prepared using a loading dye with or without reducing agent 2-mercaptoethanol as labelled, followed by Coomassie Blue staining. **b)** Deconvoluted MS (1500–4000 m/z) of **14**. Peak height is referenced to most intense signal. Expected 49862 Da, observed 49862 Da. **c)** Raw MS of **14**; intensity vs. m/z. **d)** Deconvoluted MS (1500–4000 m/z) of **14a**. Peak height is referenced to most intense signal. Expected 49998 Da, observed 49999 Da. **e)** Raw MS of **14a**; intensity vs. m/z. **f)** Deconvoluted MS (1500–4000 m/z) of **14b**. Peak height is referenced to most intense signal. Expected 50120 Da, observed 50121 Da. **g)** Raw MS of **14b**; intensity vs. m/z.

6.7. αSdrF Fab binding kinetics analysis (Figure S8)

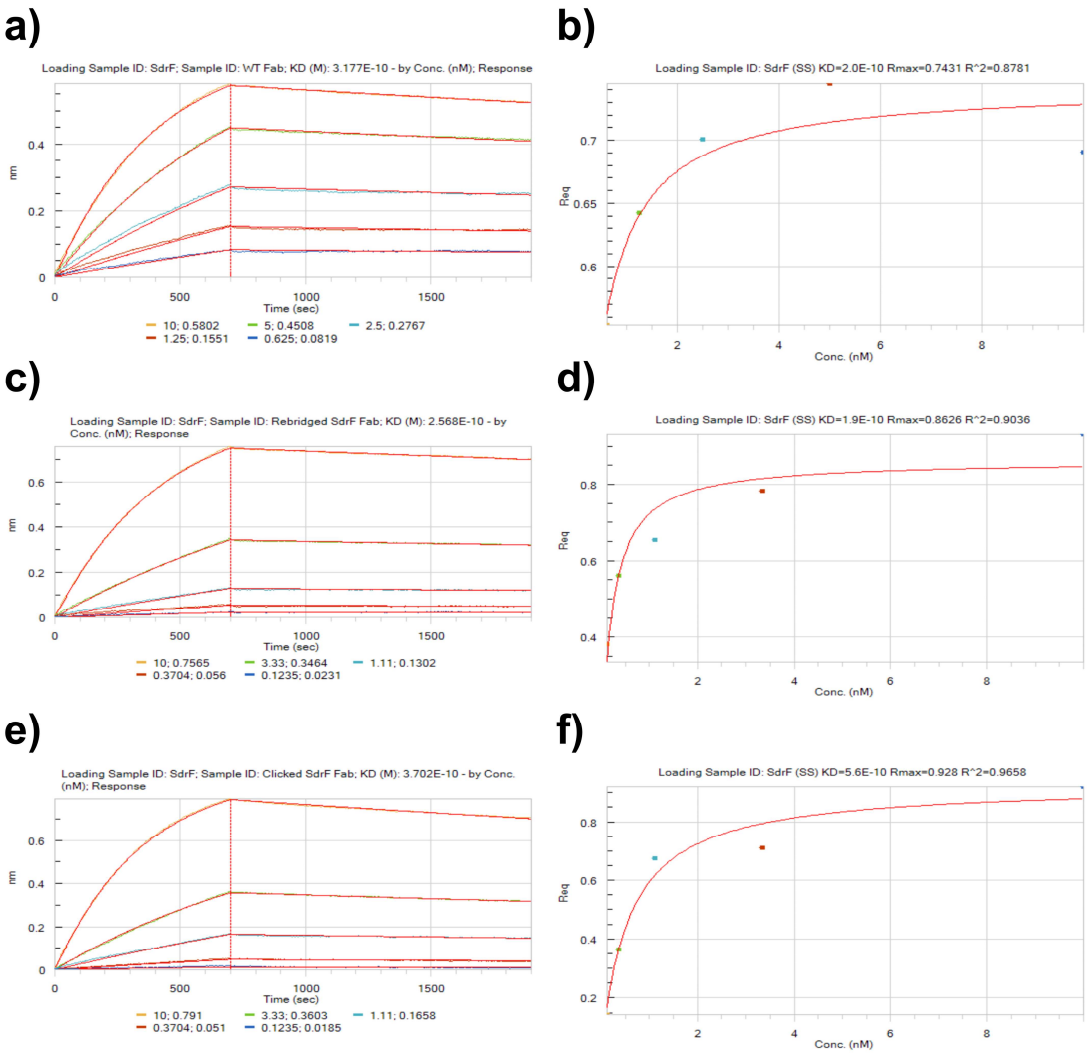

Figure S8: αSdrF Fab binding kinetics analysis. Biotinylated SdrF was loaded onto streptavidin sensors and unmodified αSdrF Fab (**14**), αSdrF Fab-DvTz (**14a**) and αSdrF Fab-DvTz-BCN (**14b**) were used as analytes in PBS-T (pH 7.4, 0.05% Tween-20). **a)** BLI curves (association and dissociation phases, marked by the vertical red dashed line) of **14**. The corresponding K_d ± fitting error is 0.3 nM ± 0.002 nM. The red lines correspond to a fit with a 1:1 standard binding model. **b)** Steady state analysis of **14** from BLI. The corresponding steady-state K_d is 0.2 nM. **c)** BLI curves of **14a**. The corresponding K_d ± fitting error is 0.3 nM ± 0.001 nM. The red lines correspond to a fit with a 1:1 standard binding model. **d)** Steady state analysis of **14a** from BLI. The corresponding steady-state K_d is 0.2 nM. **e)** BLI curves of **14b**. The corresponding K_d ± fitting error is 0.4 nM ± 0.001 nM. The red lines correspond to a fit with a 1:1 standard binding model. **f)** Steady-state analysis of **14b** from BLI. The corresponding steady-state K_d is 0.6 nM.

6.8. General Procedure E: Trastuzumab disulfide re-bridging and IEDDA functionalisation via DvTz

To a 10 μM solution of trastuzumab in TBS buffer (25 mM Tris-HCl, 25 mM NaCl, 0.5 mM EDTA, pH 8.0, 100 μL) was added tris(2-carboxyethyl)phosphine hydrochloride (TCEP, 10 eq.) and the solution was incubated for 1 h at 37 °C on a thermal shaker at 400 rpm. **DvTz** (60 eq., stock solution in MeCN) was subsequently added in MeCN (10% of the total reaction volume), and the solution was incubated at 37 °C for a further 2 h. The reaction was filtered through a Zeba™ spin desalting column (equilibrated into PBS, 10,000 MW cut-off, Thermo-Fisher Scientific) and buffer-exchanged into PBS *via* an Amicon-Ultra 15 diafiltration spin-concentrator (10,000 MW cut-off, Merck Millipore) to yield trastuzumab-DvTz (**15a**).

To a 10 μM solution of **15a** in PBS buffer was added **2** (100 eq.) in DMSO (10% of the reaction volume), and the reaction was incubated for 16 h at 37 °C on a thermal shaker at 400 rpm. The reaction was filtered through a Zeba™ spin desalting column (equilibrated into PBS, 10,000 MW cut-off, Thermo-Fisher Scientific) and concentrated *via* an Amicon-Ultra 15 diafiltration spin-concentrator (10,000 MW cut-off, Merck Millipore) to yield trastuzumab-DvTz-BCN (**15b**).

6.9. Optimisation of trastuzumab re-bridging (Figure S9)

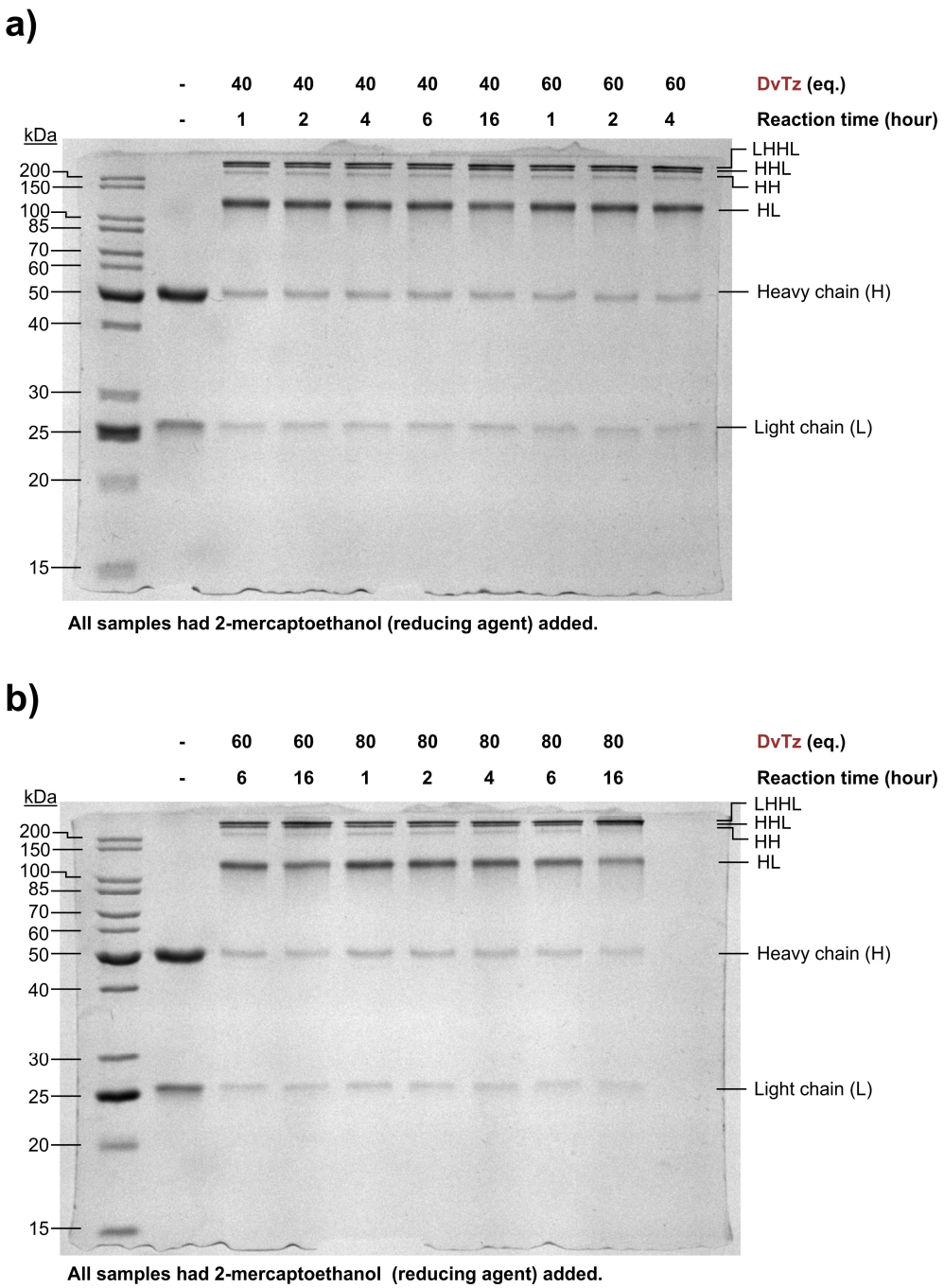

Figure S9: Optimisation of Trastuzumab conjugation via **DvTz** re-bridging titration. **a)** SDS–PAGE analysis of the **DvTz** re-bridging titration. Trastuzumab (**15**) is shown alongside trastuzumab treated under identical reduction and reaction conditions with increasing equivalents of **DvTz** and increasing reaction time to give trastuzumab–DvTz (**15a**); **15** and **15a** were resolved on 12% acrylamide gel with samples prepared using a loading dye with reducing agent 2-mercaptoethanol, followed by Coomassie Blue staining. **b)** 12% acrylamide gel with samples prepared using loading dye with reducing agent 2-mercaptoethanol, followed by Coomassie Blue staining. L = native antibody light chain; H = native antibody heavy chain; HL= re-bridged heavy-light chains (half antibody); HH= re-bridged antibody heavy-heavy chains; HHL = re-bridged antibody heavy-heavy-light chains; LHHL= fully re-bridged antibody

6.10. Trastuzumab conjugate analysis (Figure S10)

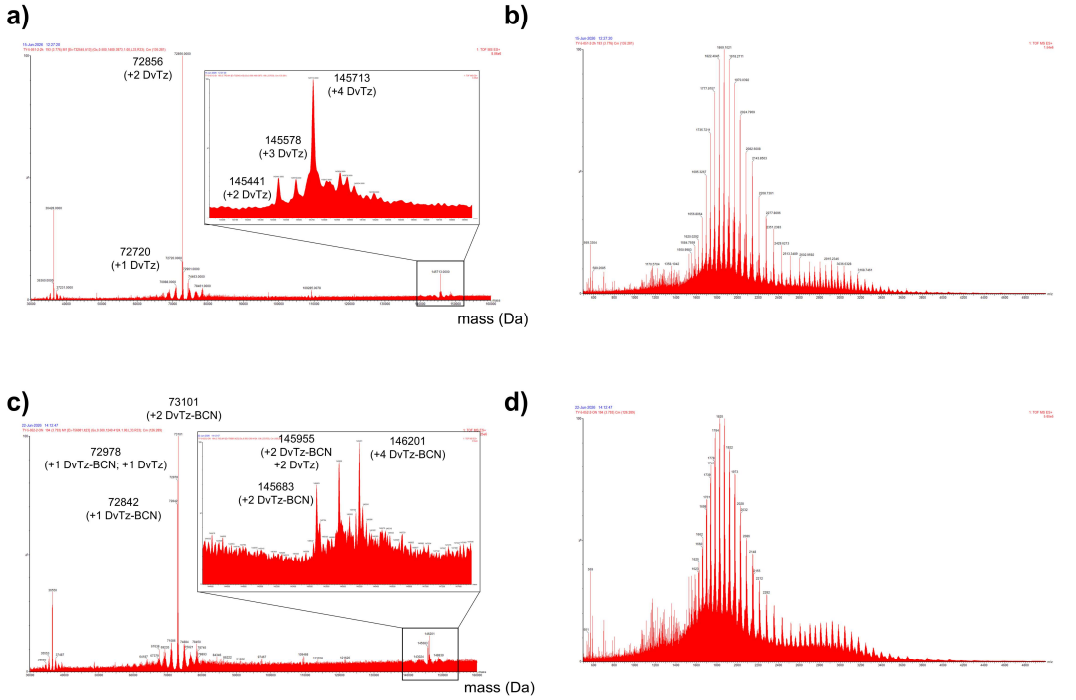

Figure S10: Analytical data for trastuzumab-DvTz (**15a**) and trastuzumab-DvTz-BCN (**15b**). **a)** Deconvoluted MS (1500–4000 m/z) of **15a** formed with 60 eq. of DvTz for a 2-hour reaction. Peak height is referenced to most intense signal. Half antibody mass+1 DvTz, expected 72719 Da, observed 72720 Da; Half antibody mass+2 DvTz, expected 72853 Da, observed 72856 Da; Full antibody mass+2 DvTz, expected 145438 Da, observed 145441 Da; Full antibody mass+3 DvTz, expected 145572 Da, observed 145578 Da; Full antibody mass+4 DvTz, expected 145706 Da, observed 145713 Da; **b)** Raw MS of **15a**; intensity vs. m/z. **c)** Deconvoluted MS (1500–4000 m/z) of **15b** formed with 100 eq. of BCN for a 16-hour reaction. Peak height is referenced to most intense signal. Half antibody mass+1 DvTz-BCN, expected 72841 Da, observed 72842 Da; Half antibody mass+1 DvTz-BCN+1 DvTz, expected 72975 Da, observed 72978 Da; Half antibody mass+2 DvTz-BCN, expected 73097 Da, observed 73101 Da; Full antibody mass+2 DvTz-BCN, expected 145682 Da, observed 145683 Da; Full antibody mass+2 DvTz-BCN+2 DvTz, expected 145950 Da, observed 145955 Da; Full antibody mass+4 DvTz-BCN, expected 146194 Da, observed 146201 Da; **d)** Raw MS of **15b**; intensity vs. m/z.

6.11. Trastuzumab binding kinetics analysis (Figure S11)

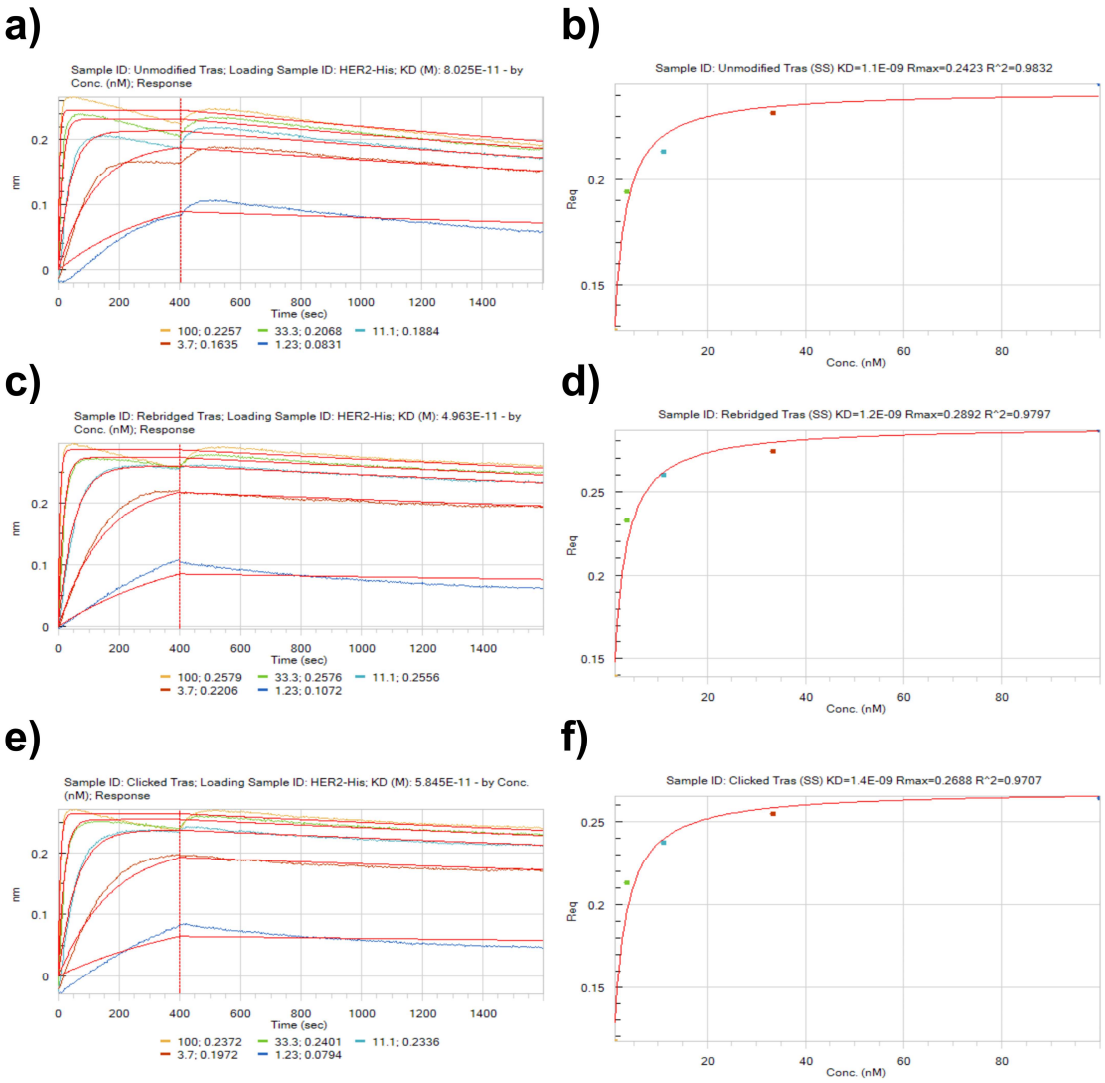

Figure S11: Trastuzumab binding kinetics analysis. Human HER2-HisTag was loaded onto HIS1K sensors and unmodified trastuzumab (**15**), trastuzumab-DvTz (**15a**) and trastuzumab-DvTz-BCN (**15b**) were used as analytes in PBS-T (pH 7.4, 0.05% Tween-20). **a)** BLI curves (association and dissociation phases, marked by the vertical red dashed line) of **15**. The corresponding K_d is 0.08 nM. The red lines correspond to a fit with a 1:1 standard binding model. **b)** Steady-state analysis of **15** from BLI. The corresponding steady-state K_d is 1 nM. **c)** BLI curves (association, dissociation, marked by the vertical red dashed line) of **15a**. The corresponding K_d is 0.05 nM. The red lines correspond to a fit with a 1:1 standard binding model. **d)** Steady-state analysis of **15a** from BLI. The corresponding steady-state K_d is 1 nM. **e)** BLI curves (association, dissociation, marked by the vertical red dashed line) of **15b**. The corresponding K_d is 0.06 nM. The red lines correspond to a fit with a 1:1 standard binding model. **f)** Steady-state analysis of **15b** from BLI. The corresponding steady-state K_d is 1 nM.

7. References

1 H. E. Gottlieb, V. Kotlyar and A. Nudelman, *J. Org. Chem.*, 1997, **62**, 7512–7515.

2 B. Pinto-Pacheco, W. P. Carbery, S. Khan, D. B. Turner and D. Buccella, *Angew. Chem. Int. Ed.*, 2020, **59**, 22140–22149.

3 X. He, J. Li, X. Liang, W. Mao, X. Deng, M. Qin, H. Su and H. Wu, *Nat. Commun.*, 2024, **15**, 2831.

4 A. J. Counsell, S. J. Walsh, N. Ashman, M. Park, F. M. Dannheim, T. A. King, T. Wharton, J. S. Carroll and D. R. Spring, *Chem. Sci.*, 2026, **17**, 2722–2731.

5 R. A. Hills, T. K. Tan, A. A. Cohen, J. R. Keeffe, A. H. Keeble, P. N. P. Gnanapragasam, K. N. Storm, A. V. Rorick, A. P. West, M. L. Hill, S. Liu, J. Gilbert-Jaramillo, M. Afzal, A. Napier, G. Admans, W. S. James, P. J. Bjorkman, A. R. Townsend and M. R. Howarth, *Nat. Nanotechnol.*, 2024, **19**, 1216–1223.

6 M. Fairhead and M. Howarth, in *Methods in Molecular Biology*, Humana Press Inc., 2015, vol. 1266, pp. 171–184.